Universidade de Lisboa

Faculdade de Farmácia

Astrocyte-specific Transcriptomic Response to PGC-1α Isoforms

Mariana Messias de Jesus Rufino Ribeiro

Master Thesis supervised by Elsa Rodrigues, Ph.D., and co-supervised by Jorge Lira Ruas, Ph.D.

Master's Degree in Biopharmaceutical Sciences

Dissertation submitted to obtain a master's degree in Biopharmaceutical Sciences

September 2018

Universidade de Lisboa

Faculdade de Farmácia

Astrocyte-specific Transcriptomic Response to PGC-1α Isoforms

Mariana Messias de Jesus Rufino Ribeiro

Master Thesis supervised by Elsa Rodrigues, Ph.D., and co-supervised by Jorge Lira Ruas, Ph.D.

Master's Degree in Biopharmaceutical Sciences

Dissertation submitted to obtain a master's degree in Biopharmaceutical Sciences

September 2018

Astrocyte-specific Transcriptomic Response to PGC-1α Isoforms

Part of the results discussed in this thesis were presented in the following meetings:

Ribeiro, M.M., Nunes, M.J., Cervenka, I., Jannig, P., Gama M.J., Castro-Caldas M., Ruas, J.L. & Rodrigues E., Astrocyte-specific Transcriptomic Response to PGC-1α Isoforms. 10th iMed.UL Postgraduate Students Meeting, 24th July 2018, Lisbon, Portugal [Abstract and Poster Presentation]

This work was supported by FEDER and national funds from Fundação para a Ciência e Tecnologia (FCT) (PTDC/MED-FSL/30104/2017 (to J.L.R) and UID/DTP/04138/2013), research grant SFRH/BPD/95855/2013 (to M.J.N.) and Swedish Research Council Consolidator Grant (to J.L.R.).

ACKNOWLEDGEMENTS

Os meus primeiros agradecimentos vão, como não podia deixar de ser, para a Professora Doutora Elsa Rodrigues. Não só por este ano de dissertação, mas também por me ter acolhido logo no primeiro ano de mestrado. Por me ter introduzido no mundo da investigação e por me ter ajudado a dar os primeiros passos no laboratório. Pela constante boa-disposição, atitude positiva e divertida, mas também por me pôr no lugar quando fazia coisas com "excesso de confiança" ou à pressa. Por partilhar comigo o seu infame "caderno das experiências falhadas". Por todo o entusiamo como novos resultados. Por me ter dado a oportunidade única de trabalhar num dos melhores institutos da Europa. Por nunca me deixar à deriva e encontrar sempre uma hipótese alternativa e um rumo para o nosso trabalho. Um muito obrigado por ter sido a melhor orientadora que podia ter pedido, mas também por ser um exemplo de que me irei lembrar sempre.

Ao Professor Doutor Jorge Ruas, por me ter aceite no seu grupo no Karolinska. Por me pôr completamente à vontade e ter sempre a porta aberta para mim. Pelos *mini meetings*, pela boa disposição e pela orientação. Por expandir os meus horizontes no mundo da investigação e por me obrigar a pensar fora da caixa.

À Maria, muito obrigada por estares sempre disponível para me ajudar, mesmo quando o Manel não te dava muito descanso. Por esclareceres todas as minhas dúvidas e seres um dos maiores exemplos de organização que conheço. Por todas as culturas extra que tiveste de fazer para me enviar para Estocolmo. Aprendi imenso contigo e quero agradecer-te por todos os bons momentos e por nunca desistires do nosso trabalho.

To Igor. Thank you for your crucial help with all the bioinformatics analysis. You taught me everything I know about RNA-Seq analysis. All the problem solving, failed and successful attempts, building scripts on my own were vital for my learning process. Your collaboration was, without a doubt, indispensable for the sucess of this project.

À professora Maria João Gama, à Andreia e à professora Margarida por animarem a nossa salinha, por toda a disponibilidade e espírito de entreajuda.

Agradeço também à Professora Doutora Cecília Rodrigues a oportunidade de fazer parte do seu grupo "Cellular Function and Therapeutic Targeting", por enriquecer os meus conhecimentos e pelo esforço constante para nos dar as melhores condições de trabalho.

A todos os restantes membros do CellFun: André, Dionísio, Pedro, Maria, Diane, Vanda, Hugo, Simão por me ajudarem sempre precisava e por tornarem os meus dias mais alegres. Um especial obrigado ao André por todos momentos de diversão e ao Dionísio por nos entreter com o seu canto inconfundível.

À Raquel, ao Sebastião e ao Paulo por uma amizade desde os tempos da licenciatura e por partilharmos as nossas frustrações e também os nossos sucessos (mas principalmente as frustrações). Por todo o apoio, por me darem uma perspetiva diferente e bons conselhos e força para ultrapassar os obstáculos que foram surgindo.

To Arthur. Thank you for being my biggest support in Stockholm. For not giving up on me and always trying to make me feel comfortable with the people from the lab. For trying (quite successfully) to improve my arm strength and my jumping rope skills. For explaining

me the pronunciation difference between “owe” and “own”, “beach” and “bitch”, “sheet” and “shit”. My English is now way better thanks to you. For always looking out for me when we went out with the guys. I will never forget what you have done for me. For showing me so many good cafes, from the most popular to the “granny’s place”, taking me around Stockholm, Sigtuna and Uppsala. For showing me the *lagom* vibe and for taking me to the lake on those unpredictably hot days so that I could swim. If it wasn’t for you, my experience in Stockholm wouldn’t have been half as fun. Thank you for being my “big brother” while I was there.

To Maja. For actually putting me into shape. I honestly thought that that would never happen in my life. Thank you. But also for all those fun moments, inappropriate jokes and support. For being an example of perseverance will power and honestly a bit of madness. But a good one. Eating kale everyday and then working out like you do is an example of good madness. I wish you the best of luck for your new journey in Italy!

Speaking about Italians, how could I forget i miei italiani, Laura and Michele. Laura, ragazza mia, you were a breath of fresh air when you arrived to Stockholm. Super kind, nice and amazingly pretty. Even I fell for you. I enjoyed all our conversations superficial and deep ones, in the gym or in the lake and I’m super glad to have been able to see you grow and becoming a bit more independent and confident. Thank you for all the good advices, for always being available to talk and listen and, of course, for helping me making fun of Michele.

Michele Assolini… Ah, sorry, Azzolini. When I arrived to the lab, I thought you were a girl. Like 90% of the people I think. I saw the drawers saying “Michele” and, in Portugal, that’s a girl’s name. So, I wondered in the lab for a while looking for a girl called Michele. And one day, I saw you open those drawers. And, in that moment, I found that Michele was truly a girl. Thank you for always reminding me that I was not the only one screwing up in the lab, since day one, when we were talking in the qPCR room and you messed up your plate up (let’s hope Jorge doesn’t read this part). But now for real, thank you for always making my days way way funnier and nicer. For constantly admiring my “youthness” and also for making fun of my less young face (aka completely dying face). And of course, we will always remember, “ERAASMUUUUUS!”. I mean, you will.

Ao Paulo, por me surpreenderes logo no primeiro dia. Quando te conheci, pensei que eras sueco. Cabelo loiro, olhos claros… Mas depois cumprimentaste com um típico “oi, tudo bem?” e um grande abraço e eu pensei “não foi isto que li sobre os suecos”. Obrigada por toda a tua ajuda com a bioinformática. Sem ti, teria demorado e por seres o meu companheiro de sala. Por me alertares para os *lab meetings* e por todas as gargalhadas e debates sobre português europeu vs. português do Brasil.

A big thank you to all “Molecular and Cellular Exercise Physiology” group. To Serge, Duarte, Jorge, Lars, Vicente, Paula, Margareta, Yildiz, Shamim, Kyle, Manizheh and to Maria Manti for all your help and guidance in the lab. A special thank you to Serge, for being my quiet buddie, to Duarte for always being available to help and for all the patience with Agilent and my samples to Paula for all the help with the cultures and to Maria for all the fun we had in the office.

Last, but not least, a more personal thank you to my “supervisor”, Igor. The best way I have to describe you is like a gigantic teddy bear. Because, on the outside, you are big and strong and people usually think twice before they mess with you. But then, when I started to

know you, I saw that you were the sweetest, kindest soul I have ever met. Although our first interactions were by changing emails, you were always available to help in the lab and always checking if I had broken something. Besides a great help in the lab, you have been my biggest support during this last year. We understand each other very well and that makes it easier to talk to you. No matter what happens from now on, I know that I can always count on you. Thank you very much for everything.

À Marta e à Inês, as minhas sincronistas desde sempre. Por me ouvirem a qualquer altura e serem as minhas maiores confidentes.

Ao Sérgio e ao Tiago, por todo o apoio enquanto estive em Estocolmo. Ajudaram-me a ultrapassar os primeiros tempos mais do que imaginam. Obrigada por me terem ido visitar. Obrigada por tudo o que me ensinaste Sérgio. Obrigada por atenderes a minha chamada às três da manhã quando pensava que ia morrer Tiago.

Por fim, os meus agradecimentos mais especiais vão para a minha família. Aos meus avós e ao meu pai, por sempre me apoiarem em qualquer decisão que tome e por apostarem na minha educação e no meu bem-estar.

À minha irmã. Sei que temos a relação clássica de amor ódio, mas quero que saibas o quanto te admiro. Não sei como és capaz de conciliar o Técnico com a natação, com cursos, vida social. É verdadeiramente incrível. Admiro a tua capacidade de organização e de gestão de tempo. Vejo em ti um exemplo a seguir, o que posso melhorar e como o posso fazer. Tenho realmente orgulho em ti, que consigas atingir todos os teus objetivos e na mulher que te estás a tornar. Claro que ainda me irrita a tua ligeira preguiça, mas com todo o esforço que fazes durante o dia, cá no fundo, sabes que te compreendo. Obrigada por todo o apoio que me deste enquanto tive em Estocolmo. Foi à nossa maneira, mas eu sei que esteve lá.

Mas sobretudo à minha mãe. Obrigada por tudo. Por dares 200% para que tenhamos tudo de melhor. Por dedicares a tua vida a nós. Por seres a melhor mãe e o melhor exemplo que podia ter. Se eu um dia crescer e me tornar metade da mãe e mulher que és, vou ficar muito feliz. Fizeste muito por nós. Espero que um dia conseguir retribuir toda a tua dedicação. Obrigada por todas as palavras de apoio, coragem e motivação que me deste ao longo deste ano e de toda a minha vida. Amo-te muito.

Com carinho,

Mariana

ABSTRACT

Peroxisome proliferator-activated receptor-gamma coactivator-1α (PGC-1α) transcriptional coactivators are key regulators of energy metabolism-related genes and are expressed in energy-demanding tissues. There are several PGC-1α variants that exert differential and specific biological functions. In the brain, PGC-1α1 has been implicated in reactive oxygen species detoxification but our understanding of the role of the other isoforms is far from complete. Previous results have shown that PGC-1α isoform expression levels can be modulated in the brain by stress conditions, suggesting a functional role for these proteins. Moreover, we have observed that increased expression of PGC-1α3 in astrocytes could be deleterious to neurons. In the adult brain, astrocyte-neuron crosstalk is crucial for neurite outgrowth, dendritic spine maintenance and synaptic function.

The main objective of this study was to characterize the molecular pathways controlled by PGC-1α3 in *in vitro* neuronal and astrocytic experimental models. In parallel, we analysed the transcriptome of astrocytes transduced with a viral vector encoding PGC-1α3 by massively parallel sequencing (RNA-seq) in order to identify its downstream targets.

The most striking hits, as well as the expression of other astrocyte-specific genes that could be involved in the neuronal response to PGC-1α3-overexpressing astrocytes, were determined by qPCR. We also used the Ingenuity Pathway Analysis suite to determine which pathways were being modulated as a result of differential expression of the identified hits. Our results show that PGC-1α3 can trigger G_q-coupled protein-mediate calcium dysregulation within astrocytes, inducing secretory pathways and neuroinflammation. In addition, our observations suggest a severe impairment of cell migration.

Since proteins secreted by astrocytes play an important role in different neuronal physiological functions, we analyzed our RNA-seq data in order to predict the astrocytic secretome profile. Using a suite of bioinformatic tools we were able to identify candidate proteins putatively secreted through both canonical and non-canonical pathways. Combining these results with the analysis of the differentially expressed genes, led to the identification of Serpini1, Angptl4, galectin 9 and TGFβ as putative PGC-1α3 target genes. Interestingly, an extensive number of transcripts regulated by PGC-1α3 map to pseudogenes, which could potentially include miR sequences.

Our results identify for the first-time an astrocyte-specific transcriptomic response to PGC-1α3 expression and highlight PGC-1α isoforms as novel therapeutic targets for the treatment of neurodegenerative diseases.

Keywords: PGC-1α, astrocytes, crosstalk, transcriptome, neurodegeneration

RESUMO

O co-ativador 1 alfa do recetor gama ativado por proliferadores de peroxissoma (*Peroxisome Proliferator-activated receptor-gamma Coactivator-1α* - PGC-1α) é um regulador transcricional envolvido maioritariamente na expressão de genes relacionados com metabolismo energético, que, por sua vez, são expressos em tecidos com alta necessidade energética. Existem várias isoformas do PGC-1α que exercem funções biológicas específicas e distintas. No entanto, o nosso conhecimento sobre o seu papel no correto funcionamento do encéfalo está longe de estar completo. Os nossos resultados anteriores mostram que as diferentes formas do PGC-1α têm efeitos particulares em neurónios e astrócitos. Nomeadamente, observámos que o PGC-1α3 aumenta o conteúdo de colesterol nos neurónios e que aumento da expressão desta isoforma em astrócitos tem efeitos deletérios nos neurónios. No cérebro adulto, o *crosstalk* entre astrócitos e neurónios é essencial para o crescimento de neurites, manutenção das espinhas dendríticas e para a correta funcionalidade das sinapses.

Como tal, o principal objetivo deste estudo foi o de caracterizar as vias sinalização controladas pelo PGC-1α3 em modelos experimentais astrocíticos e neuronais *in vitro*. Em paralelo, analisámos o transcriptoma de astrócitos infetados com um vetor viral que codifica para o PGC-1α3 através de sequenciação paralela massiva de RNA (RNA-Seq) com o objetivo de identificar os seus genes alvos diretos.

Resultados obtidos em neurónios mostram que, após infeção de culturas primárias com o vetor adenoviral que codifica para o PGC-1α3, há uma diminuição significativa da expressão de proteína pós-sinápticas. No entanto, ao avaliarmos a atividade transcricional dos respetivos genes, observamos que esta não se correlaciona com o observado ao nível da expressão proteica. Assim, isto levou-nos a concluir que a ação do PGC-1α3 não será direta, mas sim sobre genes que codificam para proteínas envolvidas em modificações pós-transcricionais. Por exemplo, a ativação de calpaínas poderá justificar estes resultados, já que a sua função consiste na clivagem proteolítica induzida por aumento da concentração de cálcio intracelular.

Através do processamento dos dados obtidos por RNA-Seq, observámos que o transcriptoma associado à expressão ectópica do PGC-1α3 em astrócitos apresenta uma diminuição transversal da expressão génica. Estes resultados vão de acordo com o previamente observado por outros estudos em que se mostra que o PGC-1α3 tem um perfil regulatório contrário ao do PGC-1α1 (forma canónica). De entre os mais de 300 genes diferencialmente expressos identificados por esta análise, determinámos os níveis de mRNA dos alguns dos que nos pareceram mais relevantes, na perspetiva da comunicação entre astrócitos e neurónios. Avaliámos ainda os níveis expressão de genes-chave envolvidos na comunicação entre astrócitos e neurónios, como transportadores de glutamato e genes envolvidos na sinalização do cálcio. Também utilizamos a lista dos genes identificados como diferencialmente expressos através da análise bioinformática para determinar quais as vias de sinalização que seriam mais afetadas pela alteração na expressão destes genes. Os nossos resultados mostram que o PGC-1α3 induz desregulação de cálcio mediado pela ação de recetores acoplados à proteína G e, consequentemente, a modelação das vias celular secretórias, assim como desempenha um papel na regulação da neuroinflamação. Para além disso, também observámos que a migração celular poderá estar fortemente reduzida.

A análise efetuada aos resultados de RNA-Seq teve como propósito servir como ferramenta de descoberta, sendo que as tendências de expressão previstas pela mesma têm de ser validadas posteriormente por RT-qPCR. Surpreendentemente, observámos uma sobreexpressão de todos os genes que validámos. Tem sido sugerido que o PGC-1α3 poderá estar envolvido na regulação do *splicing* alternativo e, consequentemente, poderá induzir a produção de novos transcritos para diferentes genes. Isto poderá explicar as discrepâncias entre os nossos resultados obtidos pela análise bioinformática e os resultados de RT-qPCR, já que os novos transcritos não constam na nossa base de dados e, portanto, não conseguem ser identificados, indicando ausência de expressão.

Os astrócitos são considerados como as principais células secretórias do sistema nervoso. Sendo que proteínas secretadas pelos menos desempenham um papel crucial em diferentes funções fisiológicas neuronais, analisámos novamente a nossa lista de genes diferencialmente expressos, mas desta vez para determinar o perfil secretório associado à expressão ectópica do PGC-1α3. Através de uma seleção de ferramentas bioinformáticas especificas que preveem através da sequência de um gene a presença ou ausência de péptido sinal, localização celular, domínios transmembranares e a probabilidade de ser secretada por vias não-convencionais, identificámos proteínas potencialmente secretadas através da via canónica e não canónica. Ao combinarmos estes resultados com as tendências de expressão previstas pela análise dos resultados de RNA-Seq, identificámos a Serpini1, Angptl4, galectina 9 e TGFβ como potenciais alvos da ação do PGC-1α3.

Apesar do perfil de expressão génica previsto pela análise bioinformática seja maioritariamente repressivo, é de notar que os transcritos que se encontram aumentados são, em grande parte, identificados como pseudogenes. Os pseudogenes têm uma sequência nucleotídica muito semelhante a genes funcionais, só que, aparentemente, não desempenham nenhuma função celular. Devido à sua semelhança com outros genes, o aumento previsto da sua expressão poderia ser fruto de alinhamentos incorretos durante a análise bioinformática. Fomos então verificar se estes genes continham marcas epigenéticas relacionadas com a ativação da transcrição. Na verdade, nos *loci* onde os pseudogenes identificados se localizam, foram já identificámos marcadores de transcrição ativa, inclusivamente, marcadores específicos de *long noncoding* RNAs. Tanto os pseudogenes como os *long noncoding* RNAs têm sido descritos como reguladores da expressão génica, mais concretamente, estes pseudogenes podem estar envolvidos no *buffering* de miRs.

Novamente, com base na nossa lista de genes diferencialmente expressos, identificámos miRs cujos níveis de expressão poderão estar a ser modulados pela sua expressão. Curiosamente, prevê-se que todos os miRs identificados estejam aumentados como consequência da sobreexpressão do PGC-1α3. Diferentes miRs têm sido descritos como essenciais à manutenção da homeostase cerebral assim como a sua desregulação tem sido associada ao desenvolvimento de neurodegeneração e, consequentemente, à patogénese de doenças neurodegenerativas.

Assim, os nossos resultados identificam pela primeira vez o transcriptoma específico de astrócitos em resposta à sobreexpressão de PGC-1α3 e evidencia as isoformas do PGC-1α como novos alvos terapêuticos, abrindo assim novas estratégias terapêuticas em doenças neurodegenerativas.

Palavras-chave: PGC-1α, astrócitos, *crosstalk*, transcriptoma, neurodegeneração

TABLE OF CONTENTS

ABBREVIATIONS

ABC	ATP-binding cassette transporter
Ad	Adenovirus
AD	Alzheimer's Disease
ADP	Adenosine diphosphate
AMPA	α-Amino-3-hydroxy-5-methyl-4-isoxazole propionate
AMPK	AMP-activated protein kinase
ApoE	Apolipoprotein E
ARE	Antioxidant response element
ATF2	Activating transcription factor 2
ATP	Adenosine triphosphate
BAT	Brown adipose tissue
BDNF	Brain-derived growth factor
Ca^{2+}	Calcium
CaM	Calmodulin
CaMK	Calmodulin kinase
cAMP	Cyclic adenosine monophosphate
CaN	Calcineurin
CBP	CREB binding protein
CNS	Central nervous system
CREB	cAMP response element-binding
DAPI	4′,6-Diamidino-2-phenylindole dihydrochloride
DEG	Differentially expressed gene
DMEM	Dulbecco's Modified Eagle Medium
DTT	Dithiothreitol
EAAT	Excitatory amino acid transporter
ECM	Extracellular matrix
EEF	Eukaryotic elongation factor
ER	Endoplasmic reticulum
FBS	Fetal Bovine Serum
FM	Ferramiza-Muller Transform
GABA	γ-Aminobutyric acid
GAT	GABA transporters
GCL	γ-glutamylcysteine synthetase
GFAP	Glial fibrillary acid protein
GFP	Green fluorescence protein
glm	Generalized linear model
GSEA	Gene Set Enrichment Analysis
GSH	Glutathione
GST	Glutathione S-transferase
HBSS	Hanks' Balanced Salt solution
IGV	Integrate Genome Viewer
IP_3	Inositol-3-phosphate
IPA	Ingenuity Pathway Analysis
LDCV	Large dense-core vesicles
LXR	Liver X receptor
MAP2	Microtubule-associated protein 2

MAPK	Mitogen-activated protein kinase
MEF	Myocyte enhancer factor
Mg^{2+}	Magnesium
miR	microRNA
MRP1	Multidrug resistance protein 1
NADH	Nicotinamide adenine dinucleotide
NFAT	Nuclear factor of activated T cells
NL	Neuroligin
NMDA	N-methyl-D-aspartate
NOS	Nitric oxide species
NRF1	Nuclear respiratory factor 1
Nrf2	Nuclear factor erythroid 2-related factor 2
NRX	Neurexin
OXPHOS	Oxidative Phosphorylation
PCA	Principal Component Analysis
PD	Parkinson's Disease
PGC-1α	PPARγ coactivator-1 alpha
Pi	Inorganic phosphate
PKA	Protein Kinase A
PLC	Phospholipase C
PMSF	Phenylmethanesulfonyl Fluoride
PPARγ	Peroxisome proliferator-activated receptor gamma
PRC	PGC-1-related coactivator
PSD-95	Postsynaptic density protein 95
ROS	Reactive oxygen species
RRM	RNA recognition motif
RS	Serine/arginine-rich domain
RT-qPCR	Quantitative RT-PCR
SDS	Sodium dodecyl sulphate
SHANK3	SH3 and multiple ankyrin repeat domains 3
SIRT1	Silence information regulator 2-like 1
SLMV	Synaptic-like microvesicles
SNARE	N-ethylmaleimide-sensitive fusion attachment receptor
SPARC	Secreted protein acidic and cysteine rich
SRC1	Steroid receptor coactivator 1
SREBP	Sterol regulatory element binding protein
SYP	Synaptophysin
TCA	Tricarboxylic acid
TGFβ	Transforming growth factor
TSP	Thrombospondin
WB	Western-Blot
YY1	Ying-yang 1

INDEX OF FIGURES

I. Introduction

II. Materials and Methods

III. Results

IV. Discussion

INDEX OF TABLES

II. Materials and Methods

III. Results

I. INTRODUCTION

1 Central nervous system cell types and functions

The nervous system is responsible for controlling the body's actions through somatic and autonomic functions by processing and transmitting signals arriving to and from different parts of the body. It detects changes in the environment and then, working together with the endocrine system, produces a response appropriate to the given stimulus [1]. The nervous system is divided into two main parts: the central nervous system (CNS) and the peripheral nervous system (PNS).

The CNS consists of the two major organs of the nervous system: the brain and spinal cord. These two structures are enclosed by the meninges and protected by the cranial cavity and the spinal canal, respectively [1]. The CNS is divided into white matter, which consists of myelinated axons (conferring the white colour) and oligodendrocytes, and into grey matter, which is predominantly made of neuronal cell bodies [1].

The brain is the most complex organ of the body and the centre of the nervous system since it is responsible for processing and integrating information received from the whole body as well as deciding accordingly [1]. Brain stem, cerebellum and cerebrum are three substructures that compose the brain. The brain stem can be seen as an extension of the spinal cord and is in control of some autonomic functions such as breathing, blood pressure, balance, hearing and taste. The cerebellum is localized on the posterior surface of the brain stem, and is responsible for motor control, namely, control of posture and coordination of movements. It also plays a role in cognitive functions, such as attention and language [2].

The cerebrum is the largest region of the brain and it is divided into cerebral cortex, amygdala and hippocampus. Both the amygdala and the hippocampus reside in the limbic system, but they have different functions. The amygdala has a key role in fight-or-flight response and is also involved in memory processing and emotional responses, such as anxiety [3]. On the other hand, the hippocampus plays an important part in consolidation of information from short and long memory and in spatial memory, which influences navigation [1]. The cerebral cortex is the largest region of the cerebrum and plays a role in several functions, such as memory, cognition, language, awareness and attention, which are individually associated with different regions of the cortex [4].

Neurons are a functionally important cell type since they are responsible for all the communication network of the nervous system [5,6]. Carrying information is a metabolically intensive task, therefore neurons require a constant metabolite supply and structural maintenance, requirements fulfilled by glial cells [5,6]. Glial cells include oligodendrocytes, microglia and astrocytes which provide a framework that supports neurons by maintaining brain homeostasis [5,6]. Thus, glial cells have a critical role in the development and function of the nervous system and in neuropathogenesis.

1.1 Neurons

Neurons are asymmetric, extremely elongated and electrically excitable cells that are able to respond to external stimuli by generation of an action potential, which is propagated throughout the neuronal network [5,6]. The journey of the stimulus starts in sensory neurons, which have specialized receptors that are able to sense environmental cues, such as sound, touch and light and convert them into electric pulses [7]. These signals are then converted into chemical signals that are carried out to other interneurons until they reach the motor neurons, which receive and act on the information [7].

Structurally, neurons have a distinctive morphology, with the nucleus being found in the rounded part of cell (soma), and typical proteins which regulate the ion flow present across the cellular membrane [5,6]. Branching cell processes extend from the soma into opposite directions, forming the other two neuronal main structures: dendrites and axons [5].

Dendrites branch into complex dendritic spines, which all together constitute dendritic trees [5]. These allow single neuron to receive and integrate multiple signals from different cells [5,6]. Whether or not a neuron is excited into transmitting the signal depends on the sum of all of the excitatory and inhibitory inputs it receives. For the neuron to fire, the total amount of inputs needs to cause a depolarization of the membrane. If this depolarization is powerful enough that surpasses the threshold, an action potential is induced. Action potentials operate under the “all-or-none” law which means that, independently of the signal intensity, once the threshold is reached, a firing occurs and the action potential is conducted down the neurons’ axon [7].

Axons arise from the soma at a specialized area, called the axon hillock, which is where the action potential is initiated [6,7]. Morphologically, axons have long, extended arms which are essentially information transmission wires [5,6]. Axonal growth needs to be correctly regulated so that the right connections with the dendrites of adjacent neurons are made. This process, called axon guidance, is mediated by microtubules that promote the assembly of a growth cone made mostly of actin. Actin is a central part of the mechanism that controls the growth direction of the growth cone, while microtubules are involved in the extension and development of the axon [8].

One of the structural components that form the described microtubule network is beta tubulin III (βIII-tub). It is specifically expressed in neurons and it is involved not only in axon guidance, but also in axon maintenance and neurogenesis [9]. Thus, βIII-tub is commonly used as a positive marker of neuronal cells and activity in many research studies [9,10].

The majority of axon length is electrically insulated by myelin, a lipid-rich laminated membrane structure produced by oligodendrocytes [5,6]. This insulation allows the electrical transmission to be carried out faster because it forces the electrical pulse to jump between nodes of Ranvier (axonal myelin-sheath gaps). Towards its end, the axon divides itself into round-shaped swelled branches, known as axon terminals, that transmit the signal to target neurons dendrites through synapses [5–7].

1.1.1 Synapses

Electrical pulses are transmitted along the neurons until they reach the axon terminal, where the electrical signal is converted into a chemical signal in order to be communicated to target neurons or other effector cells. Synapses are structures located in-between the axon terminal of the presynaptic neuron (sender of the chemical signal) and the dendrite spine of the postsynaptic neuron (receiver of the chemical signal) where the neurotransmitter-mediated chemical signal is transmitted [6,7].

When the action potential reaches the axon terminal of the presynaptic neuron, its cellular membrane depolarizes, and opening of voltage-sensitive calcium (Ca^{2+}) membrane channels causes an influx of Ca^{2+}. This triggers the fusion of synaptic vesicles to the cellular membrane, releasing their content into the synaptic cleft, a tight space between the pre- and postsynaptic neurons [6,7]. These vesicles carry neurotransmitters, small molecules that diffuse through the synapse and bind to postsynaptic cell receptors inducing changes in its membrane potential [11].

Neurotransmitters can induce two types of signals: excitatory, which results on postsynaptic membrane depolarization and consequent opening of transmembrane sodium (Na^{+}) channels, inducing an action potential on the postsynaptic neuron; or inhibitory, which results on hyperpolarization of the postsynaptic membrane and subsequent opening of chloride or potassium (K^{+}) channels, blocking the generation of an action potential in the postsynaptic neuron [7,11]. Glutamate is the main inducer of excitatory synapses, also called glutamatergic synapses, and its action is mediated through metabotropic as well as ionotropic glutamate receptors such as N-methyl-D-aspartate (NMDA) and α-amino-3-hydroxy-5-methyl-4-isoxazole propionate (AMPA) receptors. On the other hand, the most common inhibitory synapses are the so-called GABAergic synapses which are activated by γ-aminobutyric acid (GABA) and mediated by metabotropic and ionotropic transmembrane receptors $GABA_B$ and $GABA_A$ [11,12].

After binding to the respective postsynaptic receptor, neurotransmitters are rapidly removed from synaptic cleft ceasing the transmission and allowing a new round of signals to be transmitted to the postsynaptic neuron. Neurotransmitters clearance concentration can happen through different means: neurotransmitters either diffuse away, are broken down through enzyme degradation or re-absorbed either by the presynaptic neuron or by surrounding glial cells, such as astrocytes [7,11].

Neurons form more than 10^{14} synapses that can integrate and transmit millions of impulses in split second [6]. Consequently, all this processing power requires a lot of maintenance and support, a role carried out by glial cells, namely, by astrocytes.

1.2 Astrocytes

Astrocytes are star-shaped glial cells which constitute the most abundant cell type in the CNS. They exhibit several long branched cellular processes, which originate from their soma and terminate in the formation of endfeet, and express unique intermediate filaments: vimentin and glial fibrillary acid protein (GFAP) [5,13]. GFAP is a member of intermediate filament proteins family and it has become a reliable marker for identification of astrocytes [13].

Although it has mostly structural cellular functions, *in vivo* studies showed that GFAP expression is not essential for normal astrocyte function and morphology [14,15]. In fact, in healthy CNS tissue, many mature astrocytes do not express detectable levels of GFAP and its labelling does not correlate with the total volume of an astrocyte [16,17]. Astrocytes can also be identified by the expression of other constitutive markers, such as S100β, aldehyde dehydrogenase 1 family member L1 and aquaporin 4, although these are specific for this glial cell type [18].

According to their morphology and anatomical locations, astrocytes can be classified into two main types [5]. Fibrous astrocytes present an elongated morphology, have thin and long processes and are located in white matter (Figure I.1B) [5]. By contrast, protoplasmic astrocytes are found throughout gray matter and display a radial morphology in which main processes divide into numerous and irregular finely branching processes (Figure I.1A) [5]. Fibrous astrocytes form endfeet at the surfaces of myelinated axons, namely, nodes of Ranvier, and oligodendrocytes whereas protoplasmic astrocytes display a strategic framing as their endfeet are in close contact with intraparenchymal blood vessels and their perisynaptic processes sheath most of synapses [5].

Communication between neighbour astrocytes is organized as a network, provided by gap-junction channels, which are assembled by two connexons, each as a result of the assembly of an hexameric connexin structure [19,20]. These channels are mainly composed by connexin 30 and 43 and are permeable to small molecules, such as Ca^{2+} and K^{+} ions, energy substrates, second messengers (cyclic adenosine monophosphate (cAMP), inositol-3-phosphate (IP_3)) or neurotransmitters, such as glutamate [19–21]. Thus, astrocytic activity is mostly regulated by extra- and intracellular signals.

Astrocytes are strategically located close to neurons, surrounding mostly dendrites and synaptic clefts. They strongly influence the extracellular ion concentration, affecting neurons' membrane potential, and produce a wide variety of extracellular matrix (ECM) proteins, some of which are used as guides for migrating neurons.

This characteristic organization coupled to their close interactions with neurons and other glial cells, allows astrocytes to be not only key sensors of brain homeostasis, but also essential to maintain a suitable environment for proper neuronal function.

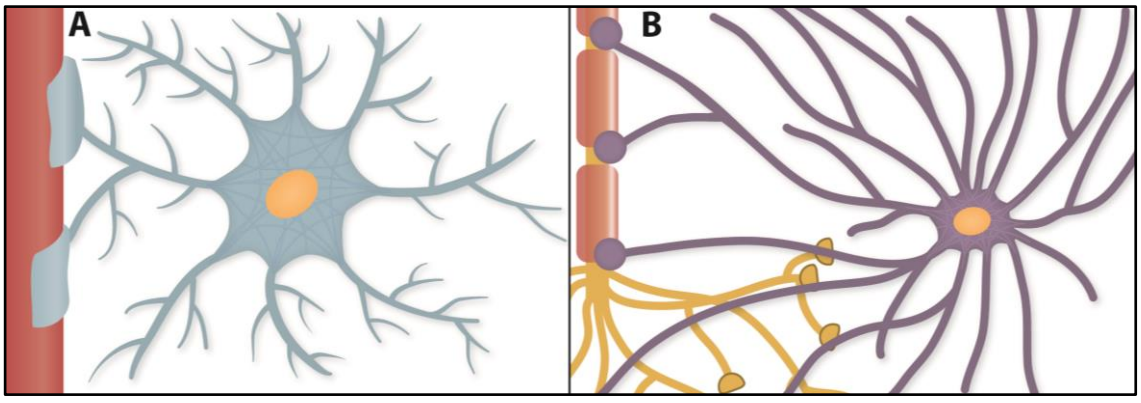

Figure I.1 – Representative diagram of the different classes of astrocytes. (A) Protoplasmic astrocytes display a radial morphology and are present in the grey matter. They present finely branching processes and their endfeet sheath synapses and directly contact with blood capillaries. (B) Fibrous astrocytes are present in the white matter and have elongated processes which endfeet contact with surfaces of myelinated axons, namely, nodes of Ranvier.

1.3 Crosstalk between astrocytes and neurons

Astrocytes are the secretory cells of the CNS. They release a wide variety of gliotransmitters that contribute to ionostasis maintenance, ECM remodelling, synaptic plasticity and transmission, metabolism regulation and blood flow [22]. Some of these signals include neurotransmitters, glucose, lactate and other metabolic substrates, trophic factors such as brain-derived growth factor (BDNF), glutathione (GSH) and other reactive oxygen species (ROS) scavengers, cytokines and chemokines [11,23–25]. Astrocytes can release the same gliotransmitter through several mechanisms.

Most of proteins are secreted by the classical pathway, which depends on the presence of an N-terminal signal peptide [26]. That signal directs trafficking to the endoplasmic reticulum (ER) and Golgi complex where proteins are glycosylated and go through post-translational modifications, respectively [26]. Then, proteins are transported by secretory vesicles to the cellular membrane and exported by exocytosis [22,26]. Exocytosis can occur via synaptic-like microvesicles (SLMVs), exosomes, dense-core vesicles (LDCV) or secreting lysosomes, which transport, respectively, glutamate and other neurotransmitters, microRNAs (miRs), peptides and adenosine triphosphate (ATP) [22,27–29]. Nonetheless, proteins lacking a signal sequence can also be secreted through the non-classical pathway, which bypasses the ER-Golgi route and diffuses metabolites through membrane ion channels, such as hemichannels and connexins [30,31].

These different secretory pathways are crucial for the transmission of neurochemical signals which play a major role not only in regulation of the entire CNS metabolism, but primarily in neuronal microenvironment, synaptic homeostasis and neural network activity.

1.3.1 Metabolic support and antioxidant defence to neurons

Twenty five percent of all our glucose and oxygen supply are used by the brain, which only represents 2% of our total body mass. The reason behind this high metabolic demand has to do with synaptic activity, since carrying and processing information received from the entire body is a metabolically demanding task [32,33]. Release of neurotransmitters and intake of ions during this process causes major shifts into ionic gradients which, in turn, require a great consumption of those metabolites in order to be re-established [32,33]. Astrocytes have been proposed to be key players in the mediation of this process, which is called neuro-metabolic coupling [21].

The unique cytoarchitectural and phenotypic characteristics of astrocytes, namely, their processes, are tailored to efficiently sense neuronal activity and quickly fulfil metabolic deficits by uptaking vital molecules from intracerebral blood vessels, metabolizing and shuttling them to neurons [21]. For instance, it has been shown that glutamate uptake triggers an increase in both glucose import and its transport through astrocytic gap junction towards active synapses [34]. Glutamate released by neurons to the synaptic cleft is imported by astrocytes together with Na^+ and hydrogen (H^+) ions through excitatory amino acid transporters (EAATs) [35,36]. This leads to an intracellular accumulation of Na^+, which, in turn, activates Na^+/K^+ ATPase pump, creating an ATP deficit and, consequently, an increase in adenosine diphosphate (ADP) and inorganic phosphate (Pi) concentrations [36]. This induces glucose uptake through glucose transporter 1 (GLUT1) and triggers glycolysis, leading to the

production of lactate which, in turn, is transported to neurons where is metabolized into pyruvate that enters tricyclic acid (TCA) cycle (Figure I.2) [36]. Also, some of the glucose enters the astrocytic TCA cycle, which leads to α-ketoglutarate synthesis that is then catalysed by glutamate dehydrogenase or an amino acid aminotransferase into glutamate [37].

Glycogen also has a role in supplying energy to the brain. Astrocytes have a high concentration of glycogen granules, which allows them to sustain neuronal function by transforming astrocytic glycogen into lactate which is then secreted and used for oxidative production of ATP by neurons [36]. Glycogenolysis is triggered under hypoglycaemia conditions or when there is intense neuronal activity that cannot be sustain only by glycolysis [38,39].

It has been shown that neuro-metabolic coupling has an important role in long-term memory formation. Amnesia and synaptic plasticity deficits were rescued by lactate but not by glucose, and inhibition of glycogenolysis prevented long-term memory formation in rat hippocampus [40]. These evidences suggest a key role of astrocyte-neuron transport of lactate in long-term memory formation.

Due to its high rate of oxidative energy metabolism and consequent increase in the production of ROS, the brain is highly vulnerable to oxidative stress. Uncontrolled ROS production is deleterious for neurons and is involved in the neurodegenerative process in diseases, such as Parkinson's (PD), Huntington's and Alzheimer's disease (AD) [41].

Astrocytes also play an important role in antioxidant defence of the brain by controlling the production of ROS [42]. They express high levels of GSH peroxidase and S-transferase (GST), catalase, superoxide dismutase and other detoxifying enzymes and release antioxidant molecules such as GSH and ascorbic acid that were shown to be used by neurons as ROS scavengers [42].

The nuclear factor erythroid 2-related factor 2 (Nrf2) pathway appears to be the main pathway responsible for the astrocyte antioxidant capability [43]. Under oxidative stress conditions, this redox-sensitive transcription factor is activated by phosphorylation, leading to its binding to the antioxidant response element (ARE) (Figure I.2) [43,44]. ARE is located in the promoter or enhancer regions of antioxidant and cytoprotective genes, such as GST isoforms, γ-glutamylcysteine synthetase (GCL) and multidrug resistance protein 1 (MRP1) [43,44]. Also, shuttling of GSH and its precursors are instrumental in the neuroprotective effect of astrocytes [45]. GSH is secreted in large amounts to the extracellular space through MRP1 transporter and then cleaved by astrocytic ectoenzyme γ-glutamyl transpeptidase into cysteine-glycine peptides [46,47]. Neurons have a poor capability to synthesize their own GSH precursor amino acids, namely, cysteine, the rate-limiting substrate of this reaction [47]. Therefore, they are highly dependent on the cleavage of astrocyte-produced cysteine-glycine by their extracellular aminopeptidase N to have free glycine and cysteine available for their own GSH synthesis through action of GCL [47,48]. It has been shown that, in astrocyte/neuronal cocultures, neuronal GSH content increases as a result of this shuttling process [49].

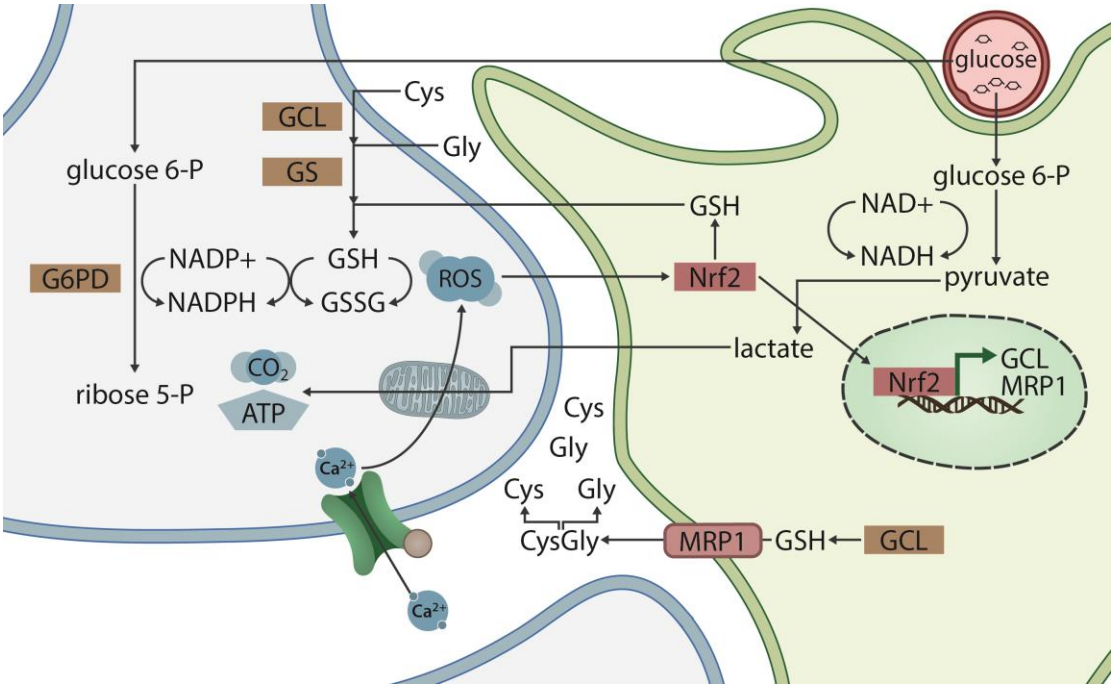

Figure I.2 – Astrocytes provide metabolic support and antioxidant defence to neurons. Glutamate import by astrocytes induces glucose uptake which, in turn, triggers glycolysis. This leads to the production of lactate is transported to neurons where is used for oxidative production of ATP or metabolized into pyruvate that enters tricyclic acid (TCA) cycle. Under oxidative stress conditions, Nrf2 is activated by phosphorylation, leading to increased levels of antioxidant and cytoprotective genes, such as GCL and MRP1. GSH is secreted to the extracellular space where it is cleaved into cysteine-glycine peptides. Neurons then import the available cysteine and glycine for their own GSH synthesis through action of GCL. In order to maintain GSH levels, GSH reductase reduces glutathione disulphide (GSSG) into GSH by using NAPDH as an electron donor. The constant NADPH supply need for maintenance of the neuronal redox state is achieved by glucose metabolism via pentose phosphate pathway.

GSH recycling is strongly coupled with glucose metabolism. In order to maintain GSH available for ROS detoxification, GSH reductase reduces glutathione disulphide (oxidized form of GSH obtained from peroxide reduction) into GSH by using nicotinamide adenine dinucleotide (NADPH) as an electron donor [50]. Consequently, it is necessary to keep a constant NADPH supply for the maintenance of the neuronal redox state, which is mainly achieved by glucose metabolism via pentose phosphate pathway (Figure I.2) [51]. It has been shown that astrocytes have higher levels of NADPH and pentose phosphate pathway activity rate than neurons [18,48]. Furthermore, astrocytes secrete ascorbic acid in response to glutamatergic activity, which is then imported by neurons inhibiting their glucose consumption and increasing lactate uptake [52]. These features also contribute to the higher antioxidant capability of astrocytes, which is strongly connected with energy metabolism derived from glutamatergic activation.

1.3.2 Synapse formation, maturation and elimination

Astrocytes are in close contact with thousands of synapses and are involved in synaptogenesis by playing a role in the formation, maturation, functionality and elimination of synapses. Development of excitatory synapses is strongly increased by the presence of astrocytes in culture or by an astrocyte-conditioned medium [53]. Several astrocyte-secreted factors have been shown to play a role in synapse formation, such as thrombospondins (TSPs), Hevin, Secreted Protein Acidic and Cysteine Rich (SPARC), Transforming Growth Factor β (TGFβ), and cholesterol.

TSPs are ECM glycoproteins involved in cell-to-cell and cell-matrix interactions. They bind to membrane receptors, growth factors and cytokines, modulating respective cellular signalling processes [54,55]. In the brain, these proteins are predominately expressed by astrocytes and are known to give a crucial contribution to astrocyte-mediated synaptogenesis [56]. There are five TSP homologs encoded by different genes which commonly form homotrimers [55]. TSP1 and TSP2 share a high degree of homology, thus they functions also overlap [55]. It was shown that TSP1 and TSP2 are essential components of synaptogenic processes, since they are able to induce ultra-structurally normal and presynaptically active synapses. However, these synapses are postsynaptically silent due to the lack of AMPA receptors [56–58]. *In vivo*, TSP1 and TSP2 double knockout mice show a significant decrease in the synapse number, which is in agreement with *in vitro* studies [56]. Furthermore, it was shown that reduced levels of astrocytic TSP1 are closely related with number and morphology of dendritic spines [59].

Synaptogenic effects of TSPs on neurons are mediated by $\alpha_2\delta$-1 subunit of voltage-gated Ca^{2+} channels and activate the Ca^{2+}-dependent signalling pathway (Figure I.3A) [60]. TSPs binding to this receptor is mediated by the interaction of type 2 epidermal growth factor-like repeats, located at their highly-conserved carboxyl region, with the $\alpha_2\delta$-1 subunit [60]. *In vitro* studies show that the drug Gabapentin, a known ligand of $\alpha_2\delta$-1, inhibits synapse formation by blocking TSP binding to this neuronal receptor [61]. Also, TSP1 was shown to interact with postsynaptic adhesion protein neuroligin 1 (NL1), resulting in an increase of speed of synapse formation [58].

Hevin and SPARC are astrocyte-secreted factors that control synapse formation in an antagonistic way [62]. Hevin potentiates synapse maturation by forming a protein complex with both presynaptic neurexin-1alpha (NRX-1α) and postsynaptic NL1B [63]. NRX-1α forms a bridge with astrocytes-secreted Hevin which, in turn, connects to NL1B (Figure I.3B) [63]. SPARC domains are very similar to Hevin's, thus, its inhibitory effect is mediated by competing with Hevin for binding with those pre and postsynaptic elements and determining the levels of AMPA receptors in the synaptic terminal [63,64] Even though their domain structures are very similar, Hevin and SPARC have different N-terminal domains, which suggests that SPARC inhibitory function of Hevin-induced synapse formation can be mediated by those [63]. It has been shown that SPARC-null mice have an increased synaptic network, while Hevin-null mice have fewer synaptic connections [62,63].

TGFβ superfamily consists of three different cytokine isoforms (TGFβ1, TGFβ2 and TGFβ3) that are secreted by glial cells, such as astrocytes, as precursor proteins [65]. When in the extracellular space, they require proteolytic activity to be activated. Several studies have identified TSP1 as the main activator of TGFβ1 [66,67]. TGFβ1, has been strongly implicated in synapse formation [68–70]. Its secretion by astrocytes leads to increased levels of amino acid D-serine, a co-agonist of the NMDA receptor, which potentiates an increase in the number of cortical excitatory synapses (Figure I.3C) [69]. It has been shown that decrease of D-serine levels leads to a depletion of the TGFβ1-induced synaptogenesis in astrocyte-conditioned medium [69]. Also, astrocyte-secreted TGFβ1 increases the formation of inhibitory synapses by inducing synaptic adhesion protein NL2 cluster formation and translocation to inhibitory postsynaptic terminal sites [70]. This effect is regulated by not only glutamatergic synaptic activity, but also by activation of Ca^{2+}/calmodulin (CaM)-dependent protein kinase II (CaMKII) pathway [70].

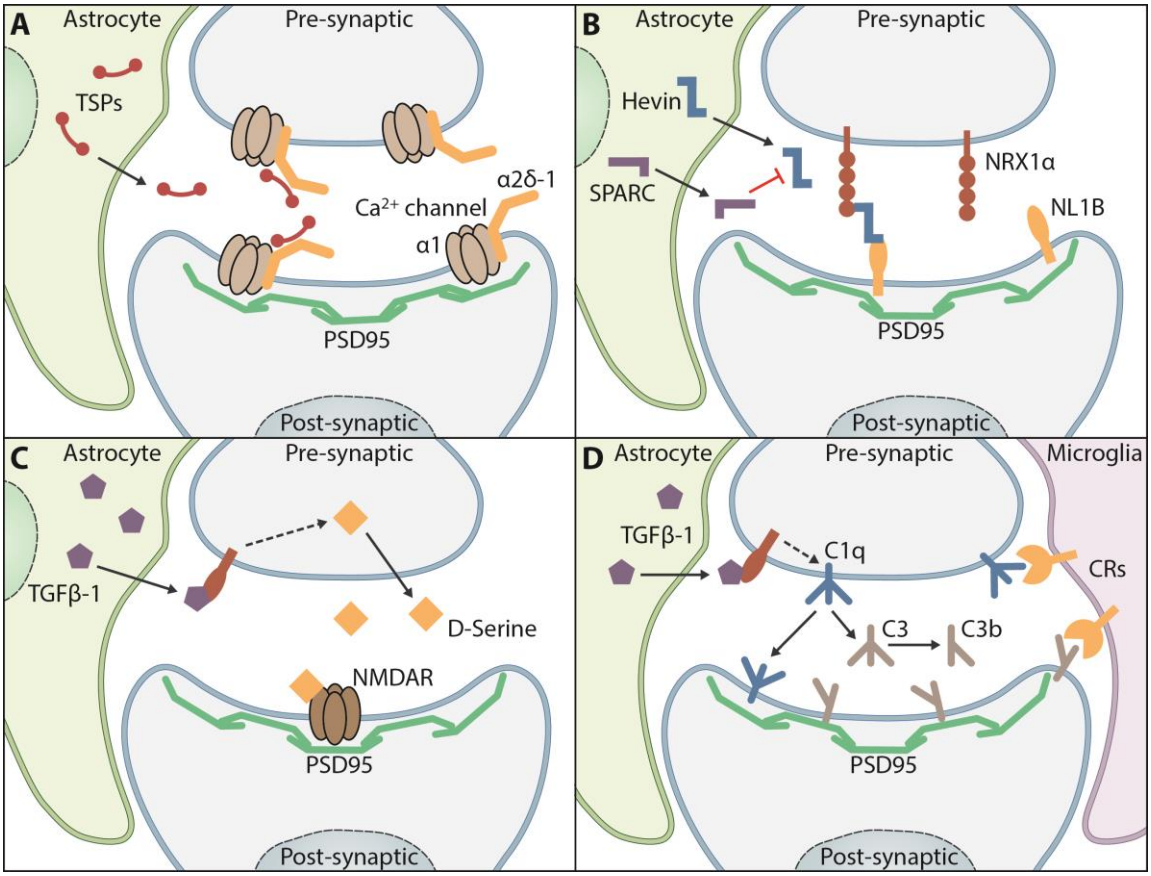

Figure I.3 – Astrocytes regulate synaptogenesis and synapse elimination. (A) Synaptogenic effects of TSPs on neurons are mediated by their binding to α2δ-1 subunit of voltage-gated Ca2+ channels and consequent activation of Ca^{2+}-dependent signalling pathway. (B) Hevin potentiates synapse maturation by forming a protein complex with presynaptic NRX-1α which, in turn, forms a bridge that connects it to the postsynaptic NL1B. SPARC inhibitory effect is mediated by competing with Hevin for binding with these pre and postsynaptic elements. (C) TGFβ1 secretion by astrocytes leads to increased levels of amino acid D-serine, a co-agonist of the NMDA receptor, which potentiates an increase in the number of cortical excitatory synapses. (D) TGFβ released by astrocytes upregulates the expression of C1q, which is then released to the extracellular space where it binds directly to neurons or to weaker synapses. C1q binding induces C3 peptide clavation into C3a and C3b. C3a triggers inflammation while C3b, as C1q, binds to weaker synapses tagging them for elimination by microglia.

Mature synapses development requires a large quantity of cholesterol. However, at the adult stage, neurons start specializing on electrical conduction and drastically reduce the energy-consuming task of cholesterol biosynthesis [71]. Therefore, they rely on astrocytes for production and delivery of cholesterol (Figure I.4) [72]. When cholesterol levels are low, the sterol regulatory element binding protein (SREBP) family, namely SREBP2, activates the transcription of genes involved in the synthesis and uptake of cholesterol, leading to an increase in its levels [73]. Cholesterol efflux is mediated by apolipoprotein E (ApoE)-containing lipoproteins that are secreted through ATP-binding cassette (ABC) transporters, namely, ABCA1 [74,75]. Then, neurons uptake cholesterol via low-density lipoprotein receptor mediated endocytosis [76]. Specific loss of ABCA1 in glial cells was shown to reduced brain cholesterol and to decreased synapse number while deficient cholesterol internalization of ApoE-containing lipoproteins by neurons reduces the formation of efficient synapses [77,78]. Also, cholesterol was shown to be essential for synaptogenesis by promoting differentiation of dendrites' presynaptic terminals through induction of cholesterol metabolism and dendrite development related genes [79,80].

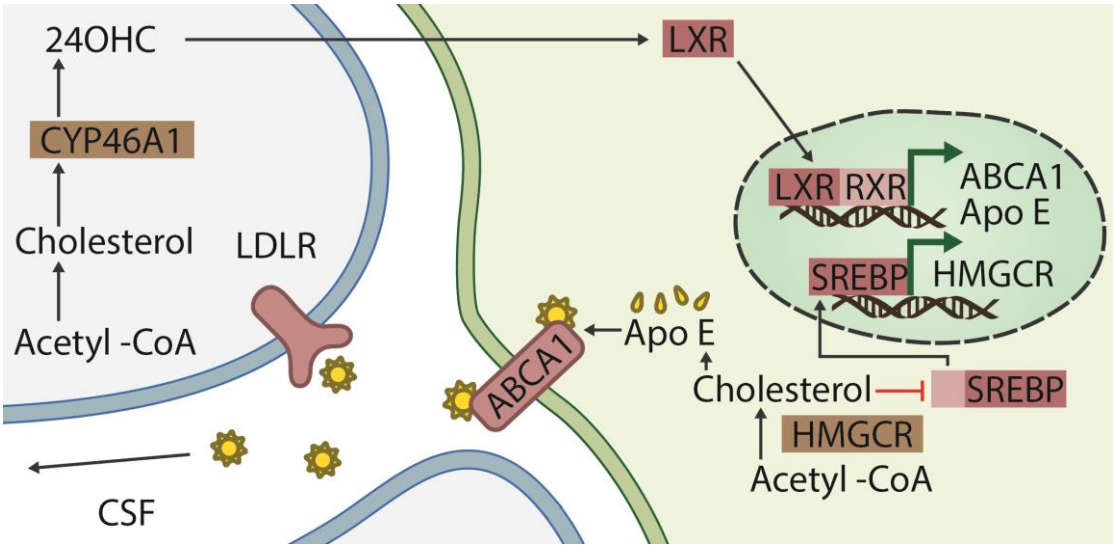

Figure I.4 – Cholesterol shuttle between astrocytes and neurons. In the adult brain, cholesterol is mainly produced by astrocytes, which secreted it through ABCA1 in ApoE-containing lipoproteins. Neurons internalize these particles by endocytosis through low-density lipoprotein receptor and cholesterol is distributed inside the cell. Excess cholesterol is converted by the neuronal-specific CYP46A1 into 24OHC, which is also a signalling molecule that induces LXR activation and, consequently, cholesterol efflux. In low cholesterol conditions, SREBPs activate the transcription of HMGCR enzyme convert more acetyl-CoA into cholesterol.

Development and refinement of neuronal networks depends on a dynamic process called synaptic remodelling, which consists in the elimination of unstable neuronal connections [81]. Several results suggest that astrocytes-secreted molecules, play a direct role in this process, either by inducing the integrin-dependent pathway or by directly eliminating synapses. This last mechanism is mediated not only by protease release, but mostly by the complement system [82,83]. In CNS, TGFβ released by astrocytes upregulates the expression of classical complement cascade member C1q in neurons (Figure I.3D) [82]. This component is then released to the extracellular space, binding either directly to neurons or to weaker synapses [82,83]. C1q binding induces its activation, leading to the formation of C3 peptide, which is then cleaved into C3a and C3b [83,84]. C3a triggers inflammation while C3b, like C1q, binds to weaker synapses tagging them for elimination by microglia [83,84].

1.3.2.1 Shuttling and recycling neurotransmitters

Besides contribution to metabolic support, antioxidant defence and synapse modulation, astrocytes play a key role in shuttling neurotransmitters, namely, glutamate, which is essential for proper neuronal activity [85]. Similarly to cholesterol, glutamate does not cross the blood–brain barrier and neurons cannot synthetize it *de novo* since they do not express pyruvate carboxylase [86]. Therefore, neurons depend on astrocytes for glutamate recycling and shuttling.

For this, astrocytes have an increased expression of two Na^+-dependent glutamate transporters: the EAAT1 and EAAT2 [35]. These high-affinity transporters uptake glutamate released to the synaptic cleft by neurons to astrocytes [87]. There, glutamine synthase transaminates glutamate to glutamine, which is then exported to neurons through synaptic vesicles, re-establishing neuronal glutamate levels [87,88]. Glutamate clearance from the synaptic cleft prevents crosstalk between synapses, limits glutamate action on pre- and postsynaptic receptors but, mostly, it protects neurons against excitotoxicity [89–91]. Namely, EAAT2 knockout mice show an increase in the levels of extracellular glutamate and, also, early neuronal death [91,92].

Astrocytic recycling and uptake of glutamate also plays an important role in the regulation of GABAergic synaptic activity by being the precursor for GABA synthesis as well as modulating the synaptic GABA content via Na^+-coupled GABA transporters (GAT) GAT1 and GAT3 [87,93]. These high-affinity GABA transporters can not only uptake GABA to astrocytes, but also to export it back to the extracellular space [94]. Astrocyte processes located near synaptic sites express GAT1, which is involved in the termination of GABA signalling at the synaptic cleft, whereas GAT3 is expressed at distal sites and regulates the action of GABA on the presynaptic GABAergic nerve endings [95].

Thus, astrocytes, by buffering and recycling glutamate and GABA, the two most important neurotransmitters, maintain brain homeostasis and regulate neuronal activity.

1.3.2.2 Tripartite synapse and synaptic transmission

Astrocytes sense neuronal activity via neurotransmitter-triggered changes in intracellular Ca^{2+} [96,97]. There are several neurotransmitter receptors being expressed at the astrocytic surface and most of them are associated with G-protein coupled receptors (GPCRs) that, when stimulated, induce phospholipase C (PLC) activity and formation of IP_3 [98]. This results in increased Ca^{2+} levels, due to its release from the endoplasmic reticulum and other intracellular IP_3-sensitive Ca^{2+} stores. Elevated Ca^{2+} concentration triggers the transmission of intracellular Ca^{2+} waves which are involved in the release of gliotransmitters, such as glutamate, to the synaptic cleft through excitatory amino acids carrier [96,97]. This bidirectional communication between astrocytes and two neurons is called a tripartite synapse (Figure I.5) [99].

Specific synaptic terminals from different brain regions induce characteristic Ca^{2+}-mediated responses. In hippocampal alveus, Ca^{2+} increases due to acetylcholine stimuli and not glutamate [100]. However, it was shown that these astrocytes can respond to glutamate, but only if released by Schaffer collateral synaptic terminals [101]. Also, *in vivo* studies show that astrocytes from separate cortical layers have different responses to glutamate inputs [102].

These specific responses of astrocytes to different synaptic terminals activity indicate that astrocytes can also modulate the transmission of synaptic information [101].

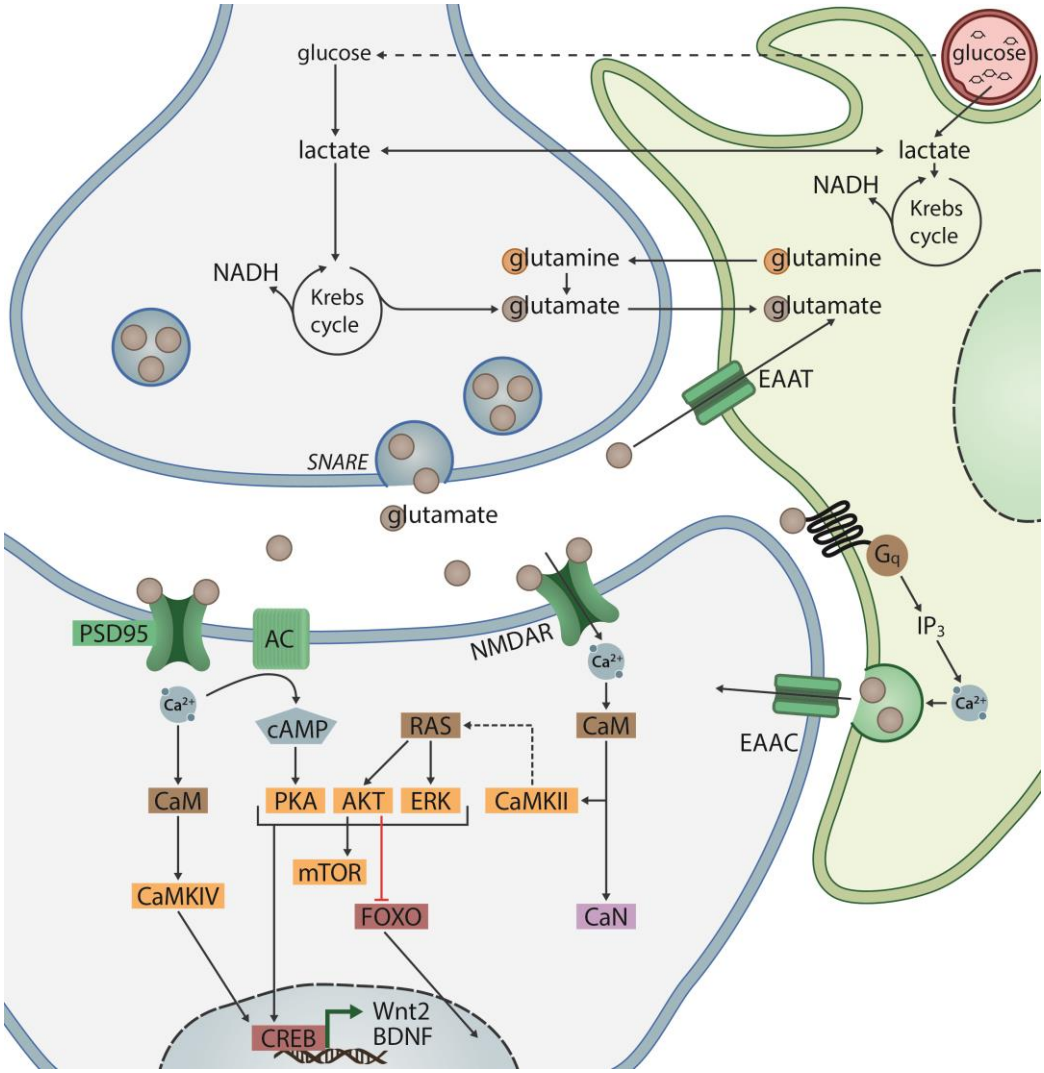

Figure I.5 – Tripartite synapse and crosstalk between neurons and astrocytes. In the presynaptic neuron, glutamine is converted to glutamate by glutaminase and packaged into synaptic vesicles. SNARE complex proteins mediate the fusion of vesicles with the presynaptic membrane. Following release into the extracellular space, glutamate binds to NDMAR inducing a Ca^{2+} influx, which promotes the assembly CaM complex that activates CaMKII, CaMKIV and calcineurin (CaN). CaMKII stimulates the small GTPase Ras activation and, consequently, induces both ERK/MAPK and PI3K/Akt pathway, resulting in CREB recruitment to the promoter of synaptic plasticity-related genes, such as BDNF and Wnt2. CaMKIV directly phosphorylates and activates CREB while Ca^{2+}-sensitive adenylyl cyclase leads to PKA-mediated activation of CREB. Besides CREB activation, PI3K/Akt pathway also induces mTOR pathway and FOXO translocation to cytoplasm, resulting in transcription of cell growth and proliferation genes. Glutamate released by the presynaptic neuron is cleared from the synaptic cleft through EAATs on neighbouring astrocytes. Glutamate is then converted to glutamine by glutamine synthetase within the astrocyte before being transported to presynaptic neurons, thereby completing the glutamate-glutamine cycle. Most of neurotransmitters receptors are associated with G proteins that, when stimulated, induce formation of IP3, which, in turn, increased Ca^{2+} levels. Elevated Ca^{2+} concentration triggers the release of gliotransmitters, such as glutamate, to the synaptic cleft where is then imported back to neurons by excitatory amino acids carrier. Besides shuttling glutamine, astrocytes also shuttle lactate and glucose to neurons as part of their role as supportive metabolic role.

Gliotransmitters are neuroactive molecules that can act on different neuronal receptors, both at the pre- and postsynaptic levels, in order to tone neuronal activity and synaptic plasticity [11]. Excitatory and inhibitory amino acids, such as glutamate, GABA and D-serine, ATP, neuropeptides, trophic factors, such as BDNF and prostaglandins, cytokines, chemokines and growth factors constitute the main bulk of this large group of astrocyte-secreted molecules [11].

Ca^{2+}-dependent and independent mechanisms of gliotransmitters release have been extensively studied in the recent years. Several Ca^{2+}-independent mechanisms have been described, including secretion by hemichannels, volume sensitive and ATP-gated ion channels and glutamate-mediated secretion, such as cystine–glutamate antiporter [30,31,103,104]. These mechanisms are mostly involved in pathological conditions, while Ca^{2+}-dependent processes occur under physiological conditions and induce exocytic release through a sharply regulated manner [27,29].

Exocytic vesicles and lysosomes secrete their content to the extracellular space by fusing with the cellular membrane through the assembly of a soluble N-ethylmaleimide-sensitive fusion attachment receptor (SNARE) complex (Figure I.5) [105]. In astrocytes, the SNARE complex is formed by v-SNAREs, such as synaptobrevin II and other vesicular associated membrane proteins, and by t-SNAREs, such as syntaxins and SNAP23, which are associated, respectively, with the vesicular membrane and with the cellular membrane [27,106]. When Ca^{2+} concentration increases, it induces SNARE-associated protein synaptotagmin 4 to bind negatively charged phospholipids, which, in turn, increase its affinity to syntaxin [107]. This leads to the formation of the ternary SNARE complex which is assembled by the interaction of v-SNARE and t-SNARE proteins, facilitating the fusion of both vesicular and cellular membranes [105]. Inactivation of synaptobrevin II by tetanus neurotoxin, a specific exocytosis inhibitor, stops glutamate release in astrocytes and transgenic mice with decreased SNARE activity showed changes in behaviour, synaptic transmission and maturation of neurons [108,109].

SLMVs, LDCVs and lysosomes are the three major types of Ca^{2+}-dependent secretory organelles released by astrocytes [27–29]. SLMVs are morphologically very similar to synaptic vesicles and transport mostly neuro and gliotransmitters, like glutamate and D-serine, through specific transport proteins, such as vesicular glutamate transporters [110]. LDCVs expression is regulated by neuron-restrictive silencer factor, a transcriptional factor involved in nerve cells differentiation. These vesicles are known to transport neuropeptides in a non-SNARE-mediated pathway [28,111]. These two findings suggest that LDCVs content might be involved in neuronal network development processes and that astrocytes might have two differentially regulated secretory pathways involved in synaptic transmission. Secretory lysosomes are known to be the main storage compartment for cytokines and play a key role in myelination since they are responsible for myelin secretion [112,113]. Also, it was shown that, in astrocytes, Ca^{2+} elevations lead to ATP release through secretory lysosomes and that blocking ATP release prevents Ca^{2+}-induced astrocyte-astrocyte communication [114].

Gliotransmitters have been described to have a role in different neuronal processes, such as synaptic plasticity, increasing neuronal excitability and network. However, astrocytic glutamate plays one of the most important roles in regulating synaptic transmission. Glutamate released by astrocytes interacts with Glutamate Ionotropic Receptor Type Subunit 2B (GRIN2B)-containing NMDA receptors, activating them which, in turn, induces slow

inward currents that depolarize and trigger neurons to fire [115]. Interestingly, NMDA receptors open only after membrane depolarization, so glutamate cannot, in theory, activate them. Thus, either these receptors targeted by astrocytic glutamate are more sensitive to depolarization or they are co-release with other depolarizing agents, such as D-serine, which facilitates the opening of the transmembrane channel [116,117]. Also, glutamate was shown to modulate excitatory synaptic flows through metabotropic glutamate receptors, which are divided into three groups. Activation of group I enhances the frequency of spontaneous and evoked excitatory synaptic currents while activation of groups II and III reduces inhibitory synaptic transmission [118,119]. Thus, a single gliotransmitter can exert multiple effects depending on the sites of action and the activated receptor subtypes.

2 Peroxisome proliferator-activated receptor-γ coactivator-1α

CNS homeostasis is regulated by changes in protein levels that are primarily induced by transcription modifications. Gene transcription is a highly regulated process that is divided into multiple steps and involves several different protein complexes. Upon activation, transcription factors bind to specific DNA sequences in the promoter or enhancer regions of their target genes, most commonly, at the 5' region to the transcription start site [120]. Coactivators are proteins recruited to gene promoters through direct interaction with transcription factors docked to specific DNA sequences [120]. Consequently, coactivators facilitate the formation of multiprotein complexes that facilitate opening of the chromatin structure and initiation of transcription itself. These multiprotein complexes include protein with methylation, phosphorylation or acetyltransferase activity that modify histones, and unwind and remodel chromatin in an ATP-dependent manner [120].

Proteins of the peroxisome proliferator-activated receptor γ (PPARγ) coactivator 1 (PGC-1) family of transcriptional coactivators are key regulators of energy metabolism-related genes and are expressed in high metabolic demanding tissues, such as brown adipose tissue (BAT), liver and brain [121–123]. PGC-1α, PGC-1β and PGC-1-related coactivator (PRC) are the three founding members of PGC-1 family [121,124,125].

The PGC-1 family has a high similarity in amino acid sequence and, consequently, core functions, especially the ability to regulate gene expression networks connected to mitochondrial biogenesis and oxidative metabolism [126]. For instance, both PGC-1α and PGC-1β increase consequently, mitochondrial respiration, although PGC-1β has a less prominent effect than PGC-1α [126]. Also, PRC and PGC-1α share the coactivation of specific transcription factors involved in expression of mitochondrial genes [125].

Although the three coactivators have partly overlapping functions, they also display functional differences depending mostly on the physiological context in which each of them act PGC-1α and PGC-1β expression seems to be more restricted to high oxidative capacity tissues when compared with PRC, which is expressed more ubiquitously [125]. PGC-1α regulates adaptive thermogenesis in BAT by coactivating several nuclear hormone receptors that are involved in the transcriptional regulation of the uncoupling protein (UCP) 1 gene, while in implicated in the skeletal muscle is involved in fiber-type switching and modulates

genes involved in glucose uptake [121,127,128]. In liver, PGC-1α directly regulates gluconeogenesis by inducing glucose-6-phosphatase and phosphoenolpyruvate carboxykinase pathways as well as increasing TCA cycle turnover, as a response to glucagon [123,129]. Unlike PGC-1α, PGC-1β does not regulate gluconeogenesis in liver, but it has a major effect in lipogenesis and lipoprotein transport [130,131]. Since PGC-1α is the most well studied member of this family and also the most relevant for our study, it will be discussed in more detail throughout this section.

2.1 Structure and mechanism of action

PGC-1 coactivators exert their modulatory function by binding to specific nuclear receptors. Indeed, one of the currently accepted model for PGC-1 mechanism of action states that they act as docking platforms that promote the interaction between DNA-bound transcription factors and enzymatically-active cofactors, which, in turn, activate gene transcription [132]

As previously mentioned, proteins from PGC-1 family have a high structural homology. They share several well-conversed domains and have very similar N- and C-terminal amino acid sequences. The amino-terminus contains highly conserved transcriptional activation and repression domains which include several major nuclear hormone receptor-interacting motifs [132]. Unlike other coactivators, PGC-1 proteins do not have any intrinsic histone acetyltransferase activity [133]. Therefore, the amino-terminal end also functions as surface for recruitment of histone acetyltransferase proteins, such as cAMP response element binding (CREB) protein binding protein (CBP)/p300 [133]. It was shown that the increase in the transcriptional activity of PPARγ and nuclear respiratory factor 1 (NRF1) nuclear receptors is due to the recruitment of histone acetyltransferases CBP/p300 and steroid receptor coactivator 1 (SRC1) to the assembly complex by PGC-1α [133].

The same study has also shown that PGC-1α exists into three different conformational stages. When not bound to any transcription factor, PGC-1α has reduced capability to interact with any histone acetyltransferases. Upon docking to a transcription factor, PGC-1α changes conformation to a more permissive state, forming a complex with CBP/p300 and SRC-1, that in turn induces gene expression [133]. Although the amino and carboxylic-terminals of PGC-1 contain well-conserved domains, the remaining unstructured region has no apparent function. Therefore, it is suggested that PGC-1 conformational changes might occur within these domains.

The C-terminus presents the highest similarity between all the three members of the PGC-1 family, containing several well conserved motifs within this region [124,134]. One of them has been identified as a binding site for the coactivator host cell factor 1, which is involved in the regulation of cell cycle[124]. The carboxy terminus also contains serine/arginine-rich domain (RS) and a RNA recognition motif (RRM) [124]. This domain is typically involved in RNA binding and splicing, suggesting that PGC-1 family may play a role in RNA processing [134]. In fact, *in vitro* studies have already shown that PGC-1α regulates gene expression by participating in mRNA processing [134].

After initiation of transcription, it is suggested that PGC-1α also interacts with elongation factors and RNA polymerase II, affecting RNA elongation rate [134,135]. Furthermore,

PGC-1α targets RNA processing of the transcribed genes, namely, by modulating mRNA capping, alternative mRNA splicing and mRNA stability [134–136]. Thus, PGC-1α is considered to be a versatile and dynamic coactivator, which plays a crucial role in regulating several aspects of gene expression.

2.2 Regulatory properties

As seen before, PGC-1α carries out different metabolic functions according to the tissue where it is being expressed. Thus, PGC-1α expression needs to be finely tuned to effectively respond to increased energy demands and fulfil cellular energy needs. Its activity is controlled through diverse transcriptional and posttranslational mechanisms.

PGC-1α responds differently to several signalling pathways according to the tissue where it is being induced. AMP-activated protein kinase (AMPK) is a key sensor of cellular energetic demands and is activated by high ratio of AMP/ATP, triggering a wide range of metabolic pathways in order to increase ATP concentration within the cell. One way to boost production of ATP is through increasing mitochondrial function and biogenesis. In muscle, PGC-1α is very sensible to AMPK activation [137]. Expectedly, activation of AMPK signalling increases PGC-1α transcription levels, which, in turn, induces mitochondrial biogenesis activation [137,138].

In the liver, PGC-1α is induced by fasting through p38 mitogen-activated protein kinase (MAPK) pathway [139]. p38 is activated by cAMP signalling and activation of protein kinase A (PKA), as response to the pancreatic hormone glucagon (Figure I.7) [139]. PKA activation promotes CREB binding to PGC-1α promoter, which, in turn, increases its expression and consequently gluconeogenesis [139]. p38 also increases PGC-1α transcription in BAT as a response to cold stimuli sensed by β3-adrenergic receptors through activating transcription factor 2 (ATF2) [121,140].

Calcium signalling is also involved in the regulation of PGC-1α expression through the activation of CaMKIV and calcineurin (CaN) [141]. CaMKIV activates CREB by phosphorylation, inducing its binding to PGC-1α promoter, while CaN interacts with myocyte enhancer factor 2 (MEF2) which results in increased PGC-1α transcription (Figure I.6) [141,142]. *In vivo* imaging shows increased CREB/MEF2-dependent PGC-1α transcript expression upon nerve stimulation in muscle [143]. Remarkably, MEF2 is a known target of PGC-1α action, which creates feed forward loop where PGC-1α increases its own expression [142].

Posttranslational mechanisms, such as phosphorylation and acetylation, are crucial players in regulating PGC-1α protein levels and activity. AMPK and p38 MAPK, not only influence PGC-1α expression, but also are the most well-known protein kinases that control PGC-1α phosphorylation. Besides inducing PGC-1α transcription, AMPK enhances its co-transcriptional activity through phosphorylation of its threonine-177 and serine-538 residues (Figure I.6) [137]. p38 MAPK activates PGC-1α through phosphorylation of specific threonine and serine residues upon cytokine stimulation [144]. This phosphorylation increases PGC-1α short half-time life by improving its stability and also disrupts PGC-1α interaction with co-repressors, resulting in an overall enhancement of its transcriptional activity [144,145].

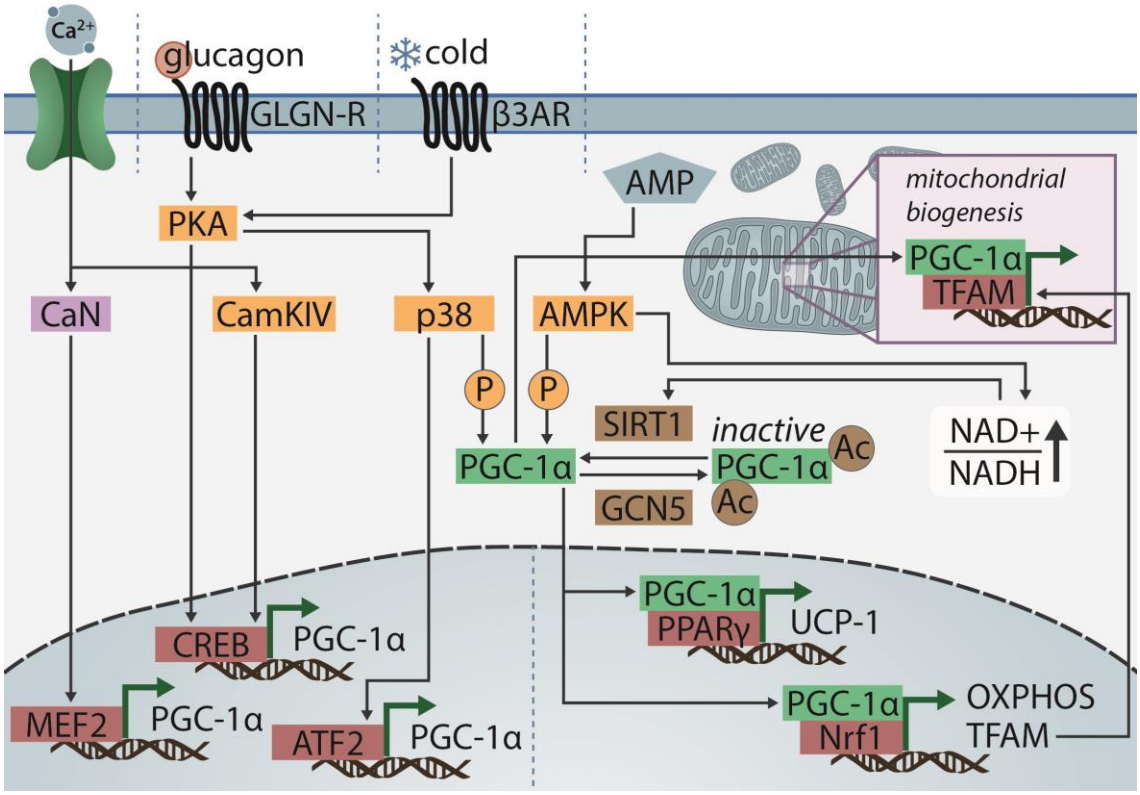

Figure I.6 – Regulation of PGC-1α expression by transcription mechanisms and posttranslational modifications. PGC-1α transcription is induced by several transcription factors, which are modulated by different signalling pathways. Ca^{2+} signalling induces CaMKIV and CaN action which, respectively, promote CREB and MEF2-mediated PGC-1α transcription. PKA is activated both through glucagon and cold stimuli, leading to CREB and ATF2 binding, respectively, to PGC-1α promoter, although ATF2 activation is mediated through p38 MAPK. p38 MAPK and AMPK can also directly activate PGC-1α through phosphorylation. In low energy situations, AMPK increase NAD^+ amounts, enhancing Sirt1 activity and deacetylation of PGC-1α. Upon activation, PGC-1α interacts with several transcription factors, such as PPARγ and NRF1, which induce the transcription of genes related with energy metabolism, such as uncoupling protein 1, and genes related with oxidative phosphorylation (OXPHOS) and mitochondrial transcription factors, such as Tfam. Furthermore, PGC-1α directly interacts with Tfam within the mitochondria, resulting into augmented mitochondrial biogenesis. When energy is abundant in the cell, GCN5 acetylates and inhibits PGC-1α.

PGC-1α is highly susceptible to transient regulation by deacetylation since the whole protein sequence contains several acetylated residues [146]. Silence information regulator 2-like 1 (Sirt1) activity depends on NAD^+/NADH ratio and uses NAD^+ as a substrate. This connects this histone deacetylase to the regulation of cell energy metabolism [147]. AMPK increases NAD^+ concentration by activating fatty acid oxidation, thereby enhancing Sirt1 activity [148]. Thus, AMPK not only induces PGC-1α expression and enhances its stability through phosphorylation, but also promotes its deacetylation by increasing Sirt1 activity [148]. Sirt1-mediated deacetylation activates PGC-1α and increases the coactivation of its target genes such as Tfam [149]. Interesting, prior AMPK phosphorylation of PGC-1α is necessary for subsequent Sirt1 deacetylation, suggesting a highly specific mechanism of posttranslational regulation [148].

Histone deacetylase GCN5 functions in an antagonistic way to Sirt1 since it acetylates PGC-1α and PGC-1β *in vitro* and *in vivo*, decreasing their activity [150,151]. Calorie excess triggers GCN5 expression and reduces Sirt1 levels which enhances GCN5-mediated acetylation of PGC-1α, reducing its activity [152]. On the other hand, GCN5 is down-regulated

and Sirt1 is increased under calorie restriction conditions, promoting PGC-1α deacetylation and hence its activity (Figure I.6) [152]. Moreover, it is thought that GCN5 dependent acetylation of PGC-1α can also be regulated by levels of acetyl-CoA within the nucleus [153].

As seen, PGC-1α activation and biological activity is extensively regulated by several transcription mechanisms as well as posttranslational modifications. To make the matters even more complicated, PGC-1α gene codes for different isoforms regulated by multiple promoters and alternative splicing [154].

2.3 Isoform structure and function

PGC-1α protein structure and function have been intensively studied in different physiological conditions, ranging from energy metabolism to muscle physiology and neurodegenerative diseases. However, after PGC-1α gene was first identified, other transcripts have been reported to be induced under specific stimuli, such as cold exposure in BAT and resistance training in skeletal muscle [154].

Two distinct promoters drive PGC-1α gene transcription [155,156]. The proximal promoter is located at 5' of exon 1, while the alternative promoter is located at 14kb upstream. PGC-1α promoters are differentially activated depending on tissue expression and specific stimuli [157]. Transcripts encoded by the alternative promoter give rise to a novel exon 1 sequence (exon 1b), which has a short and a long variant of 12 and 3 amino acids, respectively [155,158].

PGC-1α alternative promoter activation in mice, coupled with alternative splicing, gives rise to three core variants with unique structural characteristics, named PGC-1α2, PGC-1α3 and PGC-1α4 [154]. To be consistent with the isoform nomenclature, the canonical PGC-1α was renamed to PGC-1α1. All isoforms share exon 2 with PGC-1α1, however, PGC-1α2 and 4 contain the long splicing variant of exon 1b while PGC-1α3 contains the short one (exon 1b') [154].

PGC-1α2 and 3 have very similar structural features and length, 379 and 370 amino acids respectively [154]. As mentioned before, both isoforms have distinct first exons, but their remaining intron/exon structure is identical (Figure I.7) [154]. Nonetheless, their conformation notably differs from the other isoforms. Due to several splicing events, PGC-1α2 and 3 exons 4–6 and 9–13 are eliminated and a new stop codon originated from splicing of exon 8 to the 3' UTR is inserted [154]. Thus, all the previously described PGC-1α1 C-terminal motifs are missing in these two proteins, together with parts of both activation and repression domains.

PGC-1α4, on the other hand, contains the full activation domain present in PGC-1α1 but both the repression domain and the C-terminal end are missing (Figure I.7) [154]. These structural changes are mediated by downstream alternative splicing events, which lead to the introduction of a premature stop codon at amino acid 266 and to the insertion of a new exon 6, making PGC-1α4 the smallest isoform encoded by the alternative promoter [154]. Apparently, PGC-1α4 sequence modifications alter its half-time life and, consequently, its degradation rate, increasing its stability when compared to PGC-1α1 [159].

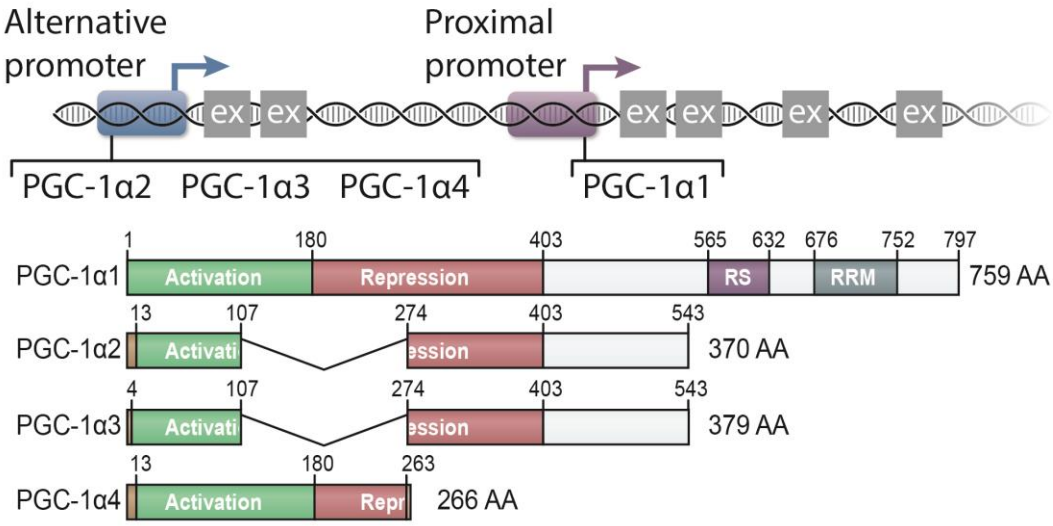

Figure I.7 – PGC-1α proximal and alternative promoter and isoform structure. Schematic representation of PGC-1α different promoters, respective encoded isoforms, and domain conservation between the different PGC-1α variants. PGC-1α1 is expressed under the control of the proximal promoter (in purple) while the remaining PGC-1α isoforms are expressed from the alternative promoter (in blue). Activation and repression motifs located at N termini mediate PGC-1α interaction with transcription factors and other coactivator complexes. The distinct N termini of the different isoforms are represented in brown. The RS and RRM domains are involved in RNA splicing.

Regarding the biological function of PGC-1α isoforms, PGC-1α4 was shown to induce muscle hypertrophy by promoting IGF-1 expression and reducing levels of muscle growth repressor, myostatin [154]. Furthermore, PGC-1α4 splicing patterns and gene regulation cluster very well with PGC-1α1 targets as opposed to PGC-1α2 and 3 [159]. This shows that, unlike what was initially thought, the preservation of the N-terminal activation domain plays a greater role in setting gene programs and splicing events than the RNA recognition motif present at the C-terminal of PGC-1α1 [159].

Furthermore, PGC-1α2 and 3 lack part of activation domain sequence that interacts with PPAR [160]. This might explain the differences found in regulation of gene networks when compared to PGC-1α1 and also the observed contra-regulation most of PGC-1α1 target genes [159]. PGC-1α2 and 3 do not modulate mitochondrial biogenesis, however they do increase pyruvate mitochondrial respiration [159]. Thus, apart from affecting metabolism through transcription, PGC-1α2 and 3 might also modulate cellular homeostasis by inducing splicing events such as in pyruvate metabolism related genes [159]. Also, it was shown that in the muscle both PGC-1α2 and 3 reduce the expression of proliferation-related genes and that PGC-1α2 exclusively regulates cholesterol synthesis metabolism while PGC-1α3 plays a role in cell cycle control, proliferation and ECM remodelling [159].

Besides the alternative promoter other transcription starting sites for PGC-1α human gene were identified. It was observed that a promoter encoding for brain-specific isoforms lies 587kb upstream of exon 2 [161]. Interestingly, this promoter is located in the genomic region associated to onset of Huntington's disease, a neurodegenerative disease where normal PGC-1α function seems to be impaired. Transcripts produced from this promoter contain specific exons encoded by the brain promoter (B1–5) followed by the canonical exons 2–13. Studies in a neuroblastoma cell line show that these transcripts have higher expression levels than PGC-1α1 [161].

2.4 PGC-1α role in brain development

During CNS development, emerging neurons grow axons and dendrites in order to form synapses, and consequently functional neuronal circuits. Mitochondria are not only the major energetic supplier for this process, but also play a role in structuring the architecture of neuronal cytoskeleton. PGC-1α, as a major regulator of cellular adaptions to changes in energy requirements and other key metabolic pathways, such as oxidative phosphorylation (OXPHOS), is thought to play a putative role in CNS correct functioning.

In fact, expression of several neurofilaments and Na^{2+} pumps α2 subunit is reduced in PGC-1α null brain [122]. Furthermore, complete deletion of PGC-1α gene in the brain induces hyperactivity and axon degeneration in the striatum [122]. Likewise, it was shown that neuronal dendritic spines formation and maintenance are regulated by PGC-1α by BDNF–cAMP axis [162]. PGC-1α also modulates the magnitude of neurotransmitter release through regulation of synaptotagmin 2 and complexin 1 expression levels [163].

As mentioned before astrocytes are the metabolic supporters of neurons, therefore any interference with the astrocytes-neuron shuttles may deprive neurons of necessary metabolites, leading to neurodegeneration. PGC-1α has been shown to play an important role in this crosstalk. Indeed, important regulators of cholesterol and lipid metabolism, such as SREBP and the Liver X receptor (LXR) were shown to be regulated by PGC-1α coactivator activity [164,165]. Moreover, PGC-1α2 has a specific role in regulating cholesterol metabolism in myotubes, which might translate to the same behaviour in brain [159].

Recently, a novel mechanism was discovered in which PGC-1α1 activation in skeletal muscle has a protective role against stress-induced depression [166]. Under normal circumstances, kynurenine enters the brain from circulation and is metabolized along kynurenine pathway into several compounds with neurotoxic effects, such as 3-hydroxy kynurenine, or quinolinic acid [166]. It is known that brain accumulation of kynurenine results in neuroinflammation and depression as well as impair glutamate transmission [166,167]. After exercise, PGC-1α1 induces expression of kynurenine amino transferases in skeletal muscle, which transform kynurenine into kynurenic acid that can no longer cross the blood brain barrier.

Several neurodegenerative diseases, especially AD and PD, have been connected to impaired mitochondrial OXPHOS and reduced expression of mitochondria related genes [168]. The forebrain of high fat diet fed mice shows that a decrease in PGC-1α levels is coupled with an increase of β-secretase whereas the opposite was observed in fasting mice [169]. Interestingly, it was shown PGC-1α1 protein stabilization can be neuroprotective against the complex I of electron transport chain blocker 1-methyl-4-phenyl-1,2,3,6-tetrahydropyridine-induced mitochondrial damage [170].

As we have seen, PGC-1α isoforms extensively regulate cellular metabolism and are essential for the excitability and survival of neurons. Therefore, targeting them with a functional therapeutically approach can have body-wide applications, including obesity and diabetes, muscle dystrophy and neurological diseases.

3 Hypothesis and aims

PGC-1α gene encodes four coactivator variants but scarcely anything is known about the role of these different PGC-1α proteins in the brain [154]. Unpublished results from the Ruas' lab have shown that these different isoforms are differentially expressed throughout the brain, and their expression levels can be modulated by stress conditions (Agudelo and Ruas, unpublished), suggesting a functional role of these proteins. Therefore, the main goal of this work is to characterize the molecular pathways controlled by PGC-1α isoforms, focusing on PGC-1α3. We seek to understand how PGC-1α3 specifically affects neuronal and astrocytic function. Understanding these mechanisms is important for discovery of new strategies of treatment for neurodegenerative diseases, namely the characterization of novel therapeutic targets. To achieve our goal, we will characterize the molecular pathways modulated by PGC-1α3 in *in vitro* neuronal and astrocytic experimental models.

The specific objectives are:

- Evaluate changes in neuronal morphology and synaptic activity markers by performing gain-of-function studies in primary cultures of mouse neurons.
- Identify downstream targets of PGC-1α3 in astrocytes by RNA-sequencing and characterization of the transcriptome using bioinformatic tools.
- Characterize modifications in the astrocytic secretome induced by PGC-1α3 that may affect neuronal function, through transcriptome processing using bioinformatic tools.

II. MATERIALS AND METHODS

1 Materials

1.1 Supplements and chemicals

Poly-D-Lysine hydrobromide, Bovine Serum Albumin, Fetal Bovine Serum (FBS), Dithiothreitol (DTT), Phenylmethanesulfonyl fluoride (PMSF), 4′,6-Diamidino-2-phenylindole dihydrochloride (DAPI), Triton X-100, phosphate buffered saline (PBS) were purchased from Sigma-Aldrich (St Louis, MO, USA); Neurobasal, Dulbecco's Modified Eagle Medium (DMEM), normal goat serum, horse serum, Penicillin/Streptomycin (PenStrep), GlutaMAX, B-27 Supplement and TrypLE Express were obtained from GIBCO® (Life Technologies, Inc., Grand Islands, USA).

IzolRNA lysis reagent was secured from 5 Prime (Hamburg, Germany); DNase I Amplification Grade kit was purchased from Invitrogen (Grand Island, NY, USA); High-Capacity RNA-to-cDNA™ and SYBR™ Green PCR Master Mix kits were obtained from Applied Biosystems (Foster, CA, USA). Primers for qRT-PCR were purchased from Integrated DNA Technologies (Illinois, USA).

Quick Start™ Bradford 1x Dye Reagent was purchased from Bio-Rad Laboratories (Hercules, CA, USA); Polyvinyl difluoride (PVDF) membrane was obtained from Millipore (Bedford, MA, USA); WesternBright^{TM} ECL HRP substrate was secured from Advansta (CA, USA); SuperSignal® West Femto Maximum Sensitivity was acquired from Thermo Scientific (Rockford, USA).

1.2 Antibodies

The antibodies used in Western Blot and immunocytochemistry assays are listed in Tables II.1 and II.2.

Table II.1 – List of the primary antibodies used in Western Blot and immunocytochemistry assays.

Primary antibody	*Host*	*Dilution*	*Supplier*
β-actin	Mouse	1:10000 (WB)	Sigma
βIII-tubulin	Mouse	1:2000 (IC)	Biolegend
GFAP	Mouse	1:1000 (IC)	Sigma
MAP2	Rabbit	1:2000 (WB)	Merck
PSD-95	Mouse	1:500 (WB)	Merck
Shank3	Rabbit	1:500 (WB)	Santa Cruz Biotechnology
SYP	Mouse	1:500 (WB)	Millipore

Table II.2 – List of the secondary antibodies used in immunocytochemistry assays.

Secondary antibody	*Target*	*Dilution*	*Supplier*
Alexa Fluor® 488	Mouse	1:1000	Invitrogen
Alexa Fluor® 594	Rabbit	1:1000	Invitrogen
Texas Red®	Mouse	1:500	Invitrogen

2 Methods

2.1 Primary neuronal cell culture and transduction conditions

Primary cultures of mouse cortical/hippocampal neurons were prepared from 16 to 17-day-old embryonic C57BL/6 mice as previously described [171]. Pregnant mice were sacrificed in a CO_2 chamber, the fetuses were collected in Hank's balanced salt solution (HBSS) with Ca^{2+} and Mg^{2+} (Gibco™, TermoFisher) and quickly decapitated. Brain cortices were collected in HBSS without Ca^{2+} and Mg^{2+}, after removal of olfactory bulbs, white matter and meninges. Cortices were then mechanically fragmented, transferred into a trypsin-DNaseI solution (0.25% trypsin, 1mg/mL DNAseI in HBSS w/o Ca^{2+}/Mg^{2+}) and incubated for 15 min at 37 °C. Following trypsinization, cells were washed three times in HBSS w/o Ca^{2+}/Mg^{2+} and resuspended in plating medium (Neurobasal, supplemented with 10% horse serum and 50U/mL of PenStrep (penicillin and streptomycin)).

Isolated neurons were plated on culture plates pre-coated with poly-D-lysine with and maintained at 37ºC in a humidified atmosphere of 5% CO_2. After 3 hours, the media was changed to Neurobasal with B-27 Supplement, 2mM of GlutaMAX and 50U/mL of PenStrep. A third of the media was changed every three days.

For RNA extraction and Western Blot, cells were plated in 6-well cell culture plates at a concentration of 1 $x10^6$ cells/well. For immunocytochemistry, cells were plated in 24-well cell culture plates at a concentration of $2{,}5x10^5$ cells/well.

Cells were transduced with an adenovirus expressing Green Fluorescence Protein (GFP) and FLAG-tagged PGC-1α3 isoform (AdPGC-1α3) at 15 days in vitro. Control cells were transduced with an adenoviral vector expressing GFP (AdControl). Adenovirus encoding GFP or both GFP and FLAG-tagged PGC-1α3 were previously generated by using the pAdTrack/pAdEasy system [159].

Neurons were transduced overnight, the medium was then discarded, cells were washed with PBS, and new media was added. 48 hours after transduction cells were washed with PBS and lysed either with IzolRNA reagent or lysis buffer (50 mM Tris-HCl pH 7.4, 180 mM NaCl, 1 mM EDTA, 1%, Triton X-100, 15% glycerol, 1mM DTT and 0.5 mM PMSF).

2.2 Primary astrocyte cell culture and transduction conditions

Primary cultures of mouse astrocytes were prepared from 5 to 7-day-old postnatal C57BL/6 mice. Pups were quickly decapitated and their brain cortices were maintained in DMEM after removal of olfactory bulbs, white matter and meninges. Cortices were then mechanically fragmented and filtered firstly in a 100µm followed by a 75µm cut-off strainer. Following filtration, cells were resuspended in DMEM/GlutaMAX-I media, supplemented with 10% FBS and 1% PenStrep, and kept at 37ºC in a humidified atmosphere of 5% CO_2.

For RNA extraction and Western Blot, cells were plated in 6-well cell culture plates and for immunocytochemistry cells were plated in 24-well cell culture plates.

Astrocytes were transduced as described in section 2.1. A workflow diagram of the main steps performed in this section are represented in Figure II.1.

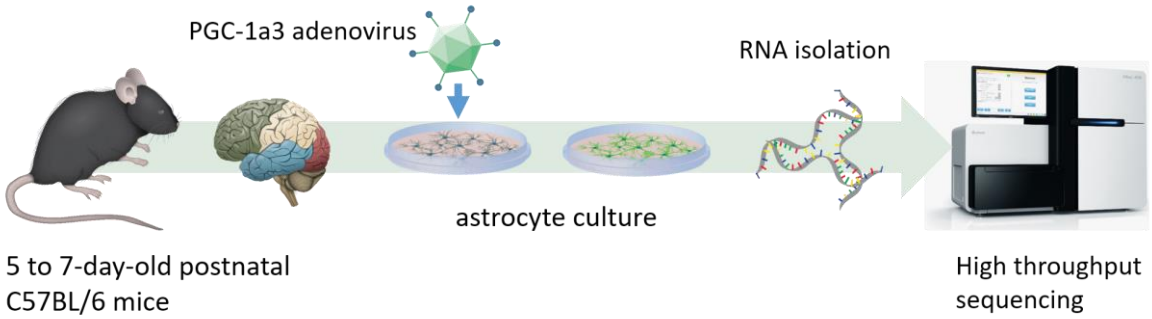

Figure II.1 – Ectopic expression of PGC-1α3 in primary cultures of mouse astrocytes. Astrocytes were isolated from 2-day-old mice, and at 15 days *in vitro* were transduced with an adenovirus encoding for GFP (AdControl) or GFP and PGC-1α3 (AdPGC-1α3) for 48h. RNA samples were isolated and subjected to Next Generation Sequencing.

2.3 Total RNA isolation and qRT-PCR analysis

Total RNA was extracted from mice cortex/hippocampal samples in accordance with manufacturer's instructions (Izol-RNA lysis reagent) [172]. RNA integrity was tested using an Agilent 2100 Bioanalyzer (Agilent Technologies, Waldbronn, Germany) in accordance with manufacturer's instructions (Agilent RNA 6000 Nano Kit) [173]. RNA Integrity Number (RIN) of samples varied between 9 to 9.6.

RNA concentration and quality were measured by spectrometry at UV light and 260/280 ratio, respectively, using the Nanodrop 1000 (Thermo Scientific, Rockford, USA). We typically obtained 100–300 ng of RNA from each 6-well neuronal culture plate and 400–800 ng from astrocytes cultures.

RNA samples were treated with DNaseI recombinant RNase-free for 15 minutes at room temperature followed by EDTA mediated enzyme inactivation for 10 minutes at 65ºC. Reverse transcription of 500 µg of treated RNA was performed with High-Capacity RNA-to-cDNA kit for 1 hour at 65ºC.

Quantitative real-time PCR (RT-qPCR) reactions were performed using SYBR Green PCR Master Mix kit in an ABI QuantStudio™ 6 Flex Real-Time PCR System (Applied Biosystems, Foster, CA, USA), using the following cycle conditions: 50ºC for 2 minutes; 95ºC for 10 minutes; followed by 40 cycles at a temperature of 95ºC for 15 seconds and at 60ºC for 1 minute. A final step of 95ºC for 15 seconds, 60ºC for 1 minute and 95ºC for 15 seconds was added to determine the melting curves in order to check for non-specific amplicons and primer dimers. Primers used are listed in Table II.3. Data analysis is based on the ΔΔCt method with normalization of the raw data to housekeeping genes. Four candidate genes (β-actin, GAPDH, eukaryotic elongation factor (EEF) and HPRT) were analysed with the Norm Finder algorithm and EEF was found to be the most stable gene to be used as an endogenous control for qPCR, in the experimental conditions used [174]. mRNA expression levels of the genes of interest were normalized to eukaryotic elongation factor (EEF) expression levels. All PCR reactions were performed in technical duplicates from at least three independent experiments.

Table II.3 – Sequences of mouse primers used for qRT-PCR analysis.

Gene	*Forward (5'-3')*	*Reverse (5'-3')*
Angptl4	GTTGCCGTGGGATAGAGTGG	TTAACCCTATAGGTGGCTGGT
Apbb1ip	ACCCAGAGTTTAGGAGTGGAC	CTTCCAGTGCATTTAAGGACTCA
Arhgap4	GCCAGTTGGAGAGCCTCATT	CCTCCTGGTCATCCTCCTGA
Atp2a3	TGGATGGTGTTCTCGGGACAT	GTCCTGGAAGTAGTCGGCA
CaM	ACGGGGATGGGACAATAACAA	TGCTGCACTAATATAGCCATTGC
Camklδ	TGACTTTGGCTTGTCGAAAATGG	TGTACGGTTTCTGGGCGAGA
Camkllα	ACCTGCACCCGATTCACAG	TGGCAGCATACTCCTGACCA
Camkllβ	GCACGTCATTGGCGAGGAT	ACGGGTCTCTTCGGACTGG
Can	CTGGCTGCGCTAATGAACCA	GGTCTGACCATAGGATGTCACAC
Ccl5	GCTGCTTTGCCTACCTCTCC	TCGAGTGACAAACACGACTGC
Ccr5	TTTTCAAGGGTCATGTCCGAC	GGAAGACCATCATGTTACCCAC
Ctss	CGACGCCAGCCATTCCTCCTT	AGAGTCCCATAGCCAACCACAAGA
Eaat1	ACCAAAAGCAACGGAGAAGAG	GGCATTCCGAAACAGGTAACTC
Eaat2	ACAATATGCCCAAGCAGGTAGA	CTTTGGCTCATCGGAGCTGA
Eef	ACACGTAGATTCCGGCAAGT	AGGAGCCCTTTCCCATCTC
Fcγrllβ	ATGGGAATCCTGCCGTTCCTA	CCGTGAGAACACATGGACAGT
Fcγrlll	CAGAATGCACACTCTGGAAGC	GGGTCCCTTCGCACATCAG
Gria1	TCCCCAACAATATCCAGATAGGG	AAGCCGCATGTTCCTGTGATT
Gria2	AATGGACGTGTTATGACTCCAGA	CTGACATTCATTCCCATGCCA
Grin2A	ACGTGACAGAACGCGAACTT	TCAGTGCGGTTCATCAATAACG
Grin2B	GCCATGAACGAGACTGACCC	GCTTCCTGGTCCGTGTCATC
Gm14403	GAGTCTTCACAATGAAACATACCA	TGCATTCATGGGGTTTCTCTT
Hevin	GTGTTTGCCAAGATCCAGAGAC	TGGCGTAGGTTTGGTTGTCA
Itgal	AGCCTATCCTGAGACCTT	TCTTATCTTCACCACAGTTCT
Itgβ2	CAGGAATGCACCAAGTACAAAGT	CCTGGTCCAGTGAAGTTCAGC
Kcnk1	TGCTCTCCACCACAGGCTATG	AGATGATGCAGAAGGCTTTGC
Laptm5	AGCACCTGGAGGCTGGGAAGTC	TTGCCATCAGAGCAGTGGCTCAT
Lgals9	CTTTCTACACCCCCATTCCA	CTCGTAGCATCTGGCAAG
Map2	GCCAGCCTCAGAACAAACAG	AAGGTCTTGGGAGGGAAGAAC
Marco	ACAGAGCCGATTTTGACCAAG	CAGCAGTGCAGTACCTGCC
Msr1	TGAACAAGAGGATGCTGACTG	TGTCATTGAACGTGCGTCAAA
Nfatc1	CAGTGTGACCGAAGATACCTGG	TCGAGACTTGATAGGGACCCC

Nfatc2	CACACCGAGCTATGAGAAGA	GTCAGCGTTTCGGAGCTTCA
Nfatc3	GCTCGACTTCAAACTCGTCTT	GATGTGGTAAGCCAAGGGATG
Nfatc4	GAGCTGGAATTTAAGCTGGTG	CATGGAGGGGTATCCTCTGAG
Nfat5	GAGGGGTGTGGATTGGAATCT	CTGGTGCTCATGTTACTGAAGTT
Pgc-1α (exon 2)	TGATGTGAATGACTTGGATACAGACA	GCTCATTGTTGTACTGGTTGGATATG
Plau	GCGCCTTGGTGGTGAAAAAC	TTGTAGGACACGCATACACCT
Plcβ2	TGGATGTCACGAGTATCCGAG	GTTTCTGGCTCTTGGGTATCTTT
Psd-95	CTGGACCTGACCGAAACCC	GCTGGTTGTTGAGTGGGAAGA
Serpini1	AGGTGTGAAGGAGACTTGAAAC	CTGACCACTCAGTTATGGTT
Shank3	GGAACTTGCTTCCATTCGGAG	CCTCGAGTCAGCATCTGCAA
Slc16a3	AGCCCAGTGTTCCTTTGTG	ACAGCAGTTGAGCAGTAGG
Sparc	CCACACGTTTCTTTGAGACC	GATGTCCTGCTCCTTGATGC
Syt11	ATACGCCCCAGCTTTGATGT	CTTGTATGGCGGGGTCTTGT
Tgfβ	CCACCTGCAAGACCATCGAC	CTGGCGAGCCTTAGTTTGGAC
Thbs1	CACGCTACAGGACAGCAT	GGCCGCCTCAGCTCATT
Tlr7	ATGTGGACACGGAAGAGACAA	ACCATCGAAACCCAAAGACTC
Tlr9	ATGGTTCTCCGTCGAAGGACT	GAGGCTTCAGCTCACAGGG
βIII-tub	CGCACGACATCTAGGACTGA	TGAGGCCTCCTCTCACAAGT

2.4 RNA-sequencing analysis

RNA samples were analysed by massively parallel sequencing using the InView Transcriptome Explore package from GATC Biotech (Germany). Sequencing was performed on an Illumina HiSeq 4000 with a non-stranded cDNA library and single-end 50-bp reads at 25–45 million reads per sample. Raw sequencing data were demultiplexed and converted into FASTQ files and quality control of raw reads was determined using FastQC tool kit (Babraham Bioinformatics, http://bioinformatics.babraham.ac.uk/projects/fastqc).

Raw reads were aligned to NCBI's *Mus musculus* (GRCm38.p5) reference genome with Hisat2 tool using default parameters[175]. Hisat2 combines an indexing scheme based on the Burrows-Wheeler transform and the Ferragina-Manzini (FM) index in order to create a global whole-genome FM index for the exonic alignment. A high ratio of uniquely mapped reads (>75%) was confirmed, with an overall alignment rate higher than 90%.

Aligned reads were counted using HTSeq framework [176], namely htseq-count script, in which only reads mapping unambiguously to a single gene are counted, whereas reads aligned or overlapping to multiple positions are discarded. Samtools (http://samtools.sourceforge.net) was used to convert Hisat2 output SAM files into BAM files sorted by alignment position that were used as HTSeq input.

Differential gene expression between individual experimental groups was performed with DESeq2 package by applying regularized log transformation [177]. HTSeq counts were normalized for library size (total number of sequenced reads), based on the premise that most genes are not differentially expressed amongst all samples. Due to the high variability between different primary cultures, multi-factor design was used in order to perform a paired analysis between the two individual experimental groups. As rationale for pairing, we set the DESeq2 contrasts for generalized linear model (glm) to use not only the comparison of AdPGC-1α3 transduced sample with the corresponding control, but also the identity of brains

that the astrocytes come from. All differentially expressed genes (DEGs) showing p-value (adjusted by Benjamini-Hochberg method for multiple comparisons adjustment) smaller than 0.05 were further examined for functional processes and differential expression and plotted as following.

For MA plots, fold change values of DEGs were log_2-transformed and matched to the respective logarithm of expression values (baseMean) and Volcano plots compare negative logarithm p-values with log_2 fold change.

Heatmaps show the one thousand most expressed genes using their respective baseMean values standardized to mean of 0 and a standard deviation of 1. Pearson's correlation coefficient is used as clustering criterion between the different genes (rows) and Euclidean distance is used to hierarchically cluster the different samples (columns). Standardized base mean values were coloured with a blue to red gradient, respectively for down and upregulated genes, for visualization purposes.

Samtools was used to convert Hisat2 BAM files into BedGraph files that were used as Integrate Genome Viewer (IGV) input [178]. Epigenetic modifications were visualized using IVG and ChIP-Atlas (http://chip-atlas.org).

TargetP 1.1, SignalP 4.1, TMHMM 1.0 and SecretomeP 2.0 (DTU Bioinformatics, Copenhagen, Denmark) were used for secretory analysis via classical and alternative pathways. DEGs list obtained from DESeq2 analysis was submitted to the previously mentioned tools separately and the outputs combined in data frame, which was subsequently filtered. Putative classically secreted proteins were uncovered by filtering the data frame for non-mitochondrial located proteins with a reliability class equal or smaller than 2 (analysed by TargetP), containing a signal peptide (obtained by SignalP) and without transmembrane helix domains (as predicted by TMHMM). Putative unconventionally secreted proteins were obtained by applying the same filter as previously described, but without predicted signal peptide and with network score higher than 0.6 (as calculated by SecretomeP).

Ingenuity Pathway Analysis (Qiagen, CA, USA) software was used for a comprehensive pathway and network analysis for gene expression. IPA input was filtered to include only DEGs with p-value smaller than 0.05 and output includes only functions and pathways experimentally validated in nervous system. Only significant pathways ($p>0.05$) were considered for subsequent RT-qPCR validation of target genes.

Kallisto was used to convert feature counts from HTSeq analysis into transcripts per million values that were used as Gene set enrichment analysis (GSEA) input. GSEA software was used for miR enrichment analysis by running the previous data matrix against the Molecular Signature Database for miR (http://software.broadinstitute.org/gsea/msigdb, version 6.2) [179]. Statistical significance is evaluated using a phenotype-based permutation applied to our gene-expression data matrix. Differentially expressed miRs were identified by setting the cut-off for false discovery rate (FDR) lower than 25% and plotted according with their normalized enrichment score (NES).

A workflow diagram of the main steps performed in this protocol as well as the used software are represented in Figure II.2.

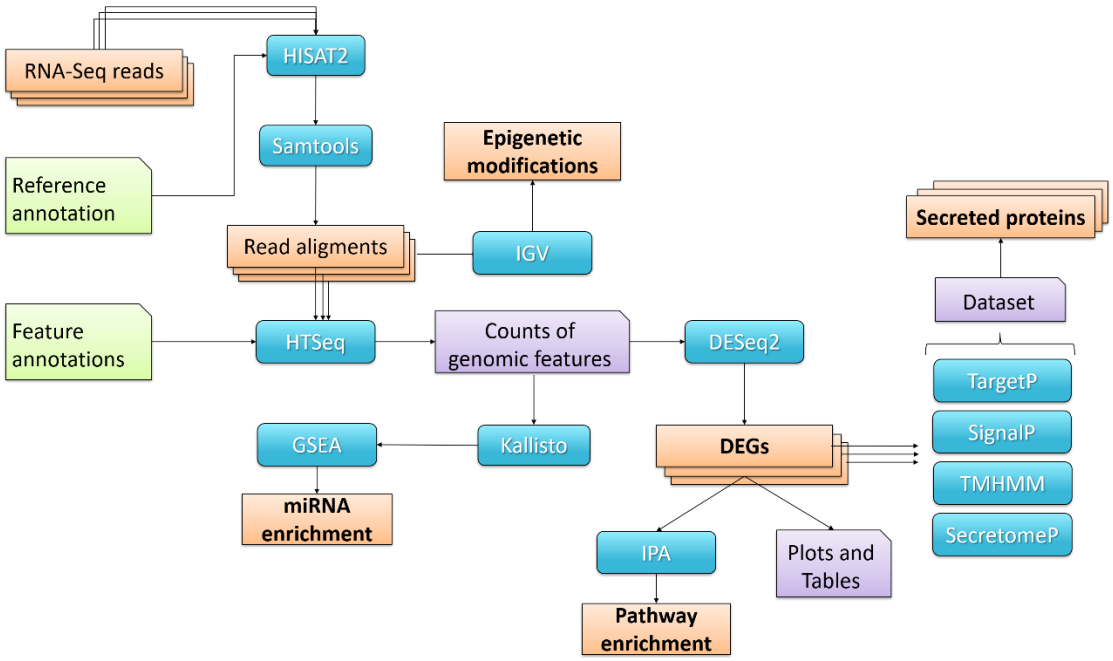

Figure II.2 – Workflow diagram of RNA-Seq analysis of DEGs. RNA-seq raw reads are first mapped to the mouse genome using HISAT2 and its output is converted by Samtools into BAM files for further analysis. BAM files are converted to BedGraph format, which are used as IGV input in order to assess epigenetic modifications. Also, BAM files reads are counted by HTSeq framework and its output is converted by Kallisto into transcripts per million values for miR enrichment analysis through GSEA. HTSeq counts of genomic features are also used for performing differential gene expression between individual experimental groups with DESeq2 package. Differential expressed genes (DEGs) obtained from DESeq2 are presented under plots and tables and are used as input for IPA analysis. Furthermore, DEGs are submitted through a bioinformatic pipeline consisting of TargetP, SignalP, TMHMM and SecretomeP softwares. The results from each bioinformatic tool are then combined to obtain a dataset which is subsequently filtered in order to obtain putative secreted proteins.

2.5 Immunocytochemistry

Primary cultures of mice neurons and astrocytes were prepared as previously described. Cells were washed with PBS three times, 30 seconds each, and fixed with 4% (w/v) paraformaldehyde. Subsequently, the cells were washed with PBS three times for 10 minutes and permeabilized with 0.1% Triton X-100 in PBS for 5 minutes at room temperature. Blocking was performed with 5% goat serum in PBS, for 20 minutes at room temperature. Cells were then incubated with anti-GFAP (1:1000 in blocking solution) or anti-βIII-tubulin primary antibody (1:2000 in blocking solution), overnight at 4ºC, in a humidified chamber. Cells were washed with PBS three times for 5 minutes and then incubated for 1 hour at room temperature with the appropriate secondary antibodies (diluted in blocking solution). After washing, nuclei were stained with 300nM of DAPI for 10 minutes. Cells were kept in PBS.

Fluorescence images of, at least, five random microscope fields were acquired per sample, under 40x magnification, using a fluorescence microscope (model AxioScope.A1) with integrated camera AxioCam HR (Carl Zeiss, Inc – North America).

2.6 Western-Blot

Lysates from mice neurons and astrocytes were homogenized in lysis buffer and sonicated, on ice, four times for 5 seconds. The sonication cycle was repeated four times. Subsequently, samples were centrifuged at 13000 rpm for 15 minutes at 4ºC and the supernatant was stored at -80ºC.

Total protein concentration was determined through the Bradford method using Quick Start™ Bradford 1x Dye Reagent (Bio-Rad Laboratories). Cell extracts with 50 µg of total protein were added to denaturing buffer (1:1) (0.25 M Tris-HCl, 4% sodium dodecyl sulphate (SDS), 4% glycerol, 0.004% bromophenol blue, 1% β-mercaptoethanol, pH 6.8), boiled for 10 min. Denatured proteins were resolved on a 10% SDS-polyacrylamide gel electrophoresis (SDS-PAGE), in running buffer (25 mM Tris Base, 190 mM glycine, 0.1% SDS, pH 8.8) with fixed amperage of 40 mA per gel, for 3 hours. Samples were electrotransferred to an activated PVDF membrane (1 min in ethanol, 2 min H_2O, 5 min in transfer buffer), in transfer buffer (25 mM Tris, 190 mM glycine, 20% methanol), with a fixed amperage of 500 mA for 2 hours.

Membranes were blocked with 5% (w/v) non-fat dry milk in TBS-T (25 mM Tris Base, 137mM NaCl, 2.7mM KCl, 0.05% Tween 20, pH 7.5), minimum 1h at room temperature (RT) and incubated overnight at 4ºC with specific primary antibodies (listed in Table II.1). After being washed with TBS-T 3 times for 15 minutes each, membranes were incubated with horseradish peroxidase-conjugated anti-mouse or anti-rabbit (1:5000, 3% non-fat dry milk in TBS-T) secondary antibodies for 1h at RT. Membranes were again washed with TBS-T and incubated with WesternBright™ ECL HRP substrate (Advansta) or SuperSignal West Femto Maximum Sensitivity Substrate (ThermoScientific) for detection of chemiluminescent immunocomplexes. Densitometric analyses were performed using ImageLab Software 5.1 Beta after scanning with ChemiDoc™, both from Bio-Rad Laboratories (Hercules, CA, USA). To reuse, membranes were stripped (1.5% glycine, 40% glacial acetic acid, 1% SDS, 10% Tween 20) for 10 minutes and washed with TBS-T. All membranes were then incubated with β-actin as endogenous control.

2.7 Statistical analysis

Principal component analysis (PCA) was used to identify the major sources of variation within the dataset without introducing inherent bias [180]. Variances of individual genes (calculated from regularized log transformed HTseq counts values) were used as input for R built-in function *prcomp()*, which uses spectral decomposition approach to evaluate the covariances/correlations between variables. Two principal components (PC1 and PC2) were determined by this analysis, which account respectively for 65% and 26% of the observed variance in RNA-sequencing data.

Significance of differences between conditions was assessed by paired t-test comparisons and one-way analysis of variance (ANOVA) followed by Tukey post hoc test analysis. Graphs were plotted using GraphPad Prism software version 7 (GraphPad Software, Inc., San Diego, CA, USA) and results are presented as mean ± standard error of the mean (SEM). Significance levels are represented as *, ** and *** when p-value is inferior to 0.05, 0.01 and 0.001, respectively.

III. RESULTS

1 Evaluation of the effects of ectopic PGC-1α3 expression in primary neuronal cultures

1.1 PGC-1α3 overexpression modulates the expression levels of postsynaptic proteins in primary cultures of neurons

PGC-1α1 is one of the master regulators of energy metabolism. As previous mentioned, one single PGC-1α gene encodes four coactivator variants (named PGC-1α1 through α4), but scarcely anything is known about the role of these different PGC-1α proteins in the brain [154]. Unpublished results from the Ruas' lab have shown that these different isoforms are differentially expressed throughout the brain, and their expression levels can be modulated by stress conditions (Agudelo and Ruas, unpublished). Importantly, complete deletion of the PGC-1α gene in the brain, generates a complex phenotype that includes hyperactivity and lesions in the striatal region, clearly indicating an essential neuronal role for these coactivators [122]. Therefore, we have started to characterize the molecular pathways controlled by PGC-1α isoforms in the brain. For that, primary cultures of mouse neurons 15DIV were transduced with a control adenoviral vector encoding GPF (AdControl) or GFP and each of the PGC-1α isoforms (AdPGC-1α1-4) for 48h, and the levels of pre- and postsynaptic proteins were determined by Western-Blotting using specific antibodies (Figure III.1).

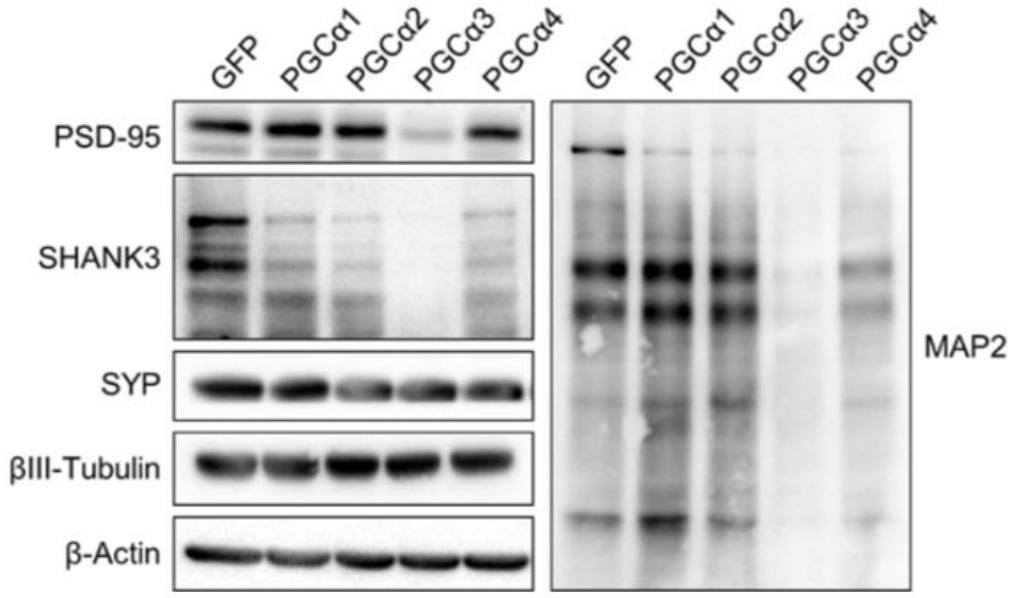

Figure III.1 – PGC-1α3 overexpression decreases expression levels of postsynaptic proteins in primary mouse neurons. Primary cultures of mouse neurons 15DIV were transduced as described in the methods section. Total protein extracts were analysed by Western-Blot to evaluate the levels of SYP, βIII-tubulin, PSD-95, SHANK3 and MAP2. β-actin was used as loading control. Representative images of the bands are shown (unpublished results Nunes et al.).

Ectopic expression of PGC-1α1, PGC-1α2 and PGC-1α4 did not significantly affect the expression levels of the evaluated pre- and postsynaptic proteins. The levels of SYP and βIII-tubulin also did not exhibit any differences between control and PGC-1α3 samples, while the levels of postsynaptic proteins, microtubule associated protein 2 (MAP2), postsynaptic density protein 95 (PSD-95) and SH3 and multiple ankyrin repeat domains 3 (SHANK3) were drastically decreased (Figure III.1), in cells with increased expression of PGC-1α3. These preliminary results suggest that PGC-1α3 targets specifically genes associated with postsynaptic proteins leading to a reduction of their expression levels.

Primary cultures of mouse neurons 15DIV were transduced as described before. As expected, transcript levels of total PGC-1α (pan PGC-1α) are significantly increased approximately 430-fold over control ($p<0.0001$), confirming PGC-1α3 overexpression (Figure III.2A). Surprisingly, SYP, SHANK3 PSD-95, MAP2 and βIII-tubulin genes showed no variation in their expression patterns in response to PGC-1α3 overexpression, which highlights the role of post-transcriptional mechanisms in the downregulation of these post-synaptic proteins.

GRIA1 mRNA levels are significantly decreased by approximately 20% ($p<0.01$), while no statistically differences were detected for GRIA2, GRIN2A, and GRIN2B mRNA levels (Figure III.2B).

The fact that there was no correlation between mRNA and protein levels for SHANK3 PSD-95, MAP2, and the fact that all these proteins are calpain subtracts, led us to analyse the expression levels of Ca^{2+} signalling-related genes CaMKIδ, CaMKIIα, CaMKIIβ and CaM2. CaMKIδ and CaMKIIβ transcript expression is significantly decreased to 0.8 and 0.7-fold change over control ($p<0.05$), respectively, whereas CaMKIIα and CaM2 expression levels remain unchanged.

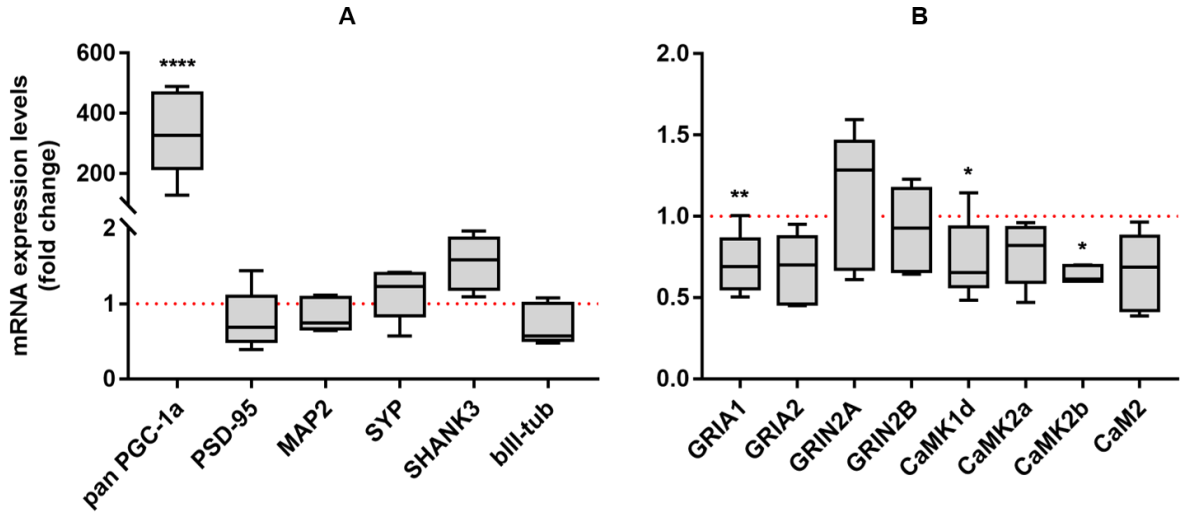

Figure III.2 – PGC-1α3 overexpression modulates transcript levels of postsynaptic proteins, neuronal markers and Ca^{2+} signalling genes in primary mouse neurons. Primary mouse neurons 15DIV transduced as described in the methods section. After mRNA isolation, transcript levels of (A) total PGC-1α (pan PGC-1α), synaptic proteins, βIII-tubulin, (B) glutamate receptors and Ca^{2+} signalling genes were analysed by RT-qPCR. Values were normalized to the housekeeping gene EEF and are expressed as fold change relative to GFP-transduced cells. Data represents means ± SEM from five individual experiments (n=5). *$p<0.05$, **$p<0.01$, $p<0.0001$.

1.2 PGC-1α3-dependent modulation of neuronal protein levels is mediated by astrocytes

So far, we observed that PGC-1α3 overexpression was modulating synaptic protein levels and, to a less extent, their corresponding gene expression. Therefore, we decided to evaluate neuronal morphology by performing immunofluorescence for neuronal βIII-tubulin in cells transduced with PGC-1α3 virus as compare it with GFP signal since this virus express GFP from a separate promoter. Surprisingly, we observed that there was hardly any colocalization between βIII-tubulin staining and GFP, indicating that cells being transduced are not neurons (Figure III.3). Indeed, our primary cultures of neurons have residual contaminations of glial cells ranging from 5-10% (data not shown). We have tried to increase and titrate the amount of virus to no avail (data not shown). Unfortunately, mice mature neurons have decreased expression of coxsackievirus and adenovirus receptor (CAR), which is correlated with attenuated adenoviral susceptibility [181]. These results suggest that the observed effects in neurons are in fact modulated by a third party, most likely astrocytes. Therefore, to determine if the GFP-positive cells are astrocytes, we performed immunocytochemistry for GFP and GFAP, a specific astrocytic marker. We indeed observed a high degree of colocalization between the two markers, meaning that GFP-expressing adenovirus is preferentially transducing resident astrocytes. This suggests that PGC-1α3 is mediating the effect seen in neuronal-specific postsynaptic proteins through modulation of astrocyte-neuron crosstalk.

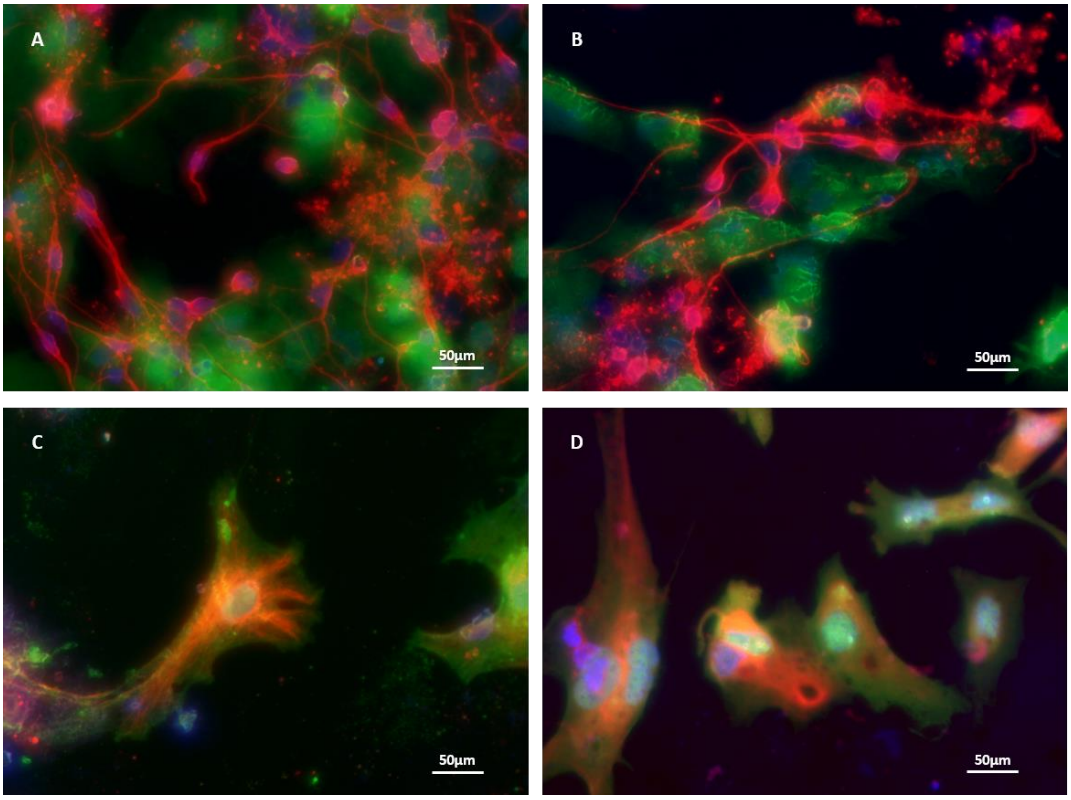

Figure III.3 – AdPGC-1α3 specifically transduces astrocytes in primary cultures of mice neurons. Primary mouse neurons 15DIV transduced as described in the methods section. Primary mouse neurons were transduced with (A, C) AdControl and (B, D) AdPGC-1α3 and stained for (A, B) βIII-tubulin, or (C, D) GFAP (red). Positive transduction can be observed by GFP fluorescence (green). DAPI was used as a nuclear marker (blue). The panels shown are representative of three independent experiments (n=3). Scale bar=50 µm.

2 Evaluation of ectopic PGC-1α3 expression in primary cultures of astrocytes

2.1 PGC-1α3 overexpression regulates glutamate transport and Ca^{2+} signalling genes in primary cultures of astrocytes

The results presented so far suggest that PGC-1α3 overexpression in astrocytes induce a decrease in postsynaptic proteins levels. Astrocytes are considered to be the secretory cells of CNS and have a pivotal role in the tripartite synapse by recycling glutamate and releasing several other factors through modulation of Ca^{2+} intracellular levels. Therefore, we decided to determine expression levels of genes involved in secretory pathways, namely Hevin, Sparc and Thbs1, as well as glutamate transporters EAAT1 and EAAT2 and Ca^{2+} signalling related genes CaN, CaMKIδ, CaMKIIα, CaMKIIβ and CaM2. In addition, we measured expression levels of Nuclear Factor of Activated T cells (NFAT) isoforms, transcription factors that are regulated by calcium signalling, and verified PGC-1α3 overexpression as performed previously.

Expression levels of total PGC-1α (pan PGC-1α) are significantly increased to about 3000-fold over control ($p<0.001$), confirming PGC-1α3 overexpression (Figure III.4A). EAAT1 and EAAT2 levels are significantly decreased by 25 and 35% ($p<0.05$ and $p<0.01$, respectively), while there are no variations in the gene expression of Hevin, Thbs1, and Sparc.

CaMKIδ transcript levels are significantly increased by 1.4-fold ($p<0.05$) (Figure III.4B), while CaMK2β, CaM2, CaN and CaMK2α expression levels show no variation when compared to control. Interestingly, NFATc1 and NFATc3 mRNA levels values are significantly increased to 1.3 and 1.7-fold over control ($p<0.05$ and $p<0.001$), respectively, while NFATc4 is significantly downregulated by 60% ($p<0.001$).

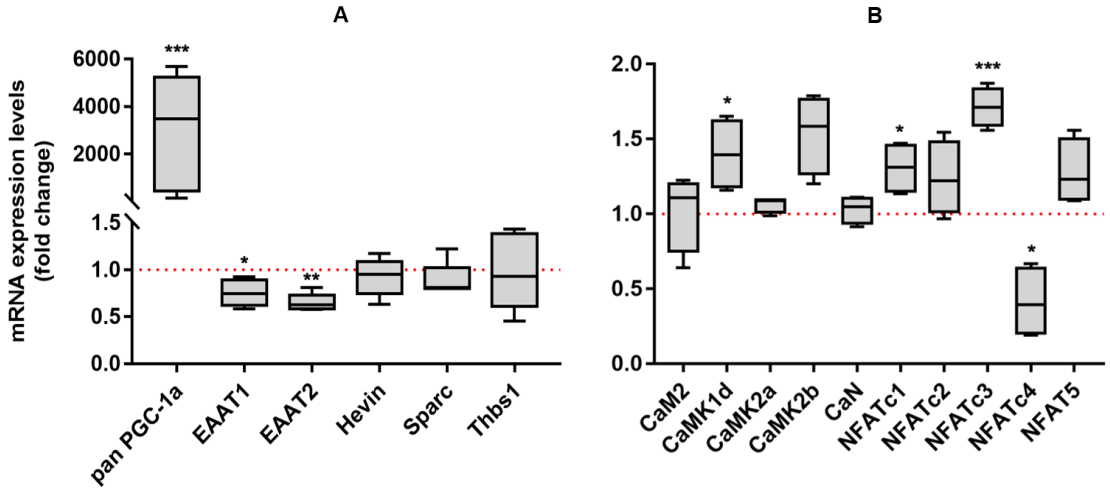

Figure III.4 – PGC-1α3 overexpression modulates transcript levels of glutamate transporters and Ca^{2+} signalling-related genes in primary mouse astrocytes. Primary mouse astrocytes 15DIV were transduced as described in the methods section. After mRNA isolation, transcript levels of (A) total PGC-1α (exon2), glutamate transporters, secretory proteins and (B) Ca^{2+} signalling-related genes were analysed by RT-qPCR. Values were normalized to the housekeeping gene EEF and are expressed as fold change relative to GFP-transduced cells. Data represents means ± SEM from five individual experiments (n=5). *p<0.05, **p<0.01, ***p<0.001.

2.2 PGC-1α3 overexpression reduces overall gene expression and signalling pathways in primary cultures of astrocytes

Our initial approach revealed that astrocytic function is also affected by PGC-1α3 overexpression, especially with regard to glutamate transport and Ca^{2+} signalling. In order to identify PGC-1α3 downstream targets, we performed an unbiased next generation sequencing of RNA (RNA-seq) and identified the genes that are differentially expressed in PGC-1α3 transduced astrocytes. We isolated and sequenced RNA from total of six samples, three biological replicates of astrocytes cultures with ectopic expression of PGC-1α3 and the three respective control conditions, in order to provide a reference for determining differential gene expression. Raw reads were aligned using the Hisat2-HTSeq-DeSeq2 inhouse pipeline as described in Methods.

Clustering of different samples revealed that there is a reasonable reproducibility and gene expression similarity between biological replicates (Figure III.5A). This result is supported by principal component analysis that indicates a good clustering within the two conditions with the exception of one PGC-1α3 sample that has gene expression profile more similar to GFP controls (Figure III.5B). Sequenced samples come from different pools of mouse brains, which were processed separately. Each pool was then used to be plated and transduced adenovirus expressing either GFP or GFP and PGC-1α3. To decrease inter-sample variability, we decided to use a pairwise comparison approach in order to minimize the error induced by the variability between the different brain pools. This provided us a better dataset to determine gene expression changes in astrocytes overexpressing PGC-1α3.

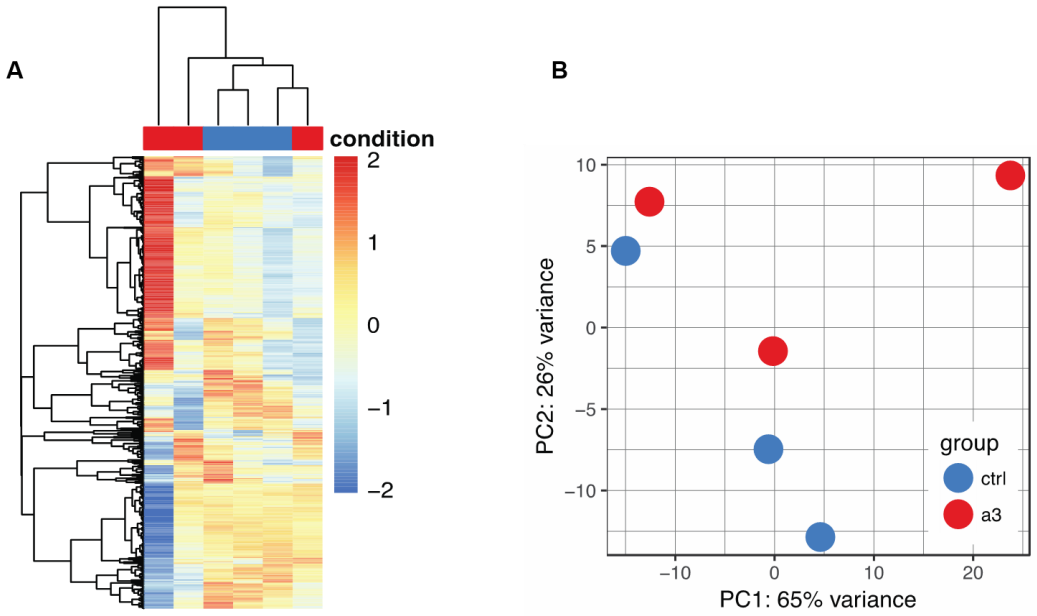

Figure III.5 – Transcript enrichment analysis in astrocytes transduced with AdControl and AdPGC-1α3. (A) Clustered heatmap of expressions of the 1000 most abundant transcripts expressed by AdControl transduced (red bar) and AdPGC-1α3 transduced astrocytes (blue bar). Transcript expression is plotted using standardized baseMean values (see Materials and Methods). Pearson's correlation coefficient is used to cluster genes (rows) and Euclidean distance to cluster samples (columns). Standardized base mean values were coloured with a blue to red gradient, respectively for down and upregulated genes. (B) Principal component analysis (PCA) plot represents the two principal components (PC1 and PC2) responsible for, respectively, 65% and 26% of the observed variance within AdControl transduced (blue dots) and AdPGC-1α3 transduced astrocytes (red dots).

We detected significant changes in gene expression profile of astrocytes transduced with PGC-1α3 (adjusted p-value<0.05). In total, we obtained 389 differential expressed genes of which 343 genes are downregulated and, besides PGC-1α gene, other 43 genes are shown to be upregulated (Figure III.6). These results are consistent with the previously published RNA-sequencing data of PGC-1α3 overexpression in myotubes where the downregulation of gene expression is more prominent and is also according with the current working model that suspects that PGC-1α3 acts as a transcriptional repressor [159].

To better understand which biological functions are controlled by PGC-1α3 isoform, we performed a comprehensive pathway and network analysis of our DEGs dataset using IPA platform. This analysis revealed that the effect of PGC-1α3 on astrocytes is manifold. As expected, it significantly upregulates PPARα signalling pathway, but it also downregulates several pathways involved in mitochondrial biology (CREB signalling in neurons, nitrogen oxide species (NOS) and ROS production), as well as transmembrane transport (GPCR pathway, PLC and Ca^{2+} signalling), integrin signalling, synaptic plasticity (synaptic long-term depression and axonal guidance) and neuroinflammation (NFAT in regulation of immune response, complement system, chemokine signalling) (Figure III.7A). Also, it is shown that PGC-1α3 overexpression strongly regulates cell cycle control and cell movement, results consistent with what was observed in myotubes (Figure III.7B).

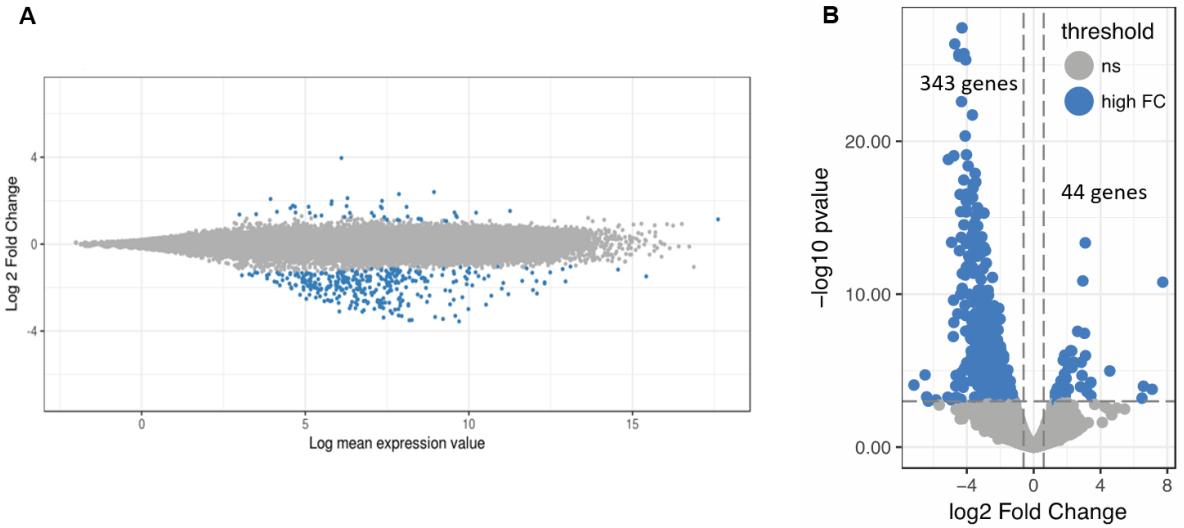

Figure III.6 – PGC-1α3 overexpression downregulates overall gene expression in primary mouse astrocytes. Graphical representations of differentially expressed genes (DEGs) in astrocytes transduced with AdControl and AdPGC-1α3. Blue dots represent significant DEGs with a high fold change (fold change higher or lower than $\log_2(0.6)$ and adjusted p-value<0.05), while grey dots represent the remaining genome. (A) MA plot represents logarithm of expression values (baseMean) against the $\log_2$ fold change values of genes compared AdContol. (B) Volcano plot shows negative $\log_2$ fold change of genes against negative of $\log_{10}$ p-values.

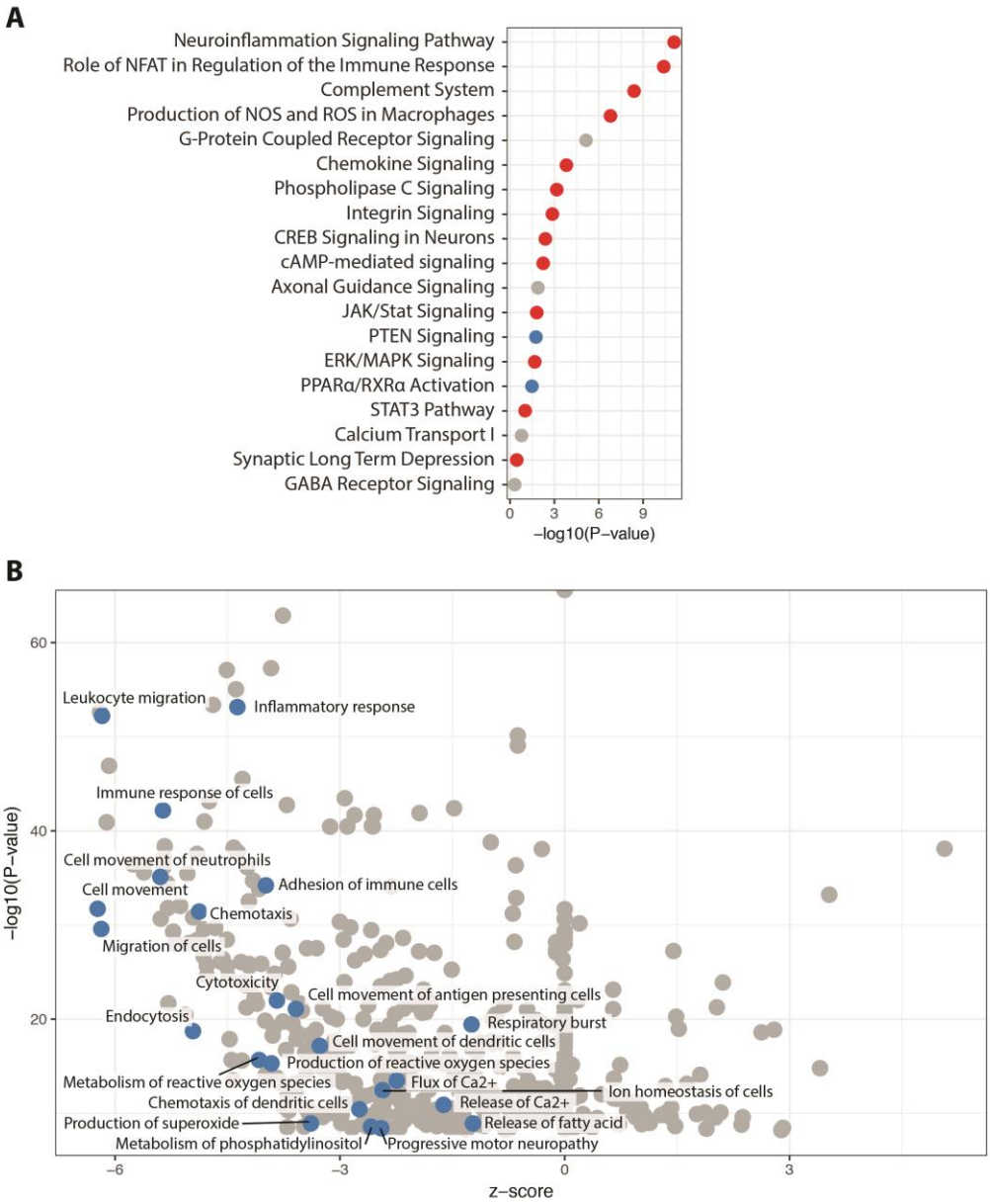

Figure III.7 – Principal IPA canonical pathways and functions modulated by PGC-1α3 ectopic expression in astrocytes. Graph presents -$\log_{10}$p-values determined for each (A) canonical pathway and (B) function. Directionality of change is indicated by colour of dots. (A) Red and blue dots represent down- and upregulated pathways, respectively, with significantly changed z-score and grey ones represent significantly modulated canonical pathways and functions with no clear directionality. (B) Blue dots represent downregulated functions with significantly changed z-score and grey ones represent significantly modulated functions with no clear directionality.

After obtaining the most differentially expressed pathways in response to PGC-1α3 overexpression, we analysed which DEGs were associated with each pathway and to what extent did they contribute for the observed effects (Table III.1). Furthermore, we also verified if there was any other DEGs that, when combined, could be affecting other biological functions. Indeed, we observed that PGC-1α3 upregulates many transcripts that map to pseudogenes and zinc finger proteins and regulates the expression of different transport channels and secreted proteins such as Serpini1, TGFβ1, Angptl4 and galectin 9. This analysis indicates that PGC-1α3 might play a role in the secretory abilities of astrocytes.

Table III.1 – Main up- and down-regulated DEGs involved in each differentially regulated canonical pathways. Canonical pathways were obtained through IPA and DEGs analysis. Fold change (FC) values were coloured with a blue to red gradient, respectively for down and upregulated DEGs.

PPAR Signalling	
Pparγc1α	2.208
Tnfrsf1β	0.452
Gnas	0.454
Tgfβ1	0.267
Plcβ2	0.297
Ptk2β	0.441
Adcy7	0.374
Ptgs2	2.412
Ptpn6	0.291
Ptprc	0.253
Ptpn7	0.262
Plcg2	0.314
Pik3cγ	0.202
Tlr9	0.290
Angptl4	3.370

Transcription Regulation	
Gm4631	2.881
Gm7478	4.222
Gm13341	5.277
Gm14295	3.927
Gm14296	4.934
Gm14305	3.599
Gm14403	3.280
Gm14410	3.977
Zfp966	4.333

NOS and ROS Production	
Apod	0.423
Tnfrsf1β	0.452
Ncf1	0.124
Pik3r5	0.400
Tlr9	0.290
Spi1	0.116
Ncf2	0.301
Pik3cγ	0.202
Plcg2	0.314
Irf8	0.174
Pik3cδ	0.355
Ptpn6	0.291
Cybb	0.225
Cyba	0.366

Neuroinflammation	
Cx3cr1	0.170
Tgfβ1	0.267
Tlr9	0.290
Trem2	0.126
Csf1r	0.101
Tlr8	0.394
Syk	0.309
Irf7	0.207
Tyrobp	0.166
Cd86	0.352
Tlr7	0.216
Ccl5	0.463
Pik3cγ	0.202
Nlrp3	0.240
Ptgs2	2.412
Msr1	0.308
Fas	2.729
Cybb	0.225
Plau	0.335
Fcγr1	0.154
Marco	0.401

Complement System	
Itgam	0.155
C1qc	0.092
C3	0.451
Itgβ2	0.147
C1qb	0.098
C1qa	0.085
C4b	0.401

Chemokine Signalling	
Ccr5	0.282
Ccl5	0.463
Plcβ2	0.297
Ptk2β	0.441
Pik3cγ	0.202
Plcg2	0.314
Ccl12	0.394
Cxcl16	0.427

Transport Channels	
Slc16a3	0.331
Atp1a3	0.420
Atp2a3	0.421
Kcnk1	2.112
Kcnk6	0.317

Ca^{2+}/PLC Signalling	
Plcβ2	0.297
Pld4	0.089
Plcγ2	0.314
Atp2a3	0.421
Trpc3	0.277
Lcp2	0.216
Syk	0.309
Fcγr2β	0.302
Gnas	0.454
Nlrp3	0.240
Adcy7	0.374
Btk	0.251
Fcer1γ	0.263
Pld4	0.089
Blnk	0.356
Gna15	0,234
Tlr9	0.290
Cd86	0.352
Ccr5	0.282
Ccl5	0.463

Lysossomal Regulation	
Slc11a1	0.136
Laptm5	0.126
Ctse	0.149
Syt11	2.370
Hexb	0.489
Ctss	0.145

Integrin Signalling	
Itgam	0.155
Itgal	0.152
Pik3r5	0.400
Tlr9	0.290
Itgβ2	0.147
Rac2	0.118
Pik3cγ	0.202
Plcg2	0.314
Was	0.233
Pik3cδ	0.355
Arhgap4	0.356
Arhgap9	0.282
Lgals9	0.306

Axonal Guidance	
Plcβ2	0.297
Adam8	0.346
Sema4c	0.426
Pik3r5	0.400
Tlr9	0.290
Rac2	0.118
Arpc1b	0.408
Pik3cγ	0.202
Plcγ2	0.314
Was	0.233
Pik3cδ	0.355
Gnas	0.454
Serpini1	3.308
Apbb1ip	0.330

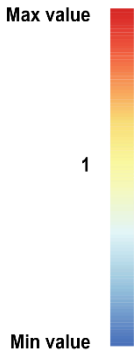

Among the genes involved in the pathways targeted by PGC-1α3, we confirmed the expression of key targets involved in one or more of the identified signalling pathways. Transcript expression levels were evaluated through RT-qPCR using specific primers. We started to validate the increase in expression levels of total PGC-1α ($p<0.01$), which increased 2800 times over control. Amongst the differentially regulated canonical pathways we selected different genes that represent the PGC-1α3-targeted pathways. Surprisingly, validation by RT-qPCR revealed that most of the genes that presented significantly changes in gene expression after PGC-1α3 expression were up-regulated. Indeed, mRNA levels of Itgβ2, Plcβ2, Laptm5, Slc16a3, Ccr5, FcγRIIb are significantly increased ($p<0.05$) as well as Apbb1ip, Msr1, Ctss, Ccl5, FcγRIII ($p<0.01$), Plau, Atp2a3 ($p<0.001$) and Tlr7 ($p<0.0001$) genes. The remaining genes show no variation in their expression patterns.

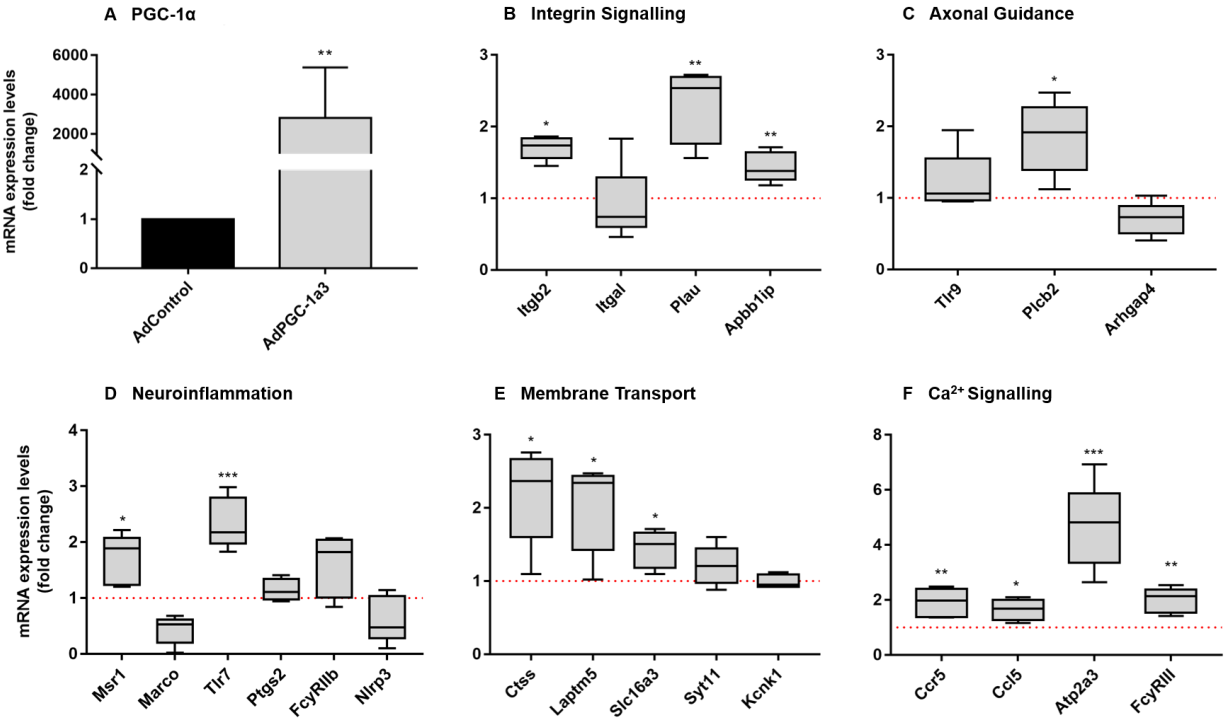

Figure III.8 – RT-qPCR validation of gene expression associated with the molecular pathways identified by IPA. Primary mouse astrocytes 15DIV transduced as described in methods section. Expression of (A) total PGC-1α and genes associated with (B) integrin signalling, (C) axonal guidance, (D) neuroinflammation, (E) membrane transport and (F) Ca^{2+} Signalling were analysed by RT-qPCR. Values were normalized to the housekeeping gene EEF and are expressed as fold change relative to GFP-transduced cells. Data represents means ± SEM from at least five individual experiments (n=5). *p<0.05, **p<0.01, ***p<0.001.

2.3 PGC-1α3 regulates astrocytic secretory function in primary cultures of astrocytes

As can be seen from the previously presented data (Table III), PGC-1α3 seems to have a strong regulatory role in genes involved in astrocyte-neuronal crosstalk. Thus, we decided to determine the secretome of astrocytes overexpressing PGC-1α3. We used a previously published bioinformatics pipeline that is able to integrate information from both canonical and non-canonical secretory pathways. We submitted protein sequences of our differentially expressed genes to TargetP, SignalP and TMHMM bioinformatic tools which determine the subcellular localization, presence of signal peptides and existence of transmembrane helix domains, respectively. By overlaying their outputs, we were able to infer the identity of proteins most likely secreted by canonical pathway. On the other hand, it doesn't have clear sequence-based rules to determine whether proteins are secreted, so SecretomeP uses trained neural networks and finds similarities between known secreted proteins secreted via non-classical pathways. This analysis yielded dataset totalling 210 secreted proteins, of which 70 are secreted through the classical pathway and 140 through the non-classical one.

Table III.2 – Ten most up- or downregulated genes encoding secreted proteins through the classical and non-classical secretory pathway. Secreted proteins were determined by submitting DEGs list to previously published pipeline containing TargetP, SignalP and TMHMM for determining classical secretion and SecretomeP for non-classical secretion. Fold change results are imported from the DEGs dataframe analysis.

Classical Pathway	Fold Change	Non-classical Pathway	Fold Change
Angptl4	3,370	Novel KRAB box and zinc finger (Predicted genes)	3,927
Serpini1	3,308	Complement component C3	0,451
Prostaglandin H2	2,412	Actin-related protein 2/3 complex	0,408
CCL5	0,463	Lymphocyte-specific protein	0,404
Apolipoprotein D	0,423	CYP4F15 enzyme	0,397
Cathepsin E	0,149	Interferon-inducible GTPase 1	0,363
Integrin β	0,147	Galectin 9	0,306
Cathepsin S	0,145	Myelin basic protein	0,298
TGFβ	0,130	Tyrosine-protein phosphatase non-receptor	0,291
Complement component C1q	0,092	Stabilin-1	0,110

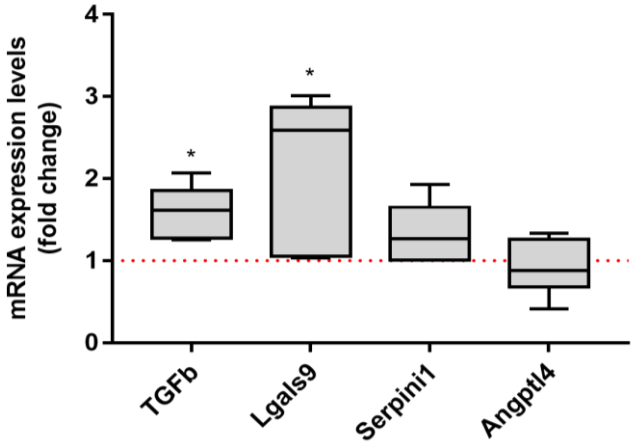

Figure III.9 – PGC-1α3 overexpression modulates transcript levels of genes encoding secreted proteins through classical and non-classical secretory pathways. Primary mouse astrocytes 15DIV transduced as described in the methods section. Transcript levels of TGFβ, Lgals9, Serpini1 and Angplt4 were analysed by RT-qPCR. Values were normalized to the housekeeping gene EEF and are expressed as fold change relative to GFP-transduced cells. Data represents means ± SEM from at least five individual experiments (n=5). *p<0.05.

As expected, the majority of identified proteins have reduced gene expression in our dataset. To proceed with further studies, we selected ten genes with the highest differences in fold change for both classical and non-classical pathways. Subsequently, we decided to validate the gene expression of the most relevant secreted proteins of that list. Transcript expression levels of TGFβ, Lgals9, Serpini1 and Angplt4 genes were evaluated through RT-qPCR using specific primers. TGFβ and Lgals9 transcript levels are significantly increased to 1.6 and 2.2-fold, respectively, over control ($p<0.05$), while Angptl4 shows no variation in its expression pattern. Serpini1 seems to have a slight increase in its mRNA levels, although not statistically significant, this time validating the tendency predicted by the bioinformatic analysis.

2.4 Pseudogene expression is strongly regulated by PGC-1α3 overexpression in primary cultures of astrocytes

As presented in Table III, PGC-1α3 transduction in astrocytes upregulates mostly pseudogenes. They are considered to be biologically dysfunctional, however they are well preserved within the genome, suggesting that they may indeed have a certain role in the cell [182]. Specifically, it was shown that pseudogenes could play a role in the regulation of miR expression [182].

Nonetheless, they highly resemble real genes, therefore it is possible that they might be just a result of misaligning reads at the beginning of RNASeq data analysis. Unfortunately, discerning those differences is difficult in batch computation pipelines, thus, we decided to verify if the differentially expressed pseudogenes correspond to genomic regions that present specific epigenetic modifications, namely, histone H3 lysine 4 mono- and trimethylation and histone H3 lysine 27 acetylation, binding of RNA polymerase II and DNAse hypersensitive sites, markers of active transcription. We displayed raw reads in the IGV genome browser alongside the tracks from ChIP-Atlas epigenetic modifications database and the reference genome used to align the reads. We observed that most of the identified pseudogenes have markers for transcriptional activity like histone H3 lysine 4 mono- and trimethylation ratios that are frequently found in long non-coding RNAs (Figure III.10A-C). In fact, we validated by RT-qPCR the upregulation of mRNA levels of Gm14403, which is significantly increased to about 1.42-fold over control ($p<0.001$) (Figure III10.D). This pseudogene is one of the

identified by the bioinformatic analysis as being increased and that displayed epigenetic markers (Table III.1 and Figure III.10C).

Suspecting that these pseudogenes are not the results of mis-mapped reads, we can evaluate at what extent in our dataset we detect the up- or downregulation of miRs. To that end, we used GSEA software platform to determine which miRs might be modulated by PGC-1α3 overexpression. This analysis is based on association of different gene sets to both single miRs and miRs clusters. Therefore, for each gene set, we might have one or several miRs as identified hits. There were identified 20 significantly differentially expressed miRs and three miRs clusters, all of them being upregulated. This adds up to 29 putative differentially expressed miRs in response to PGC-1α3 overexpression (Figure III.11A). From this 29 identified miRs, we decided to verify which are highly expressed in human brain and, therefore, the ones that can have the biggest relevance for our future studies. For that, we checked a miRs database for expression values and verified that miR-92, miR-26, miR-25, miR-186, miR520f and miR-363 are the most expressed in human brain (Figure III.11B) [183].

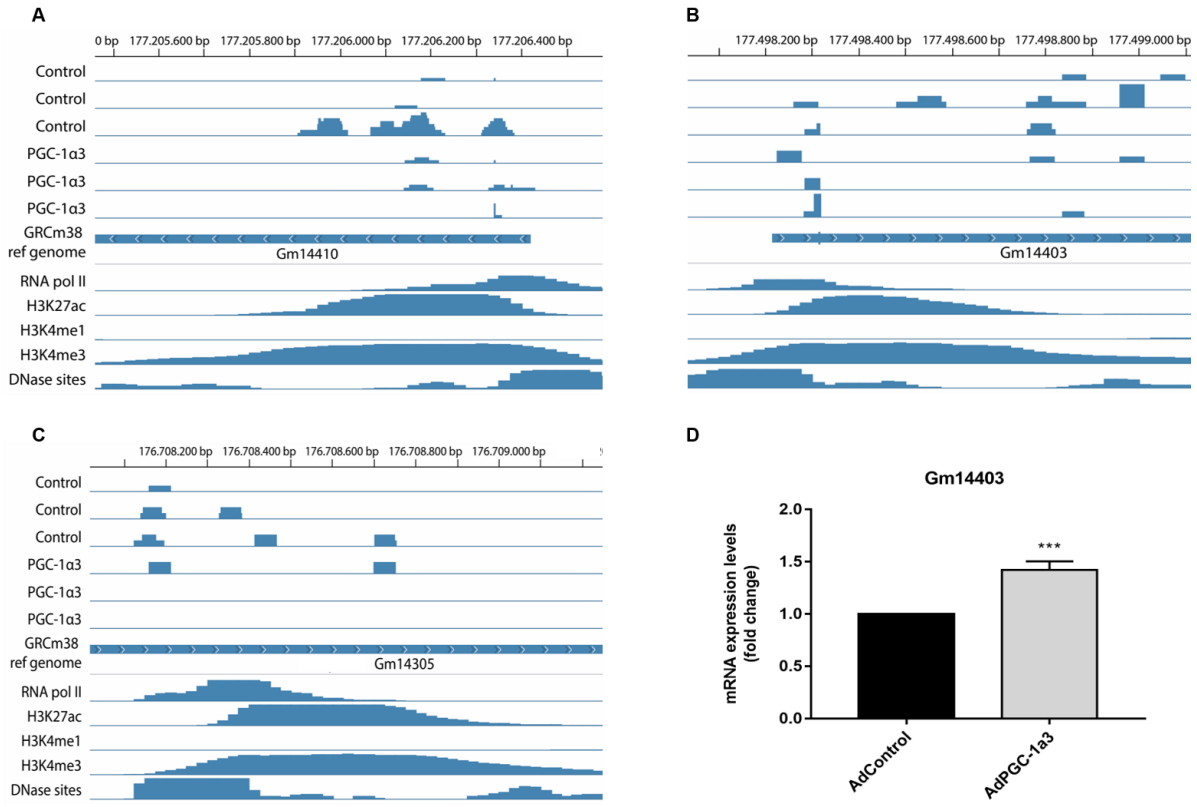

Figure III.10 – Pseudogenes regulated by PGC-1α3 are transcriptionally active in primary cultures of astrocytes. (A-C) IGV graphs top view shows aligned raw reads of (A) Gm14410, (B) Gm14403 and (C) Gm14305 pseudogenes in which the top three rows correspond to AdControl transduced astrocytes and the following three to AdPGC-1α3 transduction. Middle track shows NCBI's *Mus musculus* reference genome used to align the raw reads. Bottom view presents ChIP-seq epigenetic marks from neuronal cell line in this order (top to bottom): RNA polymerase II docking sites, H3K27 acetylation, H3K4 monomethylation, H3K4 trimethylation and DNAse sensibility site markers. Raw reads are shown as blue. (D) Primary mouse astrocytes 15DIV transduced as described in the methods section. mRNA levels of Gm14403 were analysed by RT-qPCR. Values were normalized to the housekeeping gene EEF and are expressed as fold change relative to GFP-transduced cells. Data represents means ± SEM from six individual experiments (n=6). ***p<0.001.

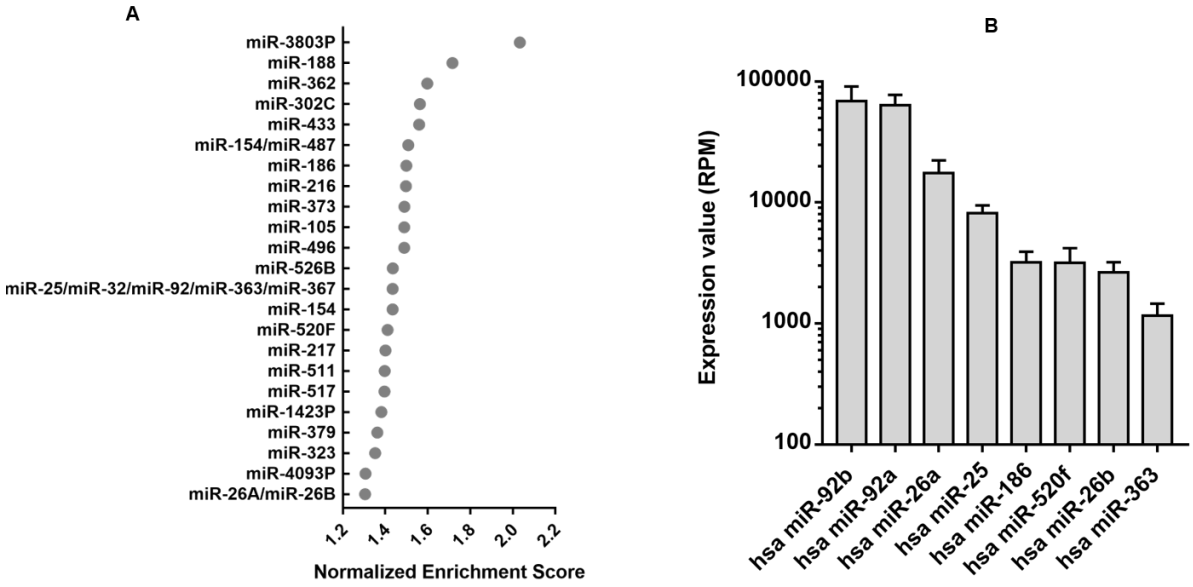

Figure III.11 – PGC-1α3 overexpression upregulates the expression of different miRs. (A) GSEA analysis enriched miRs in AdPGC-1α3 transduced astrocytes when compared with AdControl transduction. Analysis performed according with normalized enrichment score (NES) calculated by GSEA, with a cut-off of FDR<0.25. (B) Bar graph representing the five most expressed miRs identified by our analysis in human brain (hsa miR). The left axis represents the reads per million (RPM) values corresponding to each miR [183].

IV. DISCUSSION

In this thesis, we set out to characterize the molecular pathways controlled by PGC-1α3 in the brain and understand how PGC-1α3 affects astrocytic function. PGC-1α family of proteins mainly regulates energy metabolism and oxidative phosphorylation in metabolically demanding tissues to which brain certainly belongs. Aberrant mitochondrial function also links them to the progression of neurodegenerative diseases such as AD or PD. The characterization of pathways regulated by PGC-1α proteins will allow to understand if they take part of the crosstalk between astrocytes and neurons, if they may influence composition and identity of astrocyte secreted metabolites, given astrocytes previously described as the main secretory cells of CNS. And finally, we wanted to confirm our long-standing notion, that by negatively modulating mitochondrial function they might be responsible for induction of neurodegeneration.

1 PGC-1α3 modulates postsynaptic protein levels by regulating posttranslational modifications

We have chosen the viral transduction of isolated neurons and astrocytes as a core methodology to be able to successfully dissect the role of PGC-1α3 on individual CNS cell types. Initially we have tested all PGC-1α isoforms described by Ruas and collaborators for their possible influence on neuronal and astrocytic function [154]. Our preliminary results show the PGC-1α3 ectopic expression in primary cultures of mice cortical neurons leads to decreased levels of postsynaptic proteins. PGC-1α proteins act as co-activators of gene expression and therefore it seemed plausible that the decrease in levels of postsynaptic proteins would reflect changes in gene transcription. Surprisingly, our results showed that the observed decrease at the protein level of SHANK3, PSD-95 and MAP2 did not correlate with a decrease in the respective transcript levels, suggesting that PGC-1α3 does not directly affect postsynaptic gene transcription, but there is another regulation level at play. PGC-1α doesn't possess any enzymatic activity by itself, but it might be able to bind other proteins to stabilize them. Also, PGC-1α1 can induce the expression of particular enzymes that mark the postsynaptic proteins for degradation, such as components of ubiquitin proteasome system such as E3 ligases [184]. Thus, the most feasible explanation is that PGC-1α3 regulates expression of either components or enzymes capable of proteolytic cleavage. Calpains are a family of ubiquitously expressed calcium-activated cysteine proteases, known to control Ca^{2+} influx by cleaving most glutamate receptors and leading to a reduction of their function [185]. In fact, both MAP2 and PSD-95 were shown to be targets of calpains action, which supports this hypothesis [186,187]. Since PSD-95 might be degraded, its postsynaptic complex disassembles, therefore, its components, such as SHANK3 might be targeted for proteolysis, which could explain the observed decrease in its protein levels. To confirm this hypothesis, we should measure calpain transcript and protein levels and, more importantly their activity rate under the same conditions.

The fact that PGC-1α3 ectopic expression induced the downregulation of synaptic protein levels, led us to evaluate neuronal morphology by performing immunofluorescence for neuronal βIII-tubulin in cells transduced with PGC-1α3 virus. Surprisingly, and in contrary

to previous results obtained in rat cortical neurons, we observed that there was hardly any colocalization between βIII-tubulin staining and GFP, indicating that cells being transduced are not neurons [171].

Therefore, we performed an unbiased RNASeq on astrocytic cultures instead, in order to identify PGC-1α3 downstream targets that might be responsible for the observed decrease in post-synaptic proteins in neurons. Interestingly, with respect to DEGs in response to PGC-1α3 isoform overexpression, the majority of them are downregulated. This in turn translates into a strong downregulation of most of the cellular pathways identified by IPA analysis. Amongst the identified pathways and genes, we observe a strong reduction of genes related with complement system, namely C1q (the most downregulated gene of our analysis) and C3; neuroinflammation, with TGFβ1, Marco and Msr1; cell adhesion, such as Itgβ2 and Itgαm; and axonal guidance, namely PLCβ2, TLR9 and Apbb1ip. Also, as a result of IPA analysis, we observe that cell migration may be significantly decreased. This is an interesting observation, since there has been a notion that PGC-1α3 acts as a co-repressor and might be able to antagonize the functions of PGC-1α1.

2 PGC-1α3 reduces overall gene expression by regulating AMPK activation and ROS production

After CNS injury, brain cells are known to release damage-associated molecular patterns (DAMPs), which in turn are cleared by the scavenger receptor Msr1 in mice [188]. Combined deficiency of both Msr1 and Marco scavengers causes more severe inflammation and aggravated neuronal injury in a murine model of ischemic stroke [188]. TLRs are the major DAMP receptors, with TLR9 being the only one that can be stimulated by mitochondrial DNA. Recently, an alternative TLR9 signalling pathway was characterized in neurons [189]. TLR9 stimulation impairs Ca^{2+} uptake into the ER which leads to a decrease in mitochondrial calcium concentrations, increasing the AMP/ATP ratio and activating AMPK [189].

AMPK is a key inducer of PGC-1α activity and it is described as the major metabolic switch of the cell. Indeed, it was shown that AMPK-mediated PGC-1α activation regulates GCL modulatory subunit expression exclusively on astrocytes [190]. It was also observed that PGC-1α knockdown blocked its expression and, therefore, lead to increased ROS levels [190]. Thus, GCL expression is promoted in a PGC-1α-dependent way in order to regulate GSH activity and, consequently, the antioxidant activity of astrocytes.

Many upstream signals have been described to regulate AMPK activity. TLR9-dependent AMPK activation was shown to promote actin polymerization and Rho pathway in vascular smooth muscular cells [191]. Moreover, a recent study in ovarian cancer cells show that CaMKKIIβ/PLCβ-activated AMPK induces cytoskeleton rearrangements by promoting upregulation of actin-remodelling proteins through the Rho pathway [192]. TLR9 and PLCβ appear in our list of DEGs, therefore it would be interesting to determine AMPK phosphorylation levels in PGC-1α3-transduced astrocytes.

PGC-1α3 was shown to contra-regulate PGC-1α1 target genes, therefore one can suggest that PGC-1α3 could eventually potentiates ROS production by downregulating GCL subunit expression [159]. The levels of GSH would be reduced and, consequently, there will be a decrease is ROS detoxification. This hypothesis can have repercussions in neurons, since

shuttling of GSH and its precursors are instrumental in the astrocytic neuroprotective effect because neurons highly depend on GSH to detoxify ROS. To verify this hypothesis, we could measure ROS levels, and perform cell viability assays.

Moreover, since ROS is known to damage mitochondrial DNA, we could assume an increase in the activation of TLR9 and consequently an increase in AMPK activation. However, our results present decreased TLR9 levels. PGC-1α was shown to repress NF-κB transcriptional activity in skeletal muscle [193]. Therefore, we can hypothesize that PGC-1α3 might promote the same effect in astrocytes, which explains why there is no inflammatory response to ROS increase, and also there is a decreased expression of TLR9. Measuring NF-κB and assessing ATP levels will give us more conclusive regarding the putative inhibition of this pathway.

Without AMPK activation, either by TLR9 or by PLCβ, which is also downregulated in our analysis, astrocytes cannot migrate, for example, to lesion sites. This is also supported by the observed upregulation of PTEN signalling in our analysis, one of the few pathways being increased besides PPAR signalling. PTEN inhibits PI3K/Akt signalling, which is downregulated in our analysis and it is involved in promoting cell cycle and movement. Also, these results go accordingly with the observed role of PGC-1α3 in regulating cell movement in myotubes.

3 PGC-1α3 might induce different splicing events and promote the formation of unknown transcript splicing variations

RNA-Seq analysis is an unbiased methodology and therefore serves well as a discovery tool. To confirm our hypotheses, results must be further validated by qPCR. To this end, we have evaluated the expression of several representative genes, but we were not able verify the predicted global downregulation, instead we observe a general increase of the transcript levels. Although not expected, this outcome has several possible explanations.

To identify the downstream targets of PGC-1α3 in astrocytes by RNA-sequencing we used DESeq2 package with multi-factor design for paired analysis. As rationale for pairing, we set the DESeq2 contrasts for glm to use two different parameters: (i) comparing AdPGC-1α3 transduced samples with the corresponding controls and (ii) group the samples according with the brain that the astrocytes come from. The pairing for the brain was based on the fact that neuronal and astrocytic cultures coming from different brain preparations are cultivated in conditions that are difficult to reproduce. Over time, the characteristics of neurons and astrocytes in culture change together with gene expression levels. Pairing them helps to partially remove these inconsistencies. Unfortunately, DESeq2 R package is not entirely optimized for this kind of analysis. We observed some variations between the tendencies of expression of DEGs between each sample pair. For example, pair 1 shows a slight upregulation of a certain DEG, while pair 2 shows a strong downregulation and in pair 3 we observe no change in the raw read count (data not shown). In the end, the final result takes into consideration the magnitude of change, which is also dependent on basal expression level in a particular culture. This can manifest itself when the gene is upregulated in pair 1 and not differentially expressed in pair 3, it will come out of the analysis as downregulated because pair 2 strong trend will overcome all the others.

Previously published analysis of gene programs regulated by PGC-1α proteins shows their significant separation. PGC-1α3 and PGC-1α2 seem to contra-regulate the target genes PGC-1α1. Moreover, PGC-1α3 has shown to have a splicing pattern complementary to that of PGC-1α1 as demonstrated on Ndrg4, Ddx27 and Osbpl1a genes. This has several implications for the results obtained from our RNASeq analysis. If one of the roles of PGC-1α3 is to regulate splicing events, we might observe discrepancies between RNASeq data and subsequent qPCR validation. While RNASeq takes into consideration all the reads that fall within the exons of a particular gene, standard qPCR only looks at a very short stretch, usually around 100bp. Thus, it is easy to imagine that if PGC-1α3 promotes splicing of a particular isoform and increases its expression, the qPCR validation might miss such an event and it might manifest itself either as no change or even a decrease in expression. Several alternatives exist to tackle this problem. It is possible to perform differential exon expression analysis on RNASeq data with R packages such as Ballgown or DEXSeq. Unfortunately, this analysis is based on statistics and relies heavily on the depth of sequencing and length of sequenced reads in order to successfully identify exon-exon boundaries in transcripts. Array-based methodologies exist to differentiate in-between gene isoforms such as the one employed in comparing induction of splicing between different PGC-1α isoforms. Unfortunately, far more exons are present in the genome than can be reasonably placed on microarray. Therefore, only several probes are used per particular gene, introducing bias into this methodology. The third approach is to manually inspect RNASeq data for changes in read numbers in particular exons and then design specific probes for qPCR to differentiate between them. Although this approach is probably least prone to mistakes, it is also the most tedious one and unsuitable for high-throughput analysis.

Secondly, if PGC-1α3 induces different splicing events, it might promote the formation of unknown transcripts. Our pipeline uses HTSeq framework to count reads and relies on published annotation of gene features such as exons for particular reference genome. If PGC-1α3 overexpression leads to overall production of unknown transcripts, these will not be accounted for. To overcome this shortcoming, we can produce *de novo* transcript assembly instead of using a reference genome. Software packages such as Cufflink or Trinity offer this functionality.

qPCR is generally more sensitive than RNA-Seq analysis on an individual gene basis. Moreover, due to the sheer amount statistical tests of significance, genes with higher variability of expression or modest changes might not be reported as differentially expressed. For example, we had to design a specific primer for Angptl4 gene that amplified a specific sequenced site because other primers were not amplifying our transcript. This suggests that Angptl4 can be one of many DEGs where PGC-1α3 promotes new splicing events and consequently new transcripts with unknown functions.

4 PGC-1α3 overexpression in astrocytes reduces glutamate uptake and promotes excitotoxicity

Our qPCR results show an upregulation of Ca^{2+} mobilization genes through PLC pathway, namely, Atp2a3 (which encodes for Serca3 transporter), PLCβ2, CCL5, CCR5 and FcγRIII as well as increase of transcript levels of CamKIδ, NFATc1, NFATc3 and decrease of NFATc4. There are also neuroinflammation markers being upregulated, such as Msr1, TLR7 and FcγRIIb, and integrin signalling, namely, Itgb2, Plau and Apbb1ip (which encode, respectively, for uPA and RIAM proteins). Furthermore, we can also verify increased expression of Slc16a3 lactate transporter gene, increased lysosomal activity, with upregulation of Ctss and Laptm5, as well as decrease in the levels of glutamate transporters EAAT1 and 2.

Ying-yang 1 (YY1) transcription factor is known to downregulate EAAT1 and 2 transporters expression in a NF-κB dependent manner [194]. Since PGC-1α3 specific role in the NF-κB pathway has not been studied yet, we can say that NF-κB regulation might be context-dependent. Thus, PGC-1α3 overexpression might induce NF-κB activity, leading to increased YY1 promoter activity that, in turn, diminishes EAAT1 and 2 expression levels (Figure IV.1). Consequently, there will be a decrease in the uptake of glutamate from the synaptic cleft, inducing excitotoxicity. This can explain the effects observed in primary neuronal cultures, since excess extracellular glutamate causes a massive neuronal influx of Ca^{2+} through NMDAR, which activates calpains and, consequently, proteolytic cleavage of AMPAR and postsynaptic proteins. Moreover, this increase in extracellular glutamate will keep astrocytic G_q-protein-coupled receptors activated, such as metabotropic glutamate transporters, that, when stimulated, induce PLC activity and formation of IP_3. This results in Ca^{2+} release from intracellular IP_3-sensitive Ca^{2+} stores, such as ER, and increase in intracellular Ca^{2+} concentration. Our results support the activation of this pathway since we observe increased levels of PLCβ2, Atp2a3, which promotes Ca^{2+} transport back to the ER, CCL5 and FcγRIII which are also involved in regulating Ca^{2+} mobilization. Also, CamKIδ and NFAT isoforms, well-established targets of Ca^{2+} signalling, are also differentially regulated.

Astrocytic secretory properties are known to be modulated by variations in Ca^{2+} intracellular levels. Accordingly, levels of lysosomal formation-related genes, such as Ctss and Laptm5, are upregulated, meaning membrane transport might be increased due to elevated Ca^{2+} concentration. Furthermore, Ctss encodes for cathepsin S which is secreted to the extracellular space where it degrades ECM proteins, such as laminin and fibronectin. Concomitantly, our results show that Apbb1ip gene is upregulated together with other integrin signalling genes, such as Plau and Itgβ2. All these genes are related with ECM remodelling.

Secretory lysosomes are an efficient way for the cell to export several molecules to the extracellular space, such as cytokines, peptides and miRs. Galectin 9 is a secreted protein encoded by Lgals9 gene, which is upregulated in our results. Consistent with the putative ECM remodelling induced by PGC-1α3, increased secretion of this protein was also shown to reduce cell adhesion to ECM proteins of MCF7 breast cancer cell line [195]. Furthermore, it was shown that astrocytic galectin 9 potentiates microglial tumour necrosis factor secretion, inducing neuroinflammation [196].

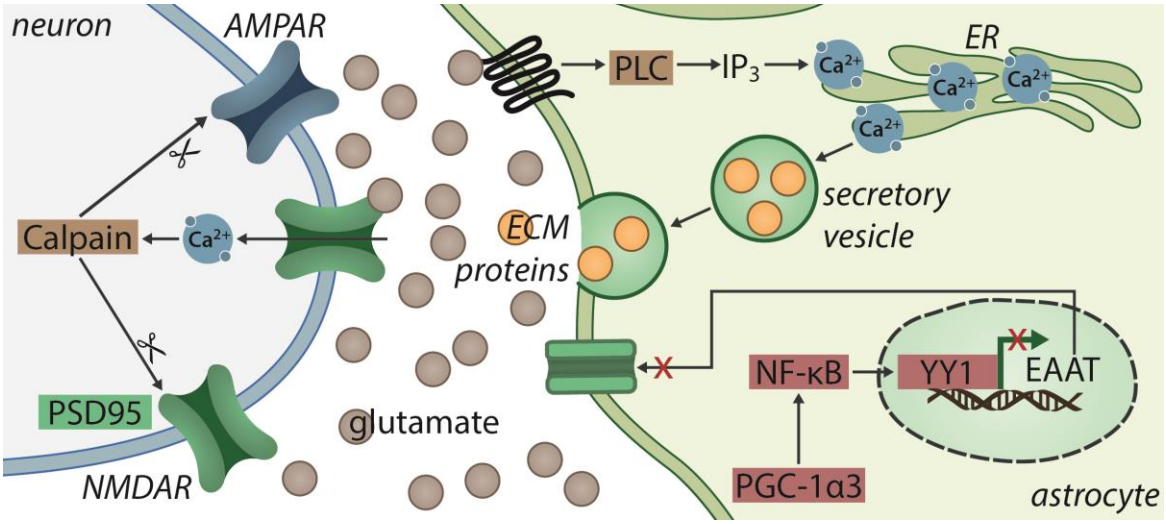

Figure IV.1 – Putative role of PGC-1α3 overexpression in excitotoxicity and secretion of ECM remodelling proteins. PGC-1α3 induces NF-κB activity, leading to increased activity of YY1 promoter which, in turn, diminishes EAATs expression levels. Consequently, there is an accumulation of glutamate in the synaptic cleft, inducing excitotoxicity. Excess extracellular glutamate causes a massive neuronal influx of Ca^{2+} through NMDAR, which activates calpains and, consequently, proteolytic cleavage of AMPAR and postsynaptic proteins. Furthermore, extracellular glutamate will keep activating astrocytic Gq-protein-coupled receptors, inducing PLC activity and IP_3 formation, which results in Ca^{2+} release from ER. This leads to an increase in intracellular Ca^{2+} concentration which activates astrocytic secretory pathways, inducing the release of ECM remodelling proteins, such as urokinase, galectin 9 and TGFβ.

TGFβ is secreted as an inactive complex containing latent TGFβ binding protein and latency associated peptide [197]. Until activation, TGFβ remains latent in the extracellular space, bind to fibronectin [197]. Upon activation by proteases, such as plasmin, TGFβ binds to TGFβ1-induced antiapoptotic factor (TIAF) that activates the SMAD pathway. Plau gene encodes for urokinase, an enzyme that catalyses the conversion of plasminogen into plasmin [198]. Therefore, upregulation of Plau leads to increased levels of plasmin that can activate TGFβ, explaining the observed transcriptional upregulation of the respective gene. Furthermore, it was suggested that TGFβ might play a role in promoting amyloid β plaque formation by inducing TIAF aggregation, which, in turn, leads to dephosphorylation of amyloid precursor protein, followed by its degradation and formation of amyloid β [199].

5 PGC-1α3 overexpression induces the expression of transcripts that map to pseudogenes, which might regulate miR expression

The characterized transcriptome presents few upregulated genes. However, most of them consist in non-characterized pseudogenes. Pseudogenes highly resemble real genes, therefore their predicted expression in the bioinformatics results could be the consequence of mis-mapped reads. Therefore, we checked if our differentially expressed pseudogenes had markers for transcriptional activity. We verified that they all markers consistent with transcription, namely, most of them have high H3K4 tri/monomethylation ratio, which is consistent with what is observed for long noncoding RNAs. Both long noncoding RNAs and pseudogenes have been described to have regulatory functions. In fact, pseudogenes were recently associated with miR buffering, meaning that, due to their high resemblance to real genes, they compete for miR binding, cancelling their effect [182].

From all the identified miR, miR-186 and miR-26 seem to have the most striking effects in brain. miR-186 suppresses glycolysis induced by hypoxia factor 1, which is, in turn, a target of PGC-1α regulation [200]. Furthermore, miR-186 also suppresses β-site amyloid precursor protein-cleaving enzyme 1 [201]. On the other hand, miR-26 modulates BDNF expression and represses PTEN signalling, promoting neurite outgrowth, regulates neuronal differentiation and its dysregulation increases Ptgs2 expression in macrophages, a tendency also observed is our astrocytic transcriptome [202–204]. Since the lysosomal pathway seems to be increased, it is plausible that these miRs could be exported and have an effect on neurons.

To better understand the putative effects of astrocytic secreted proteins and miRs in neurons, we could use astrocytic media (which contains secreted factors) in neuronal cultures and by performing PGC-1α3-transduced astrocytic/neuronal cocultures. We would verify miR expression those cultures by performing specific TaqMan assays. It would be interesting to evaluate astrocytic secreted factors effects in neurons by performing immunostaining followed by Sholl analysis in order to determine the effect of these proteins in dendritic arborization.

Neurodegenerative diseases are a truly global challenge and one of the leading medical and societal challenges faced by EU society. To date, there are no effective treatments that can slow or halt these diseases, and currently approved drugs only temporary ameliorate symptoms. Therefore, is imperative that drug discovery attempts to identify new potential therapeutic targets to open new therapeutic avenues. Thus, in the aftermath of our work, we will pursue to better characterize PGC-1α3 induced phenotype in astrocytes and the interplay between astrocytes and neurons and its role in pathogenesis of neurogenerative disorders such as AD and PD. Namely, it will be important to observe if the lack/ increased expression of astrocytic PGC-1α3 in mice effects in the age of onset and disease progression. This will help to explore possible novel therapeutic targets and pathways that can be beneficial human health in an area where no significant advances have been made.

V. REFERENCES

1. Betts, J. G. *et al.* Anatomy of the Nervous System. in *Anatomy & Physiology* Chapter 13 (2013).
2. Wolf, U., Rapoport, M. J. & Schweizer, T. A. Evaluating the Affective Component of the Cerebellar Cognitive Affective Syndrome. *J. Neuropsychiatry Clin. Neurosci.* (2009). doi:10.1176/jnp.2009.21.3.245
3. Bzdok, D., Laird, A. R., Zilles, K., Fox, P. T. & Eickhoff, S. B. An investigation of the structural, connectional, and functional subspecialization in the human amygdala. *Hum. Brain Mapp.* (2013). doi:10.1002/hbm.22138
4. Shipp, S. Structure and function of the cerebral cortex. *Current Biology* (2007). doi:10.1016/j.cub.2007.03.044
5. Ramón y Cajal, S. *Histologie du Systeme Nerveux de l'Homme et des Vertebres. Maloine, Paris: 1911. chap. II*. *Demography* (1909). doi:10.5962/bhl.title.48637
6. Lodish, H. *et al.* Nerve Cells. in *Molecular Cell Biology* Chapter 22 (2013).
7. Pereda, A. E. Electrical synapses and their functional interactions with chemical synapses. *Nature Reviews Neuroscience* (2014). doi:10.1038/nrn3708
8. Lodish, H. *et al.* Cell organization and Movement II: Microtubules and Intermediate Filaments. in *Molecular Cell Biology* Chapter 18 (2013).
9. Tischfield, M. A. *et al.* Human TUBB3 Mutations Perturb Microtubule Dynamics, Kinesin Interactions, and Axon Guidance. *Cell* (2010). doi:10.1016/j.cell.2009.12.011
10. Hamilton, W. B., Kaji, K. & Kunath, T. ERK2 Suppresses Self-Renewal Capacity of Embryonic Stem Cells, but Is Not Required for Multi-Lineage Commitment. *PLoS One* (2013). doi:10.1371/journal.pone.0060907
11. Petrelli, F. & Bezzi, P. Novel insights into gliotransmitters. *Current Opinion in Pharmacology* (2016). doi:10.1016/j.coph.2015.11.010
12. Rothstein, J. D. *et al.* Localization of neuronal and glial glutamate transporters. *Neuron* (1994). doi:10.1016/0896-6273(94)90038-8
13. Eng, L., Gerstl, B. & Vanderhaeghen, J. A study of proteins in old multiple sclerosis plaques. *Trans Am Soc Neurochem* 42 (1970).
14. Pekny, M. *et al.* Mice lacking glial fibrillary acidic protein display astrocytes devoid of intermediate filaments but develop and reproduce normally. *EMBO J.* (1995). doi:10.1002/j.1460-2075.1995.tb07147.x
15. Gomi, H. *et al.* Mice devoid of the glial fibrillary acidic protein develop normally and are susceptible to scrapie prions. *Neuron* (1995). doi:10.1016/0896-6273(95)90238-4
16. Bushong, E. A., Martone, M. E., Jones, Y. Z. & Ellisman, M. H. Protoplasmic astrocytes in CA1 stratum radiatum occupy separate anatomical domains. *J. Neurosci.* (2002). doi:22/1/183 [pii]
17. Sofroniew, M. V. Molecular dissection of reactive astrogliosis and glial scar formation. *Trends in Neurosciences* (2009). doi:10.1016/j.tins.2009.08.002
18. Cahoy, J. D. *et al.* A Transcriptome Database for Astrocytes, Neurons, and Oligodendrocytes: A New Resource for Understanding Brain Development and Function. *J. Neurosci.* **28,** 264–278 (2008).
19. Houades, V., Koulakoff, A., Ezan, P., Seif, I. & Giaume, C. Gap Junction-Mediated Astrocytic Networks in the Mouse Barrel Cortex. *J. Neurosci.* **28,** 5207–5217 (2008).
20. Kumar, N. M. & Gilula, N. B. The gap junction communication channel. *Cell* (1996). doi:10.1016/S0092-8674(00)81282-9

21. Escartin, C. & Rouach, N. Astroglial networking contributes to neurometabolic coupling. *Frontiers in Neuroenergetics* (2013). doi:10.3389/fnene.2013.00004

22. Verkhratsky, A., Matteoli, M., Parpura, V., Mothet, J.-P. & Zorec, R. Astrocytes as secretory cells of the central nervous system: idiosyncrasies of vesicular secretion. *EMBO J.* **35,** 239–257 (2016).

23. Prebil, M., Vardjan, N., Jensen, J., Zorec, R. & Kreft, M. Dynamic monitoring of cytosolic glucose in single astrocytes. *Glia* **59,** 903–913 (2011).

24. Rana, S. & Dringen, R. Gap junction hemichannel-mediated release of glutathione from cultured rat astrocytes. *Neurosci. Lett.* (2007). doi:10.1016/j.neulet.2006.12.043

25. Choi, S. S., Lee, H. J., Lim, I., Satoh, J. I. & Kim, S. U. Human astrocytes: Secretome profiles of cytokines and chemokines. *PLoS One* (2014). doi:10.1371/journal.pone.0092325

26. Lodish, H. *et al.* Vesicular Traffic, Secretion and Endocytosis. in *Molecular Cell Biology* Chapter 14 (2013). doi:NBK21471

27. Bezzi, P. *et al.* Astrocytes contain a vesicular compartment that is competent for regulated exocytosis of glutamate. *Nat. Neurosci.* (2004). doi:10.1038/nn1246

28. Prada, I. *et al.* REST/NRSF governs the expression of dense-core vesicle gliosecretion in astrocytes. *J. Cell Biol.* (2011). doi:10.1083/jcb.201010126

29. Li, D., Ropert, N., Koulakoff, A., Giaume, C. & Oheim, M. Lysosomes Are the Major Vesicular Compartment Undergoing Ca2+-Regulated Exocytosis from Cortical Astrocytes. *J. Neurosci.* (2008). doi:10.1523/JNEUROSCI.0744-08.2008

30. Haskew-Layton, R. E. *et al.* Two distinct modes of hypoosmotic medium-induced release of excitatory amino acids and taurine in the rat brain in vivo. *PLoS One* (2008). doi:10.1371/journal.pone.0003543

31. Stout, C. E., Costantin, J. L., Naus, C. C. G. & Charles, A. C. Intercellular calcium signaling in astrocytes via ATP release through connexin hemichannels. *J. Biol. Chem.* (2002). doi:10.1074/jbc.M109902200

32. Magistretti, P. J. Neuron-glia metabolic coupling and plasticity. in *Experimental Physiology* (2011). doi:10.1113/expphysiol.2010.053157

33. Bélanger, M., Allaman, I. & Magistretti, P. J. Brain energy metabolism: Focus on astrocyte-neuron metabolic cooperation. *Cell Metab.* **14,** 724–738 (2011).

34. Rouach, N., Koulakoff, A., Abudara, V., Willecke, K. & Giaume, C. Astroglial metabolic networks sustain hippocampal synaptic transmission. *Science (80-.).* (2008). doi:10.1126/science.1164022

35. Arriza, J. L. *et al.* Functional comparisons of three glutamate transporter subtypes cloned from human motor cortex. *J. Neurosci.* (1994). doi:10.1523/jneurosci.4876-07.2008

36. Pellerin, L. & Magistretti, P. J. Glutamate uptake into astrocytes stimulates aerobic glycolysis: a mechanism coupling neuronal activity to glucose utilization. *Proc. Natl. Acad. Sci.* (1994). doi:10.1073/pnas.91.22.10625

37. Pardo, B. *et al.* Brain glutamine synthesis requires neuronal-born aspartate as amino donor for glial glutamate formation. *J. Cereb. Blood Flow Metab.* (2011). doi:10.1038/jcbfm.2010.146

38. Suh, S. W. *et al.* Astrocyte Glycogen Sustains Neuronal Activity during Hypoglycemia: Studies with the Glycogen Phosphorylase Inhibitor CP-316,819 ([R-R*,S*]-5-Chloro-N-[2-hydroxy-3-(methoxymethylamino)-3-oxo-1-(phenylmethyl)propyl]-1H-indole-2-carboxamide). *J. Pharmacol. Exp. Ther.* (2007). doi:10.1124/jpet.106.115550

39. Brown, A. M. *et al.* Astrocyte glycogen metabolism is required for neural activity during aglycemia or intense stimulation in mouse white matter. in *Journal of Neuroscience Research* (2005). doi:10.1002/jnr.20335

40. Suzuki, A. *et al.* Astrocyte-neuron lactate transport is required for long-term memory formation. *Cell* (2011). doi:10.1016/j.cell.2011.02.018

41. Sofroniew, M. V. & Vinters, H. V. Astrocytes: Biology and pathology. *Acta Neuropathol.* **119,** 7–35 (2010).

42. Dringen, R. Metabolism and functions of glutathione in brain. *Prog. Neurobiol.* 649–671 (2000). doi:10.1016/S0301-0082(99)00060-X

43. Shih, A. Y. *et al.* Coordinate regulation of glutathione biosynthesis and release by Nrf2-expressing glia potently protects neurons from oxidative stress. *J. Neurosci.* (2003). doi:23/8/3394 [pii]

44. Itoh, K. *et al.* An Nrf2/small Maf heterodimer mediates the induction of phase II detoxifying enzyme genes through antioxidant response elements. *Biochem. Biophys. Res. Commun.* (1997). doi:10.1006/bbrc.1997.6943

45. Cooper, A. Role of Astrocytes in Maintaining Cerebral Glutathione Homeostasis and in Protecting the Brain Against Xenobiotics and Oxidative Stress. *Role Glutathione Nerv. Syst. Taylor Fr.* 91–115 (1998).

46. Meister, A., Tate, S. S. & Griffith, O. W. γ-Glutamyl Transpeptidase. *Methods Enzymol.* (1981). doi:10.1016/S0076-6879(81)77032-0

47. Dringen, R. & Hamprecht, B. Involvement of glutathione peroxidase and catalase in the disposal of exogenous hydrogen peroxide by cultured astroglial cells. *Brain Res.* (1997). doi:10.1016/S0006-8993(97)00233-3

48. Dringen, R., Pfeiffer, B. & Hamprecht, B. Synthesis of the Antioxidant Glutathione in Neurons: Supply by Astrocytes of CysGly as Precursor for Neuronal Glutathione. *J. Neurosci.* (1999). doi:10.1523/JNEUROSCI.19-02-00562.1999

49. Bolaños, J. P. *et al.* Nitric oxide-mediated mitochondrial damage: A potential neuroprotective role for glutathione. *Free Radic. Biol. Med.* (1996). doi:10.1016/S0891-5849(96)00240-7

50. Winterbourn, C. C. & Metodiewa, D. The reaction of superoxide with reduced glutathione. *Arch. Biochem. Biophys.* (1994). doi:10.1006/abbi.1994.1444

51. Ben-Yoseph, O., Boxer, P. a & Ross, B. D. Assessment of the role of the glutathione and pentose phosphate pathways in the protection of primary cerebrocortical cultures from oxidative stress. *J. Neurochem.* (1996). doi:10.1046/j.1471-4159.1996.66062329.x

52. Castro, M. A., Beltrán, F. A., Brauchi, S. & Concha, I. I. A metabolic switch in brain: Glucose and lactate metabolism modulation by ascorbic acid. *Journal of Neurochemistry* (2009). doi:10.1111/j.1471-4159.2009.06151.x

53. Pfrieger, F. W. Synaptic Efficacy Enhanced by Glial Cells in Vitro. *Science (80-.).* (1997). doi:10.1126/science.277.5332.1684

54. Adams, J. C. Functions of the conserved thrombospondin carboxy-terminal cassette in cell-extracellular matrix interactions and signaling. *International Journal of Biochemistry and Cell Biology* (2004). doi:10.1016/j.biocel.2004.01.022

55. Adams, J. C. Thrombospondins: Multifunctional Regulators of Cell Interactions. *Annu. Rev. Cell Dev. Biol.* (2001). doi:doi:10.1146/annurev.cellbio.17.1.25

56. Christopherson, K. S. *et al.* Thrombospondins are astrocyte-secreted proteins that promote CNS synaptogenesis. *Cell* **120,** 421–433 (2005).

57. Hennekinne, L., Colasse, S., Triller, A. & Renner, M. Differential Control of Thrombospondin over Synaptic Glycine and AMPA Receptors in Spinal Cord Neurons. *J. Neurosci.* (2013). doi:10.1523/JNEUROSCI.5247-12.2013

58. Xu, J., Xiao, N. & Xia, J. Thrombospondin 1 accelerates synaptogenesis in hippocampal neurons through neuroligin 1. *Nat. Neurosci.* (2010). doi:10.1038/nn.2459

59. Garcia, O., Torres, M., Helguera, P., Coskun, P. & Busciglio, J. A role for thrombospondin-1 deficits in astrocyte-mediated spine and synaptic pathology in down's syndrome. *PLoS One* (2010). doi:10.1371/journal.pone.0014200

60. Taylor, C. P. Mechanisms of analgesia by gabapentin and pregabalin - Calcium channel α2-δ [Cavα2-δ] ligands. *Pain* (2009). doi:10.1016/j.pain.2008.11.019

61. Eroglu, Ç. *et al.* Gabapentin Receptor α2δ-1 Is a Neuronal Thrombospondin Receptor Responsible for Excitatory CNS Synaptogenesis. *Cell* (2009). doi:10.1016/j.cell.2009.09.025

62. Kucukdereli, H. *et al.* Control of excitatory CNS synaptogenesis by astrocyte-secreted proteins Hevin and SPARC. *Proc. Natl. Acad. Sci.* (2011). doi:10.1073/pnas.1104977108

63. Singh, S. K. *et al.* Astrocytes Assemble Thalamocortical Synapses by Bridging NRX1α and NL1 via Hevin. *Cell* (2016). doi:10.1016/j.cell.2015.11.034

64. Jones, E. V. *et al.* Astrocytes Control Glutamate Receptor Levels at Developing Synapses through SPARC- -Integrin Interactions. *J. Neurosci.* (2011). doi:10.1523/JNEUROSCI.4757-10.2011

65. Gomes, F. C. A., Sousa, V. D. O. & Romão, L. Emerging roles for TGF-beta1 in nervous system development. *Int. J. Dev. Neurosci.* (2005). doi:10.1016/j.ijdevneu.2005.04.001

66. Crawford, S. E. *et al.* Thrombospondin-1 is a major activator of TGF-β1 in vivo. *Cell* (1998). doi:10.1016/S0092-8674(00)81460-9

67. Murphy-Ullrich, J. E. & Poczatek, M. Activation of latent TGF-beta by thrombospondin-1: mechanisms and physiology. *Cytokine Growth Factor Rev.* (2000). doi:10.1016/S1359-6101(99)00029-5

68. Pereira Diniz, L. *et al.* Astrocyte Transforming Growth Factor Beta 1 Protects Synapses against Aβ Oligomers in Alzheimer's Disease Model. *J. Neurosci.* **37,** 6797–6809 (2017).

69. Diniz, L. P. *et al.* Astrocyte-induced synaptogenesis is mediated by transforming growth factor β signaling through modulation of d-serine levels in cerebral cortex neurons. *J. Biol. Chem.* **287,** 41432–41445 (2012).

70. Diniz, L. P. *et al.* Astrocyte transforming growth factor beta 1 promotes inhibitory synapse formation via CaM kinase II signaling. *Glia* **62,** 1917–1931 (2014).

71. Nieweg, K., Schaller, H. & Pfrieger, F. W. Marked differences in cholesterol synthesis between neurons and glial cells from postnatal rats. *J. Neurochem.* **109,** 125–134 (2009).

72. Pfrieger, F. W. Outsourcing in the brain: Do neurons depend on cholesterol delivery by astrocytes? *BioEssays* **25,** 72–78 (2003).

73. Horton, J. D., Goldstein, J. L. & Brown, M. S. SREBPs: Activators of the complete program of cholesterol and fatty acid synthesis in the liver. *Journal of Clinical Investigation* **109,** 1125–1131 (2002).

74. Mahley, R. W. Apolipoprotein E: cholesterol transport protein with expanding role in cell biology. *Science (80-.).* **240,** 622–630 (1988).

75. Gelissen, I. C. *et al.* ABCA1 and ABCG1 synergize to mediate cholesterol export to ApoA-I. *Arterioscler. Thromb. Vasc. Biol.* **26,** 534–540 (2006).

76. Liu, Q. *et al.* Neuronal LRP1 Knockout in Adult Mice Leads to Impaired Brain Lipid Metabolism and Progressive, Age-Dependent Synapse Loss and Neurodegeneration. *J. Neurosci.* **30,** 17068–17078 (2010).

77. Karasinska, J. M. *et al.* Specific Loss of Brain ABCA1 Increases Brain Cholesterol Uptake and Influences Neuronal Structure and Function. *J. Neurosci.* **29,** 3579–3589 (2009).

78. Hirsch-Reinshagen, V. *et al.* Deficiency of ABCA1 impairs apolipoprotein E metabolism in brain. *J. Biol. Chem.* **279,** 41197–41207 (2004).

79. Goritz, C., Mauch, D. H. & Pfrieger, F. W. Multiple mechanisms mediate cholesterol-induced synaptogenesis in a CNS neuron. *Mol. Cell. Neurosci.* **29,** 190–201 (2005).

80. Göritz, C. *et al.* Glia-induced neuronal differentiation by transcriptional regulation. *Glia* (2007). doi:10.1002/glia.20531

81. Ben Haim, L. & Rowitch, D. H. Functional diversity of astrocytes in neural circuit regulation. *Nat. Rev. Neurosci.* **18,** 31–41 (2016).

82. Bialas, A. R. & Stevens, B. TGF-β signaling regulates neuronal C1q expression and developmental synaptic refinement. *Nat. Neurosci.* (2013). doi:10.1038/nn.3560

83. Stevens, B. *et al.* The Classical Complement Cascade Mediates CNS Synapse Elimination. *Cell* (2007). doi:10.1016/j.cell.2007.10.036

84. Graeber, M. B., Streit, W. J. & Kreutzberg, G. W. Axotomy of the rat facial nerve leads to increased CR3 complement receptor expression by activated microglial cells. *Journal of Neuroscience Research* (1988). doi:10.1002/jnr.490210104

85. Danbolt, N. C. Glutamate uptake. *Progress in Neurobiology* (2001). doi:10.1016/S0301-0082(00)00067-8

86. Yu, A. C. H., Drejer, J., Hertz, L. & Schousboe, A. Pyruvate carboxylase activity in primary cultures of astrocytes and neurons. *J. Neurochem.* (1983). doi:10.1111/j.1471-4159.1983.tb00849.x

87. Schousboe, A., Bak, L. K. & Waagepetersen, H. S. Astrocytic control of biosynthesis and turnover of the neurotransmitters glutamate and GABA. *Frontiers in Endocrinology* (2013). doi:10.3389/fendo.2013.00102

88. Norenberg, M. Distribution of glutamine synthetase in the rat central nervous system. *J Histochem Cytochem* 756–762 (1979).

89. DiGregorio, D. A., Nusser, Z. & Silver, R. A. Spillover of glutamate onto synaptic AMPA receptors enhances fast transmission at a cerebellar synapse. *Neuron* (2002). doi:10.1016/S0896-6273(02)00787-0

90. Mennerick, S. & Zorumski, C. F. Glial contributions to excitatory neurotransmission in cultured hippocampal cells. *Nature* (1994). doi:10.1038/368059a0

91. Kim, K. *et al.* Role of Excitatory Amino Acid Transporter-2 (EAAT2) and glutamate in neurodegeneration: Opportunities for developing novel therapeutics. *J. Cell. Physiol.* **226,** 2484–2493 (2011).

92. Tanaka, K. *et al.* Epilepsy and exacerbation of brain injury in mice lacking the glutamate transporter GLT-1. *Science (80-.).* (1997). doi:10.1126/science.276.5319.1699

93. Gadea, A. & López-Colomé, A. M. Glial transporters for glutamate, glycine, and GABA: II. GABA transporters. *Journal of Neuroscience Research* (2001). doi:10.1002/jnr.1040

94. Gallo, V., Patrizio, M. & Levi, G. GABA release triggered by the activation of neuron-like non-NMDA receptors in cultured type 2 astrocytes is carrier-mediated. *Glia* (1991). doi:10.1002/glia.440040302

95. Beenhakker, M. P. & Huguenard, J. R. Astrocytes as Gatekeepers of GABAB Receptor Function. *J. Neurosci.* (2010). doi:10.1523/JNEUROSCI.3243-10.2010

96. Cornell-Bell, A. H., Finkbeiner, S. M., Cooper, M. S. & Smith, S. J. Glutamate induces calcium waves in cultured astrocytes: Long-range glial signaling. *Science (80-.).* (1990). doi:10.1126/science.1967852

97. Charles, A. C., Merrill, J. E., Dirksen, E. R., Sanderson, M. J. & Sandersont, M. J. Intercellular signalling in glial cells: calcium waves and oscillations in response to mechanical stimulation and glutamate. *Neuron* **6,** 983–992 (1991).

98. Porter, J. T. & McCarthy, K. D. Astrocytic neurotransmitter receptors in situ and in vivo.

Progress in Neurobiology (1997). doi:10.1016/S0301-0082(96)00068-8

99. Araque, A., Parpura, V., Sanzgiri, R. P. & Haydon, P. G. Tripartite synapses: Glia, the unacknowledged partner. *Trends in Neurosciences* (1999). doi:10.1016/S0166-2236(98)01349-6

100. Araque, A., Martin, E. D., Perea, G., Arellano, J. I. & Buno, W. Synaptically Released Acetylcholine Evokes Ca2+ Elevations in Astrocytes in Hippocampal Slices. *J. Neurosci.* (2002). doi:20026212

101. Perea, G. & Araque, A. Properties of Synaptically Evoked Astrocyte Calcium Signal Reveal Synaptic Information Processing by Astrocytes. *J. Neurosci.* (2005). doi:10.1523/JNEUROSCI.3965-04.2005

102. Takata, N. & Hirase, H. Cortical layer 1 and layer 2/3 astrocytes exhibit distinct calcium dynamics in vivo. *PLoS One* (2008). doi:10.1371/journal.pone.0002525

103. Mongin, A. A. & Kimelberg, H. K. ATP potently modulates anion channel-mediated excitatory amino acid release from cultured astrocytes. *AJP Cell Physiol.* (2002). doi:10.1152/ajpcell.00438.2001

104. Moran, M. M., Melendez, R., Baker, D., Kalivas, P. W. & Seamans, J. K. Cystine/Glutamate Antiporter Regulation of Vesicular Glutamate Release. in *Annals of the New York Academy of Sciences* (2003). doi:10.1196/annals.1300.048

105. Söllner, T. *et al.* SNAP receptors implicated in vesicle targeting and fusion. *Nature* (1993). doi:10.1038/362318a0

106. Hepp, R. *et al.* Cultured glial cells express the SNAP-25 analogue SNAP-23. *Glia* (1999). doi:10.1002/(SICI)1098-1136(199908)27:2<181::AID-GLIA8>3.0.CO;2-9

107. Zhang, Q., Fukuda, M., Van Bockstaele, E., Pascual, O. & Haydon, P. G. Synaptotagmin IV regulates glial glutamate release. *Proc. Natl. Acad. Sci.* (2004). doi:10.1073/pnas.0401960101

108. Pascual, O. Astrocytic Purinergic Signaling Coordinates Synaptic Networks. *Science (80-.).* (2005). doi:10.1126/science.1116916

109. Turner, J. R., Ecke, L. E., Briand, L. A., Haydon, P. G. & Blendy, J. A. Cocaine-related behaviors in mice with deficient gliotransmission. *Psychopharmacology (Berl).* (2013). doi:10.1007/s00213-012-2897-4

110. Mothet, J.-P. *et al.* Glutamate receptor activation triggers a calcium-dependent and SNARE protein-dependent release of the gliotransmitter D-serine. *Proc. Natl. Acad. Sci.* (2005). doi:10.1073/pnas.0408483102

111. Coco, S. *et al.* Storage and release of ATP from astrocytes in culture. *J. Biol. Chem.* (2003). doi:10.1074/jbc.M209454200

112. Andrei, C. *et al.* Phospholipases C and A2 control lysosome-mediated IL-1 secretion. *Proc. Natl. Acad. Sci.* (2004). doi:10.1073/pnas.0308558101

113. Trajkovic, K. *et al.* Neuron to glia signaling triggers myelin membrane exocytosis from endosomal storage sites. *J. Cell Biol.* (2006). doi:10.1083/jcb.200509022

114. Zhang, Z. *et al.* Regulated ATP release from astrocytes through lysosome exocytosis. *Nat. Cell Biol.* (2007). doi:10.1038/ncb1620

115. Fellin, T. *et al.* Neuronal synchrony mediated by astrocytic glutamate through activation of extrasynaptic NMDA receptors. *Neuron* (2004). doi:10.1016/j.neuron.2004.08.011

116. Larsen, R. S. *et al.* NR3A-containing NMDARs promote neurotransmitter release and spike timing-dependent plasticity. *Nat. Neurosci.* (2011). doi:10.1038/nn.2750

117. Henneberger, C., Papouin, T., Oliet, S. H. R. & Rusakov, D. A. Long-term potentiation depends on release of d-serine from astrocytes. *Nature* (2010). doi:10.1038/nature08673

118. Perea, G. & Araque, A. Astrocytes potentiate transmitter release at single hippocampal synapses. *Science (80-.).* (2007). doi:10.1126/science.1144640

119. Liu, Q. S., Nedergaard, M., Xu, Q. & Kang, J. Astrocyte activation of presynaptic metabotropic glutamate receptors modulates hippocampal inhibitory synaptic transmission. *Neuron Glia Biol.* (2004). doi:10.1017/S1740925X05000190

120. Lodish, H. *et al.* Transcriptional Control of Gene Expression. in *Molecular Cell Biology* Chapter 7 (2013).

121. Puigserver, P. *et al.* A cold-inducible coactivator of nuclear receptors linked to adaptive thermogenesis. *Cell* **92,** 829–839 (1998).

122. Lin, J. *et al.* Defects in adaptive energy metabolism with CNS-linked hyperactivity in PGC-1α null mice. *Cell* **119,** 121–135 (2004).

123. Yoon, J. C. *et al.* Control of hepatic gluconeogenesis through the transcriptional coactivator PGC-1. *Nature* (2001). doi:10.1038/35093050

124. Lin, J., Puigserver, P., Donovan, J., Tarr, P. & Spiegelman, B. M. Peroxisome proliferator-activated receptor γ coactivator 1β (PGC-1β), a novel PGC-1-related transcription coactivator associated with host cell factor. *J. Biol. Chem.* (2002). doi:10.1074/jbc.C100631200

125. Andersson, U. & Scarpulla, R. C. PGC-1-Related Coactivator, a Novel, Serum-Inducible Coactivator of Nuclear Respiratory Factor 1-Dependent Transcription in Mammalian Cells. *Mol. Cell. Biol.* (2001). doi:10.1128/MCB.21.11.3738-3749.2001

126. St-Pierre, J. *et al.* Bioenergetic analysis of peroxisome proliferator-activated receptor γ coactivators 1α and 1β (PGC-1α and PGC-1β) in muscle cells. *J. Biol. Chem.* (2003). doi:10.1074/jbc.M301850200

127. Lin, J. *et al.* Transcriptional co-activator PGC-1α drives the formation of slow-twitch muscle fibres. *Nature* (2002). doi:10.1038/nature00904

128. Michael, L. F. *et al.* Restoration of insulin-sensitive glucose transporter (GLUT4) gene expression in muscle cells by the transcriptional coactivator PGC-1. *Proc. Natl. Acad. Sci.* (2001). doi:10.1073/pnas.061035098

129. Burgess, S. C. *et al.* Diminished hepatic gluconeogenesis via defects in tricarboxylic acid cycle flux in peroxisome proliferator-activated receptor gamma coactivator-1a (PGC-1a)-deficient mice. *J. Biol. Chem.* (2006). doi:10.1074/jbc.M600050200

130. Lin, J. *et al.* PGC-1beta in the regulation of hepatic glucose and energy metabolism. *J. Biol. Chem.* (2003). doi:10.1074/jbc.M303643200

131. Lin, J. *et al.* Hyperlipidemic effects of dietary saturated fats mediated through PGC-1β coactivation of SREBP. *Cell* **120,** 261–273 (2005).

132. Correia, J. C., Ferreira, D. M. S. & Ruas, J. L. Intercellular: Local and systemic actions of skeletal muscle PGC-1s. *Trends Endocrinol. Metab.* **26,** 305–314 (2015).

133. Puigserver, P. *et al.* Activation of PPARγ coactivator-1 through transcription factor docking. *Science (80-.).* **286,** 1368–1371 (1999).

134. Monsalve, M. *et al.* Direct coupling of transcription and mRNA processing through the thermogenic coactivator PGC-1. *Mol. Cell* (2000). doi:10.1016/S1097-2765(00)00031-9

135. Wallberg, A. E., Yamamura, S., Malik, S., Spiegelman, B. M. & Roeder, R. G. Coordination of p300-mediated chromatin remodeling and TRAP/mediator function through coactivator PGC-1α. *Mol. Cell* (2003). doi:10.1016/S1097-2765(03)00391-5

136. Neugebauer, K. M. & Roth, M. B. Transcription units as RNA processing units. *Genes and Development* (1997). doi:10.1101/gad.11.24.3279

137. Jager, S., Handschin, C., St.-Pierre, J. & Spiegelman, B. M. AMP-activated protein kinase (AMPK) action in skeletal muscle via direct phosphorylation of PGC-1a. *Proc. Natl. Acad. Sci.*

(2007). doi:10.1073/pnas.0705070104

138. Suwa, M., Nakano, H. & Kumagai, S. Effects of chronic AICAR treatment on fiber composition, enzyme activity, UCP3, and PGC-1 in rat muscles. *J. Appl. Physiol.* (2003). doi:10.1152/japplphysiol.00349.2003

139. Herzig, S. *et al.* CREB regulates hepatic gluconeogenesis through the coactivator PGC-1. *Nature* (2001). doi:10.1038/35093131

140. Cao, W. *et al.* p38 mitogen-activated protein kinase is the central regulator of cyclic AMP-dependent transcription of the brown fat uncoupling protein 1 gene. *Mol Cell Biol* (2004).

141. Wu, H. *et al.* Regulation of mitochondrial biogenesis in skeletal muscle by CaMK. *Science* (2002). doi:10.1126/science.1071163

142. Handschin, C., Rhee, J., Lin, J., Tarr, P. T. & Spiegelman, B. M. An autoregulatory loop controls peroxisome proliferator-activated receptor gamma coactivator 1alpha expression in muscle. *Proc. Natl. Acad. Sci. U. S. A.* (2003). doi:10.1073/pnas.1232352100

143. Akimoto, T., Sorg, B. S. & Yan, Z. Real-time imaging of peroxisome proliferator-activated receptor-gamma coactivator-1alpha promoter activity in skeletal muscles of living mice. *Am. J. Physiol. Cell Physiol.* (2004). doi:10.1152/ajpcell.00425.2003

144. Puigserver, P. *et al.* Cytokine Stimulation of Energy Expenditure through p38 MAP Kinase Activation of PPARγ Coactivator-1. *Mol. Cell* (2001). doi:10.1016/S1097-2765(01)00390-2

145. Fan, M. *et al.* Suppression of mitochondrial respiration through recruitment of p160 myb binding protein to PGC-1α: Modulation by p38 MAPK. *Genes Dev.* (2004). doi:10.1101/gad.1152204

146. Rodgers, J. T. *et al.* Nutrient control of glucose homeostasis through a complex of PGC-1a and SIRT1. *Nature* (2005). doi:10.1038/nature03314.1.

147. Houtkooper, R. H., Cantó, C., Wanders, R. J. & Auwerx, J. The secret life of NAD+: An old metabolite controlling new metabolic signaling pathways. *Endocrine Reviews* (2010). doi:10.1210/er.2009-0026

148. Cantó, C. *et al.* AMPK regulates energy expenditure by modulating NAD+ metabolism and SIRT1 activity. *Nature* (2009). doi:10.1038/nature07813

149. Gerhart-Hines, Z. *et al.* Metabolic control of muscle mitochondrial function and fatty acid oxidation through SIRT1/PGC-1α. *EMBO J.* (2007). doi:10.1038/sj.emboj.7601633

150. Lerin, C. *et al.* GCN5 acetyltransferase complex controls glucose metabolism through transcriptional repression of PGC-1α. *Cell Metab.* (2006). doi:10.1016/j.cmet.2006.04.013

151. Kelly, T. J., Lerin, C., Haas, W., Gygi, S. P. & Puigserver, P. GCN5-mediated transcriptional control of the metabolic coactivator PGC-1β through lysine acetylation. *J. Biol. Chem.* (2009). doi:10.1074/jbc.M109.015164

152. Coste, A. *et al.* The genetic ablation of SRC-3 protects against obesity and improves insulin sensitivity by reducing the acetylation of PGC-1{alpha}. *PNAS* (2008). doi:10.1073/pnas.0808207105

153. Wellen, K. E. *et al.* ATP-citrate lyase links cellular metabolism to histone acetylation. *Science (80-.).* (2009). doi:10.1126/science.1164097

154. Ruas, J. L. *et al.* A PGC-1α isoform induced by resistance training regulates skeletal muscle hypertrophy. *Cell* **151,** 1319–1331 (2012).

155. Chinsomboon, J. *et al.* The transcriptional coactivator PGC-1alpha mediates exercise-induced angiogenesis in skeletal muscle. *Proc. Natl. Acad. Sci. U. S. A.* **106,** 21401–6 (2009).

156. Yoshioka, T. *et al.* Identification and characterization of an alternative promoter of the human PGC-1α gene. *Biochem. Biophys. Res. Commun.* (2009). doi:10.1016/j.bbrc.2009.02.077

157. Martínez-Redondo, V., Pettersson, A. T. & Ruas, J. L. The hitchhiker's guide to PGC-1α isoform

structure and biological functions. *Diabetologia* **58,** 1969–1977 (2015).

158. Miura, S., Kai, Y., Kamei, Y. & Ezaki, O. Isoform-specific increases in murine skeletal muscle peroxisome proliferator-activated receptor-gamma coactivator-1alpha (PGC-1alpha) mRNA in response to beta2-adrenergic receptor activation and exercise. *Endocrinology* (2008). doi:10.1210/en.2008-0466

159. Martínez-Redondo, V. *et al.* Peroxisome proliferator-activated receptor γ coactivator-1 α isoforms selectively regulate multiple splicing events on target genes. *J. Biol. Chem.* **291,** 15169–15184 (2016).

160. Vega, R. B., Huss, J. M. & Kelly, D. P. The Coactivator PGC-1 Cooperates with Peroxisome Proliferator-Activated Receptor alpha in Transcriptional Control of Nuclear Genes Encoding Mitochondrial Fatty Acid Oxidation Enzymes. *Mol. Cell. Biol.* (2000). doi:10.1128/MCB.20.5.1868-1876.2000

161. Soyal, S. M. *et al.* A greatly extended PPARGC1A genomic locus encodes several new brain-specific isoforms and influences Huntington disease age of onset. *Hum. Mol. Genet.* (2012). doi:10.1093/hmg/dds177

162. Cheng, A. *et al.* Involvement of PGC-1α in the formation and maintenance of neuronal dendritic spines. *Nat. Commun.* **3,** 1250 (2012).

163. Lucas, E. K. *et al.* PGC-1a Provides a Transcriptional Framework for Synchronous Neurotransmitter Release from Parvalbumin-Positive Interneurons. *J. Neurosci.* **34,** 14375–14387 (2014).

164. Oberkofler, H., Schraml, E., Krempler, F. & Patsch, W. Restoration of sterol-regulatory-element-binding protein-1c gene expression in HepG2 cells by peroxisome-proliferator-activated receptor-gamma co-activator-1alpha. *Biochem. J.* (2004). doi:10.1042/BJ20040173

165. Oberkofler, H., Schraml, E., Krempler, F. & Patsch, W. Potentiation of liver X receptor transcriptional activity by peroxisome-proliferator-activated receptor γ co-activator 1α. *Biochem. J* **371,** 89–96 (2003).

166. Agudelo, L. Z. *et al.* Skeletal muscle PGC-1α1 modulates kynurenine metabolism and mediates resilience to stress-induced depression. *Cell* **159,** 33–45 (2014).

167. Schwarcz, R., Bruno, J. P., Muchowski, P. J. & Wu, H. Q. Kynurenines in the mammalian brain: When physiology meets pathology. *Nature Reviews Neuroscience* (2012). doi:10.1038/nrn3257

168. Schon, E. A. & Manfredi, G. Neuronal degeneration and mitochondrial dysfunction. *Journal of Clinical Investigation* (2003). doi:10.1172/JCI200317741

169. Wang, R. *et al.* Metabolic stress modulates Alzheimer's β-secretase gene transcription via SIRT1-PPARγ-PGC-1 in neurons. *Cell Metab.* **17,** 685–694 (2013).

170. Hasegawa, K. *et al.* Promotion of mitochondrial biogenesis by necdin protects neurons against mitochondrial insults. *Nat. Commun.* (2016). doi:10.1038/ncomms10943

171. Moutinho, M. *et al.* Neuronal cholesterol metabolism increases dendritic outgrowth and synaptic markers via a concerted action of GGTase-I and Trk. *Sci. Rep.* **6,** 30928 (2016).

172. 5 PRIME. Izol-RNA Lysis Reagent Manual. (2007). Available at: https://fnkprddata.blob.core.windows.net/domestic/data/datasheet/FPR/2302700.pdf.

173. Agilent Technologies. Agilent RNA 6000 Nano Kit Guide. (2001). Available at: https://www.agilent.com/cs/library/usermanuals/Public/G2938-90034_RNA6000Nano_KG.pdf.

174. Andersen, C. L., Jensen, J. L. & Ørntoft, T. F. Normalization of real-time quantitative reverse transcription-PCR data: A model-based variance estimation approach to identify genes suited for normalization, applied to bladder and colon cancer data sets. *Cancer Res.* (2004). doi:10.1158/0008-5472.CAN-04-0496

175. Pertea, M., Kim, D., Pertea, G. M., Leek, J. T. & Salzberg, S. L. Transcript-level expression analysis of RNA-seq experiments with HISAT, StringTie and Ballgown. *Nat. Protoc.* (2016). doi:10.1038/nprot.2016-095

176. Anders, S., Pyl, P. T. & Huber, W. HTSeq-A Python framework to work with high-throughput sequencing data. *Bioinformatics* (2015). doi:10.1093/bioinformatics/btu638

177. Love, M. I., Huber, W. & Anders, S. Moderated estimation of fold change and dispersion for RNA-seq data with DESeq2. *Genome Biol.* (2014). doi:10.1186/s13059-014-0550-8

178. Robinson, J. T. *et al.* Integrative genomics viewer. *Nature Biotechnology* (2011). doi:10.1038/nbt.1754

179. Subramanian, A. *et al.* Gene set enrichment analysis: A knowledge-based approach for interpreting genome-wide expression profiles. *Proc. Natl. Acad. Sci.* (2005). doi:10.1073/pnas.0506580102

180. Wold, S., Esbensen, K. & Geladi, P. Principal component analysis. *Chemom. Intell. Lab. Syst.* (1987). doi:10.1016/0169-7439(87)80084-9

181. Ahn, J. *et al.* Primary neurons become less susceptible to coxsackievirus B5 following maturation: The correlation with the decreased level of CAR expression on cell surface. *J. Med. Virol.* (2008). doi:10.1002/jmv.21100

182. Poliseno, L. *et al.* A coding-independent function of gene and pseudogene mRNAs regulates tumour biology. *Nature* **465,** 1033–1038 (2010).

183. Panwar, B., Omenn, G. S. & Guan, Y. MiRmine: A database of human miRNA expression profiles. *Bioinformatics* **33,** 1554–1560 (2017).

184. Wei, P., Pan, D., Mao, C. & Wang, Y.-X. RNF34 Is a Cold-Regulated E3 Ubiquitin Ligase for PGC-1a and Modulates Brown Fat Cell Metabolism. *Mol. Cell. Biol.* (2012). doi:10.1128/MCB.05674-11

185. Doshi, S. & Lynch, D. R. Calpain and the Glutamatergic synapse. *Front. Biosci. (Schol. Ed).* **1,** 466–76 (2009).

186. Fischer, I., Romano-Clarke, G. & Grynspan, F. Calpain-mediated proteolysis of microtubule associated proteins MAP1B and MAP2 in developing brain. *Neurochem. Res.* (1991). doi:10.1007/BF00965538

187. Lu, X., Rong, Y. & Baudry, M. Calpain-mediated degradation of PSD-95 in developing and adult rat brain. *Neurosci. Lett.* **286,** 149–153 (2000).

188. Shichita, T. *et al.* MAFB prevents excess inflammation after ischemic stroke by accelerating clearance of damage signals through MSR1. *Nat. Med.* **23,** 723–732 (2017).

189. Shintani, Y. *et al.* TLR9 mediates cellular protection by modulating energy metabolism in cardiomyocytes and neurons. *Proc. Natl. Acad. Sci.* **110,** 5109–5114 (2013).

190. Guo, X. *et al.* The AMPK-PGC-1α signaling axis regulates the astrocyte glutathione system to protect against oxidative and metabolic injury. *Neurobiol. Dis.* **113,** 59–69 (2018).

191. McCarthy, C. G., Wenceslau, C. F., Ogbi, S., Szasz, T. & Webb, R. C. Toll-like receptor 9-dependent AMPKα activation occurs via TAK1 and contributes to RhoA/ROCK signaling and actin polymerization in vascular smooth muscle cells. *J. Pharmacol. Exp. Ther.* jpet.117.245746 (2018). doi:10.1124/jpet.117.245746

192. Kim, E.-K. *et al.* Activation of AMP-activated Protein Kinase Is Essential for Lysophosphatidic Acid-induced Cell Migration in Ovarian Cancer Cells. *J. Biol. Chem.* **286,** 24036–24045 (2011).

193. Eisele, P. S., Salatino, S., Sobek, J., Hottiger, M. O. & Handschin, C. The peroxisome proliferator-activated receptor γ coactivator 1α/β (PGC-1) coactivators repress the transcriptional activity of NF-κB in skeletal muscle cells. *J. Biol. Chem.* **288,** 2246–2260 (2013).

194. Karki, P. *et al.* Yin Yang 1 Is a Repressor of Glutamate Transporter EAAT2, and It Mediates

Manganese-Induced Decrease of EAAT2 Expression in Astrocytes. *Mol. Cell. Biol.* **34,** 1280–1289 (2014).

195. Irie, A. *et al.* Galectin-9 as a prognostic factor with antimetastatic potential in breast cancer. *Clin. Cancer Res.* **11,** 2962–2968 (2005).

196. Steelman, A. J. & Li, J. Astrocyte galectin-9 potentiates microglial TNF secretion. *J. Neuroinflammation* **11,** 1–12 (2014).

197. Hinz, B. The extracellular matrix and transforming growth factor-β1: Tale of a strained relationship. *Matrix Biol.* **47,** 54–65 (2015).

198. Diaz, A. *et al.* A Cross Talk between Neuronal Urokinase-type Plasminogen Activator (uPA) and Astrocytic uPA Receptor (uPAR) Promotes Astrocytic Activation and Synaptic Recovery in the Ischemic Brain. *J. Neurosci.* **37,** 10310–10322 (2017).

199. Lee, M. H. *et al.* TGF-β induces TIAF1 self-aggregation via type II receptor-independent signaling that leads to generation of amyloid β plaques in Alzheimer's disease. *Cell Death Dis.* **1,** e110-11 (2010).

200. Liu, L., Wang, Y., Bai, R., Yang, K. & Tian, Z. MiR-186 inhibited aerobic glycolysis in gastric cancer via HIF-1α regulation. *Oncogenesis* **5,** e224 (2016).

201. Kim, J. *et al.* miR-186 is decreased in aged brain and suppresses BACE1 expression. *J. Neurochem.* **137,** 436–445 (2017).

202. Caputo, V. *et al.* Brain derived neurotrophic factor (BDNF) expression is regulated by microRNAs miR-26a and miR-26b allele-specific binding. *PLoS One* **6,** (2011).

203. Dill, H., Linder, B., Fehr, A. & Fischer, U. Intronic miR-26b controls neuronal differentiation by repressing its host transcript, ctdsp2. *Genes Dev.* **26,** 25–30 (2012).

204. Liu, D. *et al.* Dysregulated expression of miR-101b and miR-26b lead to age-associated increase in LPS-induced COX-2 expression in murine macrophage. *Age (Omaha).* **37,** (2015).